NEURONS AS POTENTIAL IMMUNE MODULATORS DURING CENTRAL NERVOUS SYSTEM TUBERCULOSIS

by

AVRIL WALTERS

Thesis Presented for the Degree of

DOCTOR OF PHILOSOPHY

In the Department of Pathology

Faculty of Health Sciences

UNIVERSITY OF CAPE TOWN

July 2024

Table of Contents

Declaration

I, Avril Walters, hereby declare that the work on which this thesis is based is my original work (except where acknowledgements indicate otherwise) and that neither the whole work nor any part of it has been, is being, or is to be submitted for another degree in this or any other university. I authorise the University to reproduce for the purpose of research either the whole or any portion of the contents in any manner whatsoever.

Signature: **Date:**

Acknowledgements

I would like to acknowledge and thank the following individuals and organisations for their contributions during the completion of this thesis and research project.

- I would like to thank my supervisors Prof Muazzam Jacobs, Dr Nai-Jen Hsu and Dr Roanne Keeton for the opportunity, guidance and assistance through this PhD journey.

- To Dr Sohair Geyer, thanks for the daily motivation and encouragement through these tough times. If it wasn't for you and Dr Hsu, I don't think that I would have completed this degree.

- A big thank you to Dr Khanyisile Kgoadi for always checking up on my progress and for the support and motivation.

- To other colleagues in the Jacobs lab, Faried, Dr Salie, Dr Tangie, Dr Kamanzi, Antoinette, Petr, Limpho and Marnie, thank you for the support and assistance. A special thanks to Antoinette for generating the Humanized mice which were used in this study and Petr for assistance during the experiment.

- All members of both the Burgers group and the Chigorimbo-Tsikiwa group for continuous support and encouragement during my write-up, especially while being employed. A massive thanks to Prof Burgers, Dr Keeton and Dr Chigorimbo-Tsikiwa for allowing me some time to complete my thesis while being employed.

- I would also like to acknowledge the following individuals who played a major role in the generation and analysis of the transcriptomics data for this study; Dr Hans-Joachim Mollenkopf and Dr Natalie Nieuwenhuizen (Core Facility Genomics/Microarray, Max Planck Institute for Infection Biology, Berlin, Germany), Dr Katie S. Lennard (Division of Computational Biology, Department of Integrative Biomedical Sciences, Institute of Infectious Disease and Molecular Medicine, Faculty of Health Sciences, University of Cape Town, South Africa) and Dr Conchita Kamanzi (Division of Immunology, Department of Pathology, Institute of Infectious Disease and Molecular Medicine, Faculty of Health Sciences, University of Cape Town, South Africa).

- Thanks to the National Research Foundation (South Africa), the University of Cape Town, the South African Medical Research Council (South Africa) Division of Research Capacity Development and the National Health and Laboratory Services (South Africa) for funding myself and this study.

- Thanks to all my family and friends for the kind words and best wishes.

- A special shout-out to my brothers Nico, Jordan, Earl and Buhle.

- To my daughter Nicola and wife Nicoline thanks for the motivation, encouragement and support.

- Finally, thanks to my mother Edith for motivating and encouraging me since Day 1 and for making all this possible. Thanks for being my number one fan and for never giving up on me. Thanks to Oom D (Mr Douglas Trollip) for taking such good care of my mother and for the encouragement to complete my studies.

Abstract

Background

Mycobacterium tuberculosis (*M. tuberculosis*) is the causative pathogen in the pulmonary disease tuberculosis, with both innate and adaptive immunity providing host defence mechanisms against *M. tuberculosis* infection for positive disease outcomes. There is clinical evidence that individuals with compromised immunity, such as patients with HIV, are at higher risk of bacteria dissemination to the brain and developing central nervous system tuberculosis (CNS-TB), which is often associated with high mortality and morbidity. Neurons have been identified as host cells for *M. tuberculosis* and display potential immune regulatory capability during infection. It is therefore important to understand how neurons and immune cells, whether resident or peripheral shape functional and protective immune responses against CNS-TB infection.

Objective

Neurons have demonstrated potential to participate in a tightly regulated neuro-immune networks. This study aims to investigate the immune modulatory abilities of neurons in CNS-TB. Furthermore, it aims to highlight the importance of functional systemic immune responses as an integral aspect of CNS protective immunity.

Methods

This study incorporated both a culture based *in vitro* approach as well as *in vivo* investigation using a mouse model of infection. Initial studies focused on primary murine hippocampal neurons which were infected with *M. tuberculosis* H37Rv; RNA was extracted for microarray analysis and the culture supernatants were processed for Luminex Multiplex analysis to assess neuronal secretion of 11 immunologically active analytes. To identify the immune regulatory abilities of neurons, the supernatants from infected neurons were transferred to freshly isolated leukocytes from mouse blood and used as conditioned medium for an overnight stimulation. The leukocytes were then analysed by flow cytometry. *In vivo* experiments were performed on C57BL/6, NSG and BLT-NSG humanised mice. Mice were infected with *M. tuberculosis* H37Rv by intracerebral inoculation. Mice were monitored for

body condition, weight loss and signs of neurodegeneration over the period of infection. Infected brains were harvested, and single cell suspensions were generated for flow cytometry analysis.

Results

M. tuberculosis infected primary hippocampal neurons showed transcriptional differences when compared to non-infected neurons. Genes expressed in infected neurons clustered separately from non-infected neurons representing distinct transcriptomic profiles. The transcriptomic results were validated by protein analysis, which showed significant upregulated protein expression in primary neuron cultures after *M. tuberculosis* infection. To identify the immune modulatory abilities, stimulation of leukocytes with neuronal conditioned media resulted in significant cell activation where $CD45^{+}$ leukocytes expressing MHC class II and IL1β. *In vivo* challenge studies showed that immune competent C57BL/6 mice remained healthy across the period of infection, however immune incompetent NSG and humanised BLT-NSG mice presented with deteriorating health. Furthermore, although the BLT-NSG mice were reconstituted with human immune cells and showed functional human leukocyte recruitment to the brain, mice were unable to control the infection.

Conclusion

The findings from this study show that neurons are active cell participants during CNS infections capable of generating immune responses and perform immune modulatory functions in response to *M. tuberculosis* infection. Moreover, it is imperative to have a functional systemic immune system characterised by functionally effective leukocyte recruitment to induce adequate protection as part of a comprehensive protective host immune response against CNS-TB.

List of Abbreviations

APCs	Antigen presenting cells
BBB	Blood brain barrier
BLT	Blood-liver-thymus
BLT-NSG	Humanised mice
CD	Cluster differentiation
cDCs	Conventional DCs
CFUs	Colony forming units
CM	Conditioned media
CNS-TB	Central nervous system tuberculosis
DCs	Dendritic cells
DEGs	Differentially expressed genes
EPTB	Extra pulmonary tuberculosis
GFP	Green fluorescent protein
HBSS	Hank’s balanced salt solution
HIV	Human immunodeficiency viruses
IFN-γ	Interferon-gamma
IL	Interleukin
INOS	Inducible nitric oxide synthase
KEGG	Kyoto Encyclopaedia of Genes and Genomes
LPS	Lipopolysaccharide
M. tuberculosis	Mycobacterium tuberculosis
MHC	Major histocompatibility complex
MOI	Multiplicity of infection
NF-κβ	Nuclear factor kappa beta
NK	Natural killer

NO	Nitric oxide
NOD	Nonobese diabetic
NSG	NOD-SCID-IL2Rgamma
OADC	Oleic acid-albumin-dextrose-catalase
PAMPs	Pathogen-associated molecular patterns
PBL	Peripheral blood leukocytes
PCA	Principal component analysis
pDCs	Plasmacytoid DCs
PF4	Platelet factor 4
PRRs	Pattern recognition receptors
SCID	Severe combined immunodeficiency
SD	Standard deviation
SPF	Specific pathogen free
SPIA	Signaling Pathway Impact Analysis
TB	Tuberculosis
TLRs	Toll like receptors
TNF	Tumour necrosis factor
WHO	World Health Organization

List Tables

List of figures

Chapter 1: Literature Review

1 Literature Review

1.1 Tuberculosis

The World Health Organization (WHO) reported that tuberculosis (TB) was the leading cause of mortality by a single infectious agent worldwide in 2019 before the Covid pandemic (WHO, 2022). An estimated 10 million new cases and 1.4 million TB-related deaths were reported by the WHO in 2021 (WHO, 2022). South Africa was ranked in the top eight countries globally based on new TB cases, with reports of up to 500 cases per 100 000 population in 2021 (Figure 1.1) (WHO, 2022). Even though South Africa has reached a 20% reduction in TB cases, mortality remains high (STATSSA, 2020).

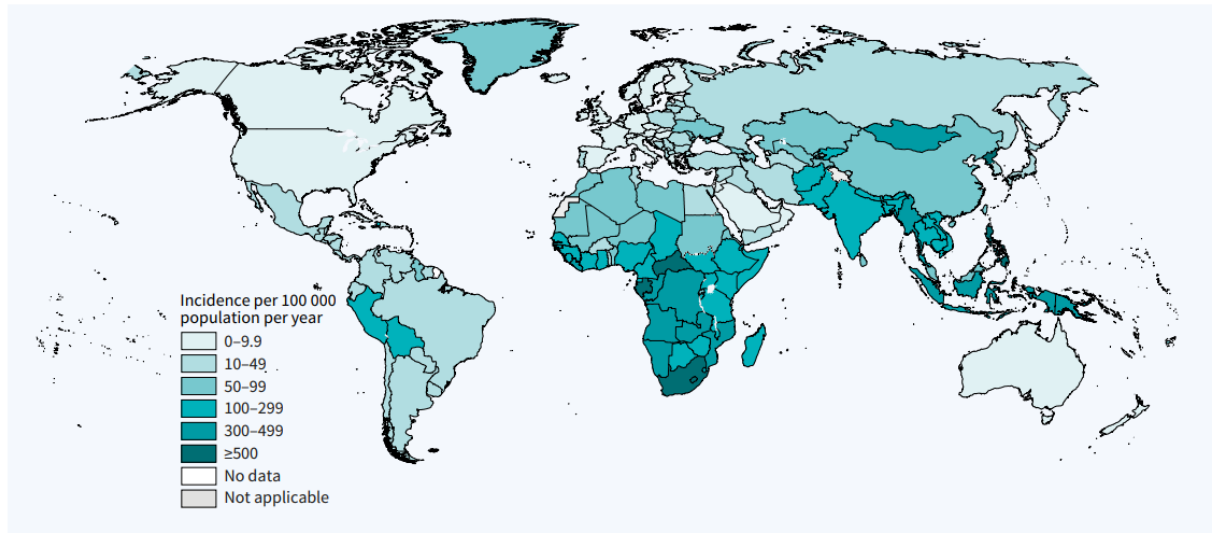

Figure 1-1: The estimated TB incidence cases per 100000 people per year.
The map shows the spectrum of estimated TB incidence cases across the world. Here South Africa is reported to have over 500 cases TB in 2021 (WHO, 2022).

TB is caused by the inhalation of bacterium *Mycobacterium tuberculosis* (*M. tuberculosis*), which is a slow growing, acid-fast, rod-shaped, gram-positive bacteria that contains peptidoglycans and lipo-arabinomannans in its cell wall (Kalscheuer *et al*., 2019, Rock *et al*., 2008). Upon inhalation, resident alveolar and interstitial macrophages phagocytose bacteria, generating initial immune responses via enhanced cytokine and chemokine production that leads to increasing cellular recruitment to focal infection sites (Walters *et al*., 2021). The influx of leukocytes such as neutrophils, macrophages and later lymphocytes are primary responding cells to *M. tuberculosis* infection.

Tuberculosis disease progression can be tracked through a spectrum of stages ranging from acute infection through latent TB to active TB presentation. This spectrum is defined by results from various tests such as the tuberculin skin test, interferon-gamma (IFN-γ) release assays, *M. tuberculosis* culture, sputum smear and symptom presentation (Pai *et al*., 2016). In 2014 an estimated 23% of the global population was said to be latently infected with *M. tuberculosis* (Houben and Dodd, 2016). Latent TB is defined as infected individuals being asymptomatic and not at risk of spreading disease (Ilievska-Poposka *et al*., 2018). Latent infected individuals can develop active TB under conditions of immune suppression. During active TB disease state, patients can actively spread the disease through the release of aerosolized droplets containing bacilli.

Compromised immunity is the leading contributor to TB disease progression. Co-infections with human immunodeficiency viruses (HIV) contributes approximately 11% of TB deaths globally (WHO, 2022). Other factors that influence TB development are individuals on immune suppressive medication and the rise of drug-resistant TB cases (Machuca *et al*., 2018). Various combinations of isoniazid, rifampicin and pyrazinamide are used over a period of six months to treat TB. *M. tuberculosis* infection primarily leads to pulmonary disease but can infect other organs due to haematogenous dissemination (Moule and Cirillo, 2020). The WHO reported that approximately 16% of the total number of new cases in 2019 were found to be extra pulmonary tuberculosis (EPTB) (WHO, 2020). EPTB takes on different forms including, lymphadenitis, musculoskeletal TB, genitourinary, and central nervous system tuberculosis (CNS-TB) (Rodriguez-Takeuchi *et al*., 2019, Rock *et al*., 2008). The symptoms presented for the various organ disease types are different and, in many instances, may resemble other diseases which increases difficulty of diagnosis and treatment.

1.2 Central nervous System Tuberculosis

The CNS is deemed to be an immune-privileged site due to the protective nature of the blood brain barrier (BBB) which isolates the CNS from the periphery (Persidsky *et al*., 2006). In the CNS under steady state, immune privilege is associated with limited surveillance by leukocytes and the restriction of large molecules as well as pathogens from infiltrating the brains (Russo and McGavern, 2015). This restrictive nature of the BBB is made possible by a combination of tight junctions joining the vascular endothelial cells along with robust structures formed by the glial limitans. These structures reduce the risk of CNS pathology and ensures neurological protection against possible neurodegenerative injury (Persidsky *et al*., 2006).

Approximately 1-10% of all TB cases are reported to be associated with CNS-TB, which mostly manifests in children and immune compromised individuals that reside in low resource regions of the world (Cherian and Thomas, 2011, Navarro-Flores *et al*., 2022). This form of TB is one of the most severe forms of the disease that can affect the spinal cord, meninges as well as the brain tissue. Symptoms of CNS-TB include but are not limited to confusion, headache, fever, neck stiffness, convulsions and ultimately mortality if left untreated (Marx and Chan, 2011).

CNS-TB occurs because of hematogenous bacilli dissemination from the lungs to the brain (Hernandez Pando *et al*., 2010). Development of CNS-TB starts from the rupture of caseating subependymal tuberculosis foci (Rock *et al*., 2008) which causes tuberculosis bacilli to enter the subarachnoid space and infect the meninges. The site of infection within the CNS is important for identifying the type of CNS-TB that is manifested. This ranges from inflammation in the CNS caused indirectly by TB infection known as TB encephalitis, to intracranial tuberculomas found in the brain tissue. Of these infections, TB meningitis is the most common, identified by tuberculosis foci formed within the meninges (Rock *et al*., 2008, Woldeamanuel and Girma, 2014).

1.3 Resident cellular immunity during CNS-TB

1.3.1 Microglia, Astrocytes and *M. tuberculosis* infection

Microglia are considered the main effector cell type essential to maintain brain homeostasis and crucial for protection against infection (Spanos *et al*., 2015). *M. tuberculosis* can target various brain cell types within the CNS and microglia are recognised as the primary target cell for infection (Rock *et al*., 2005, Curto *et al*., 2004). Microglia are professional antigen presenting cells and mediate bacilli uptake via cluster differentiation (CD) 14 mediated phagocytosis (Peterson *et al*., 1995). Microglia can migrate towards sites of CNS inflammation and proliferate (Carbonell *et al*., 2005, Giordana *et al*., 1994). Cruto *et al.* investigated differences based on bacterial virulence and rate of uptake. The authors reported rapid engulfment of *Mycobacterium avium* but longer persistence of *M. tuberculosis* within the cell cytoplasm, which was linked to downstream suppression of cytokines by *M. tuberculosis* (Curto *et al*., 2004). Various microglial subtypes have been identified by single cell RNA sequencing (Stratoulias et al., 2019) and signaling from these cells can facilitate cell recruitment for containment of bacilli infection.

Astrocytes have also been implicated as potential host cells for *M. tuberculosis* (Rock *et al*., 2005). Astrocytes are glial cells that have an important role in CNS homeostasis regulation and form part of the structural framework of the CNS. Although astrocytes constitute an important cell type in the BBB formation (Sofroniew and Vinters, 2010) they can undergo molecular changes and become “reactive” in response to CNS insult. Two different types of reactive astrocytes were identified by Liddelow *et al*. as A1 neurotoxic astrocytes and A2 neuroprotective astrocytes (Liddelow *et al*., 2017). The A1 reactive phenotype is characterized by upregulation of neuroinflammatory molecules in a microglial dependent manner, where microglial secretion of interleukin (IL) 1α, tumour necrosis factor (TNF) and C1q is pivotal. A2 is a neuroprotective phenotype and characterised by the upregulation of neurotrophic factors (Liddelow *et al*., 2017). Lipopolysaccharide (LPS) stimulation can induce A1 astrocyte activity in mice but not humans (Tarassishin *et al*., 2014). Importantly astrocytes are capable to phagocytose *M. tuberculosis* bacilli (Rock *et al*., 2005, Othman *et al*., 2018). More recently, a study using single cell RNA sequencing identified transcriptional diversity within astrocyte

populations across six CNS disorders (Qian et al., 2023). This suggests the existence of a spectrum of astrocytic subtypes similar to those found in microglia.

1.3.2 Neurons and *M. tuberculosis* infection

Neurons are specialized functional cells of the nervous system responsible for converting stimuli into electrical or chemical signals. Neurons are not considered to functionally influence immune responses while many disease outcomes result in neurological sequelae associated with neuronal damage and related CNS complications (Ronca *et al*., 2016). This drives the narrative that neurons are passive recipients and not active participants during an immune response. However, growing evidence indicates that neurons play an active role in modulating the immune response during infection (Baral *et al*., 2019).

Expression of toll like receptors (TLRs) allows neurons to recognise and respond to pathogens (Faridgohar and Nikoueinejad, 2017, Kaul *et al*., 2012). Previous studies showed neuronal internalization of bacteria such as *M. tuberculosis*, *Listeria monocytogenes*, *Mycobacterium leprae* and *Mycobacterium bovis* bacille Calmette-Guérin (Randall *et al*., 2014, Dramsi *et al*., 1998, Aung *et al*., 2007). Neuronal phagocytosis leads to the internalisation of small particles and debris (Bowen *et al*., 2007), while Randall *et. al.* showed uptake of *M tuberculosis* (Randall *et al*., 2014). The ability of neurons to internalise *M. tuberculosis* is significant and suggest that it may participate in immune regulation via antigen presentation. Largely neurons do not express major histocompatibility complex (MHC) class II except for a subpopulation of neural stem cells (Vagaska *et al*., 2016). In contrast, neurons have been recognised to express MHC class I constitutively (Shatz, 2009) which is upregulated in response to LPS stimulation (Foster *et al*., 2002). While $CD8^+$ T cells interact with neurons via MHC class I (Hennecke and Wiley, 2001, Chevalier *et al*., 2011), $CD4^+$ T cells interaction is TCR independent (Walsh *et al*., 2015). Furthermore, neurons can mediate T-regulatory cellular recruitment to the CNS (Liu *et al*., 2006).

Neurons can produce cytokines such as IL1β, IL6 and IL10 in response to *M. tuberculosis* (Randall *et al*., 2014) which constitutes an indirect mode of participation in immune regulation. The generation of a specific cytokine milieu can facilitate peripheral cell recruitment by regulating tight junctions of the BBB (Sofroniew and

Vinters, 2010). The relationship between neurons and leukocytes shows an important aspect of neuronal immune regulation. In a model of West Nile Encephalitis Virus disease, Shrestha and colleagues showed a correlation between leukocyte recruitment and increasing number of infected neurons (Shrestha *et al*., 2003). In a study with *Xenopus laevis* infected with *Escherichia coli*, the brains were removed from embryos early during embryogenesis. The animals were able to continue normal embryonic development and immune responses were compared to embryos with intact brains. The resulting outcome revealed that embryos with brains were better protected than those that had their brains removed and showed better macrophage recruitment which correlated with larger neural networks (Herrera-Rincon *et al*., 2020). The implication of these findings suggested a regulatory role of neurons in immune cellular recruitment and inflammation.

1.4 Cellular recruitment in response to CNS-TB

1.4.1 Innate Immunity to Tuberculosis

The innate arm of the immune system is the first to interact with invading pathogens and is characterised, but not limited to the activation of tissue resident immune cells. Immune modulation or regulation relies on host cells to recognise pathogens and generate an appropriate immune response. Conserved pattern recognition receptors (PRRs) such as toll like receptors, Nucleotide oligomerization domain like receptors, RIG-like receptors and C-type lectin receptors recognise pathogen-associated molecular patterns (PAMPs) present on microbes (Amarante-Mendes *et al*., 2018, Walsh *et al*., 2013). These initiate molecular events resulting in immune outcomes which require direct or indirect contact with immune cells. Direct contact is associated with MHC presentation which is critical to activate adaptive immune responses while cytokine and chemokine production characterises indirect communication important for cellular recruitment and management of pathogen containment. Various peripheral immune cell types have been proposed to surveil the CNS during homeostasis and are actively recruited under pathological conditions (Russo and McGavern, 2015). Early recruitment of systemic leukocytes such as neutrophils, macrophages and dendritic cells (DCs) are hallmarks of this defence mechanism. Innate immunity is normally considered to be essential for the control of acute infection and inflammation.

1.4.1.1 Neutrophils

Polymorphonuclear neutrophils are small innate immune cells produced in the bone marrow and are the earliest responder cells to infection. While neutrophils are the most abundant cell type in circulation, its presence within the brain is severely restricted. Neutrophils become the predominant phagocytic cell at the site of infection during early stages of *M. tuberculosis* infection due to rapid recruitment (Eum *et al*., 2010) and possess various strategies to combat foreign bodies and invasive pathogens. Amongst these are the internalization of pathogens and subsequent presentation of specific pathogen peptide motifs via MHC molecules, the production of cytotoxic reactive species and net-like structures in a process called NETosis to capture extracellular pathogens (Ramos-Kichik *et al*., 2009). While the formation of neutrophil NETs is generally considered beneficial, their presence in the CNS may hinder bacterial clearance (Mohanty *et al*., 2019). Further, capture of pathogens via NETs may allow macrophages to phagocytose infected neutrophils which enhances pathogen killing (Monteith *et al*., 2021). Neutrophils provide macrophages with anti-microbial abilities when engulfed (Tan *et al*., 2006), indicating cooperative engagement by innate cells to limit bacterial replication. Neutrophils can produce chemokines and cytokines which drives the immune response (Riedel and Kaufmann, 1997, Kasahara *et al*., 1998). However, the recruitment of neutrophils to sites of infection, although necessary, may pose a major threat because of its potential to induce non-specific neuronal damage. Allen *et al.* found that neurons exposed to transmigrated neutrophils had reduced viability which resulted in increased neuronal death (Allen *et al*., 2012). Furthermore, neutrophils have been suggested to damage the BBB causing membrane leakage and reduction of the “immune privileged” nature of the CNS (Baral *et al*., 2019).

1.4.1.2 Macrophages

Macrophages are large mononuclear professional antigen presenting cells (APCs), derived from circulating monocytes. Phagocytosis of bacilli leads to the generation of reactive species directed at terminating bacteria (Chan *et al*., 1995, Flynn *et al*., 1998, MacMicking *et al*., 1997, Scanga *et al*., 2001, Slauch, 2011). Immune evasion mechanisms employed by mycobacteria includes the production of antioxidants, the inhibition of phagolysosome fusion and hindering MHC class II upregulation, consequently causing bacilli proliferation and reduced ability of macrophages to

stimulate T cells (Chen *et al*., 1998, Bryk *et al*., 2000, Armstrong and Hart, 1971, Hart *et al*., 1972, Tufariello *et al*., 2003). Macrophages/monocytes are known to enter the CNS under steady state for routine surveillance and are actively recruited during infection or inflammation. These cells assist with infection control and tissue healing (Russo and McGavern, 2015). Sentinel macrophage populations occupy the perivascular spaces in the CNS to provide rapid immune responses (Nayak *et al*., 2012). Macrophage recruitment to the infected or inflamed CNS is characterized by an increased chemokine and cytokine concentrations as well as the increased expression of integrins and adhesion molecules (Terry *et al*., 2012). Like microglia, the peripherally recruited macrophages have previously been grouped into two polarization states, namely the M1 proinflammatory state or the M2 anti-inflammatory state. The M1 state is neurotoxic but vital to mounting an immune response against bacterial pathogens (Yin *et al*., 2017). This naming convention although still common needs to be revised because Li *et. al.* showed that macrophages exist in a spectrum of activation states rather than two specific states as previously suggested (Li *et al*., 2019).

1.4.1.3 Dendritic Cells

Dendritic cells are professional APCs positioned at the interphase of innate and adaptive immunity. DCs are recruited to the CNS during inflammation and surveil the CNS during homeostasis (D'Agostino *et al*., 2012). Furthermore, DCs are robust producers of chemoattractant molecules in response to infection which contributes to the recruitment of myeloid cells and lymphocytes. In the CNS different classes of DCs occur either as conventional DCs (cDCs) or plasmacytoid DCs (pDCs) with both subtypes being derived from bone marrow progenitor cells. The major differences between the two classes are the ability to phagocytose pathogens. cDCs express high levels of MHC class II and are functionally superior at presenting antigen while pDCs are considerable producers of type 1 interferons (Quintana *et al*., 2015). Depletion of DCs during a model of pulmonary *M. tuberculosis* infection resulted in delayed $CD4^+$ cellular recruitment and activation leading to higher bacterial burdens (Tian *et al*., 2005).

1.4.2 Adaptive Immunity to Tuberculosis

The development of antigen specific immunity is essential to control chronic infections and reinfections (Mayer-Barber and Barber, 2015). Key effector cell types are B cells and T cells that respectively facilitate humoral and cell-mediated immunity. Under homeostatic conditions, it has been suggested that T cells enter the CNS for routine immune surveillance but are maintained at very low numbers (Engelhardt and Ransohoff, 2005, Smolders *et al*., 2013, Louveau *et al*., 2018). In response to infection or inflammation, T cells are recruited into the CNS and stimulated by the resident immune cells and recruited APCs. T cell stimulation and activation occur as a result of a combination of events; T cell receptor recognition of either MHC class I or MHC class II presentation of specific pathogen peptides, binding of co-stimulatory molecules and the appropriate milieu of chemokines and cytokines (Wlodarczyk *et al*., 2014, Wieczorek *et al*., 2017).

The adaptive immune response is characterized by the recruitment and infiltration of lymphocytes to the site of infection (Wolf *et al*., 2008). T cells can be separated into various subclasses, but the most predominant ones are $CD4^+$ and $CD8^+$ T cells, both of which are required for optimal protection against *M. tuberculosis* infection (Ellis *et al*., 2017, Lin and Flynn, 2015). Upon stimulation, T cells differentiate into different cell subsets which determine the functionality of the specific T cell. The T_H1 T cell subsets are characterised by TBet transcription factor and proinflammatory cytokine production (Zhu and Zhu, 2020).

Polyfunctional T_H1 polarized T cells are considered to be the most effective at controlling *M. tuberculosis* infection, with the most notable activated cells characterised by the combined production of IFN-γ, TNF and IL2 (Jasenosky *et al*., 2015, Seder *et al*., 2008). Deficiency in the production of these proinflammatory cytokines render the host susceptible to *M. tuberculosis* infection (Flynn *et al*., 1993, Francisco *et al*., 2015, Liu *et al*., 2020c). Defects in the IFN-γ gene resulted in uncontrolled dissemination of *M. tuberculosis* bacilli in a mouse model of pulmonary infection (Cooper *et al*., 1993). Allie *et. al.* showed in a murine model of pulmonary TB that T cell specific TNF was critical for survival and control of chronic tuberculosis (Allie *et al*., 2013). Furthermore, the same group showed that myeloid and T cell derived TNF was essential for protection against CNS-TB (Hsu *et al*., 2017). The

disruption of IL2 production results in T cell developmental and proliferation complications (Liao *et al*., 2013), which may result in susceptibility to *M. tuberculosis* infection. Here, it is important to note that functional T cells are required to migrate to the CNS and regulate *M. tuberculosis* replication.

1.5 Mouse models of CNS-TB

Mouse models have historically been important to study immune responses generated during *M. tuberculosis* infection. Although, these models have inherent clinical translational limitations namely the inability to recapitulate the natural mode of infection, they have provided a platform from which ethically challenging invasive research could be conducted. The development of transgenic mice was significant as this allowed developmental and physiological functionality of specific genes and proteins to be investigated. Models such as gene deficient (knockout) mice and knock-in mice advanced knowledge of gene expression profiling and protein production (Hall *et al*., 2009). Most of these strategies, including cell specific gene expression, have been used for the investigation of immune responses to *M. tuberculosis* and has driven therapeutic innovation (Cooper, 2014).

Some transgenic mouse studies were performed to show the importance of immunocompetency in response to CNS-TB (Hsu *et al*., 2017, Francisco *et al*., 2015). Other studies made use of recombination associated gene deficient mice to highlight the importance of lymphocytes during bacterial meningitis (Hoffmann *et al*., 2015, Ribes *et al*., 2017). A mouse model of pulmonary infection showed that depletion of $CD4^+$ T cells exacerbated disease outcome (Lin *et al*., 2012). Although, these studies successfully highlighted important contributions of adaptive immunity in CNS microbial infections, none were able to provide a platform to study human immune cells *in vivo*.

To study the response of a human immune system with less complications and limitations a combination of mouse models was developed. For specific human genes, human knock-in mice were generated. Here, the specific mouse gene would be replaced by the human equivalent sequence that would result in transcription of the human gene, producing human proteins (Crespo *et al*., 2021). To develop a fully functional human immune system within a mouse, requires a combination of various

genetic alterations which renders the mouse's immune system non-functional (Chen *et al*., 2023). Nonobese diabetic (NOD) mice are characterised by defects in macrophage cytokine production, antigen presentation, natural killer (NK) cell function and T lymphocyte repertoire regulation (Fan *et al*., 2004, Piganelli *et al*., 1998, Johansson *et al*., 2004, Ferreira *et al*., 2014). On this NOD background the DNA repair complex protein *Prkdc* was mutated, generating mice with severe combined immunodeficiency (SCID) causing complete deficiency of T and B lymphocytes (Bosma *et al*., 1983). Additionally, a mutation in the IL2 receptor common gamma chain which prevents the signaling of most cytokines, resulted in a highly immune compromised strain, the NOD-SCID-IL2Rgamma^{null} (NSG) strain. Which make them ideal for engraftment of human tissue and human cells (Xia *et al*., 2019).

There are 3 general methods of engrafting a human immune system onto severely immunodeficient mice; first, by injecting human peripheral blood leukocytes (PBL) into the SCID mice resulting in Hu-PBL-SCID mice. The second approach requires direct injection of human CD34^{+} hematopoietic stem cells intravenously or intrafemorally, resulting in the Hu-SRC-SCID mouse. Finally, the third method is more invasive and requires surgical transplantation of human foetal liver and thymus tissue and injection of human foetal stem cells. This method generates a mouse referred to as blood-liver-thymus (BLT)-NSG mice (Walsh *et al*., 2017). Previously, this model has been used to study HIV-1 pathogenesis, spinal cord and brain injury responses (Evering and Tsuji, 2018, Carpenter *et al*., 2015, Diaz *et al*., 2020). A study of pulmonary TB in BLT-NSG mice demonstrated that the engraftment of human cells was able to reconstitute successfully but more importantly generate an adequate immune response to control the pathogen by granuloma formation (Calderon *et al*., 2013). This result provides an excellent avenue for alternative human TB studies where BLT-NSG mice could be used to assess the immune outcome during CNS-TB. According to the WHO report, there is an estimate of 10 million new cases annually; however, in most healthy individuals, adaptive immunity mediated by T cells controls the infection (Wolf et al., 2008). Like humans, the different genetic background of the mouse strains gives rise to the diversity of T_H1- and T_H2- responses that leads to the differences in the susceptibility to *M. tuberculosis* infection (Soldevilla et al., 2022). The current study made use of

C57BL/6 mice because these mice have been shown to be more resistant to *M. tuberculosis* infection as they preferentially develop T_H1 immune response (Turner et al., 2001) and NSG mice because they lack functional immune systems which significantly contributes to the accomplishment of the study aims and objectives.

Aims and Objectives

Neurons have widely been studied for their responses during neurodegenerative diseases and to viral infections but not much is known about their immune contributions during *M. tuberculosis* infection. Furthermore, the importance and contribution of systemic circulating cells is unclear during CNS-TB protection and finally, the relationship between neurons and leukocyte immune modulation is not well understood in response to *M. tuberculosis* infection. Therefore, this study proposes to elucidate on these critical points by investigating the tightly regulated neuro-immune network in CNS-TB.

Aim 1: To evaluate the immune modulatory properties of neurons in response to *M. tuberculosis* infection.

Objectives:

1) Assessing neuronal gene expression after *M. tuberculosis* infection.
2) Evaluating neuronal chemokine and cytokine production in response to *M. tuberculosis* infection.
3) Examining neuronal immune modulatory abilities post *M. tuberculosis* infection by assessing leukocyte activation after stimulation with neuronal conditioned media.

Aim 2: To characterise the resident and recruited cellular responses during CNS-TB.

Objectives:

1) Characterising cellular immune responses in the CNS after *M. tuberculosis* infection.
    a) Establish a successful effective intracerebral *M. tuberculosis* infection model.
    b) Investigate the immune function of microglia and neurons.
    c) Assess the responses of recruited innate immune cells.
    d) Study the response of recruited lymphocytes after acute intracerebral infection with *M. tuberculosis*.

2) Examining the role of peripheral immune cells during CNS-TB and the influence on neuronal immune responses.

Aim 3: Phenotypically characterise human immune cellular responses during CNS-TB infection using a humanised mouse model.

Objectives:

1) Analysing the recruitment of human leukocytes to the brain after *M. tuberculosis* infection.
   a) Assess the physical appearance of humanised mice and ability to control bacterial burden after intracerebral infection with *M. tuberculosis*.
   b) Describe the immune response of recruited human antigen presenting cells in the BLT-NSG mouse model.
   c) Investigate the immune responses of recruited human T cells after *M. tuberculosis* infection.

Chapter 2: Materials & Methods

2 Materials and Methods

2.1 Animal Ethics and Mouse Strains

All animal procedures were approved by the Animal Research Ethics Committee of the Health Sciences Faculty, University of Cape Town (Reference number: 018/016, 018/017). Adult C57BL/6 (Jackson Laboratories Strain #:000664) and NSG (Jackson Laboratories Strain #:005557) mice aged between 8 and 12 weeks were housed under specific pathogen free (SPF) conditions in individually ventilated cages. All animal procedures performed during this study were authorised by the Veterinary Council of South Africa (SAVC Reference Numbers: AR15/14182, AR14/13216, AR14/13213, AR15/1417). The cages were maintained, food and water were supplied by the staff at the Research Animal Facility of the University of Cape Town.

2.2 Generation of Humanised Mice (BLT-NSG)

Human foetal thymus and liver tissue from Advanced Bioscience Resources (Alameda, CA) was prepared into 1-2mm sections. $CD34^+$ stem cells were isolated from the remaining liver tissue by digestion and purification with a magnetic-activated cell sorter using anti-CD3 microbeads (Miltenyi Biotec, Auburn, CA) and stored at -80°C. Adult NSG mice were preconditioned with an intraperitoneal injection of 1.5g/kg treosulfan (medac GmbH, Hamburg, Germany) which is used for myeloablation three days before the surgical procedure (Sjoo *et al*., 2006, Gutti *et al*., 2014). All surgical procedures were performed under sterile conditions. The mice were anesthetized with an intraperitoneal injection of 100mg/kg ketamine (Bayer (Pty) Ltd, Germany) and 10mg/kg Xylazine (Intervet, Zurich-Switzerland) combination and was subcutaneously administered 100µg/kg of the pain killer Buprenorphine (Rickett Benckiser Healthcare, United Kingdom). To perform the transplant, the lower abdominal area was shaved, and an incision was made in the skin to expose the renal capsule. A 1-2mm section of human foetal thymus and liver tissue was implanted into the renal subcapsular space and was followed by the immediate closure of the incision using absorbable sutures for the muscle and sterile skin autoclips for the skin and was followed by intravenous administration of the $2x10^5$ $CD34^+$ human stem cells. The mice were housed in SPF film isolators and received acidified drinking water (pH 3.0) for two weeks. During the 12-week recovery, the mice were monitored twice a day and received Buprenorphine and

gentamicin antibiotic (8mg/kg) accordingly. The mice further received $2x10^5$ of autologous NSG bone marrow cells every 4 weeks to prevent the onset of graft-versus-host-disease. Figure 2-1 shows the presence of the human thymic organoid in the BLT-NSG mouse renal capsule, which is absent from the non-humanised NSG mouse kidney.

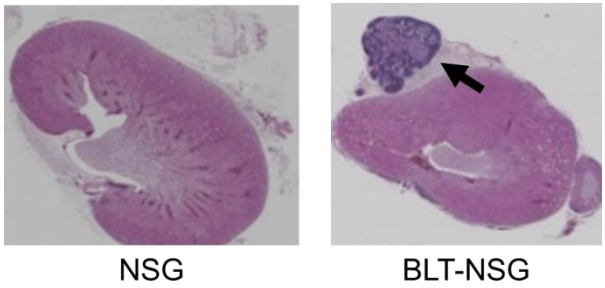

Figure 2-1: Confirmation of BLT-NSG engraftment.
The black arrow points to the clearly notable human thymus organoid under the renal capsule in the BLT-NSG mice which is not present on the non-humanised NSG mice kidney.

2.3 Mycobacterium tuberculosis Culture

M. tuberculosis strain H37Rv (Trudeau Mycobacterial Culture Collection, New York), was grown in Middlebrook 7H9 broth (Becton, Dickinson and Company, Le Pont de Claix, France) containing 0.5% Tween-80 and enriched with 10% oleic acid-albumin-dextrose-catalase (OADC) (Becton, Dickinson and Company, France). Cultures were incubated at 37°C until log phase, then aliquoted and stored at -80°C. To determine frozen stock concentration (cfu/ml), an aliquot was thawed and vortexed with glass beads to generate a homogenous solution. Next, 100µl of inoculum was plated in duplicate in 10-fold serial dilutions on Middlebrook 7H10 agar (Becton, Dickinson and Company, Le Pont de Claix, France) containing 10% OADC and 0.5% glycerol. Plates were incubated for 15-21 days at 37°C and the concentration of *M. tuberculosis* was determined by counting the colony forming units (CFUs). *M. tuberculosis* with green fluorescent expressing protein (H37Rv-GFP, provided by Joel Ernst, New York University School of Medicine, USA) was prepared similarly with 25µg/ml kanamycin.

2.4 Primary neuron culture

2.4.1 Coating plates with poly-l-lysine

Neuronal cell adhesion was improved by coating the wells with sterile 0.01% poly-l-lysine (Sigma, MO, USA) dissolved in dH_2O. The plate was incubated with 500ul of the poly-l-lysine solution per well in each 24-well plates at 4°C for 24 hours. Poly-l-lysine solution was then removed, and the plate was rinsed three times with sterile water.

2.4.2 Dissection of the hippocampus

To set up timed pregnant mice, adult mice were mated at a ratio of two female mice to one male mouse. Pregnant mice were monitored for 17 days and then euthanized with 5% Halothane (Safeline pharmaceuticals). E17 foetuses were harvested and euthanized by decapitation using sharp scissors. Brains were removed from the foetal heads and dissected in Hank's balanced salt solution (HBSS) (Lonza, MD, USA) under the microscope (Figure 2-2). Hippocampus was chosen for primary neuron cultures and meninges-free hippocampi were collected in 15ml tube containing 5ml of HBSS on ice.

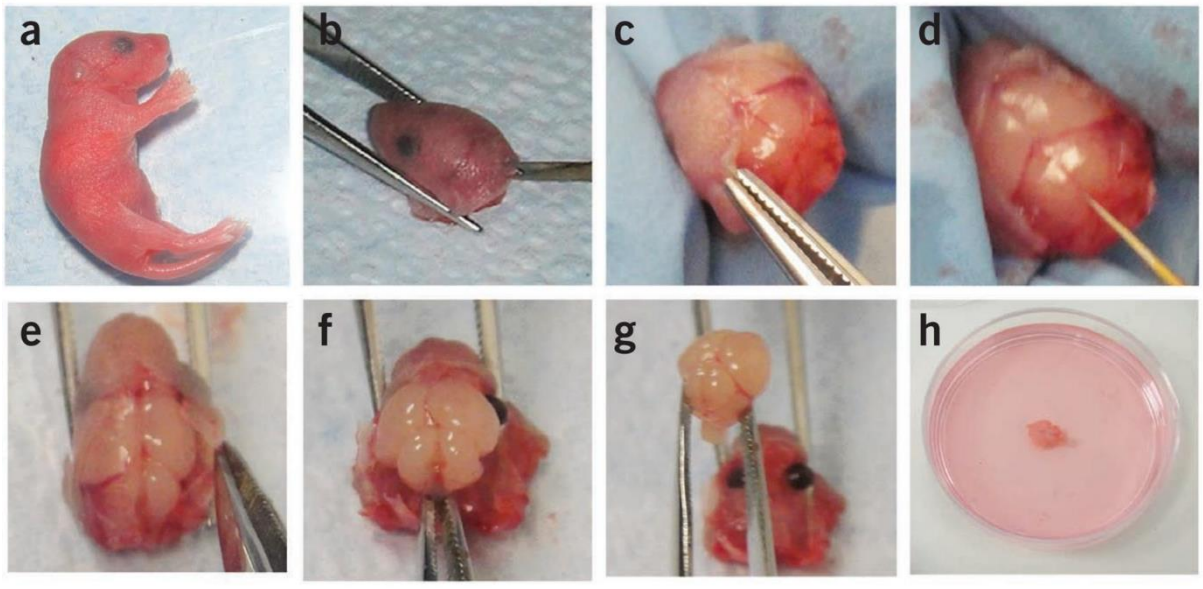

Figure 2-2: Procedure for harvesting foetal brains.
E17 foetuses (a) were euthanized by decapitation and an incision was made in the skin by the midline (b). The skull was completely exposed by removing the skin along the incision (c). An incision was then made in the skull (d) and removed in two halves (e). The brain was gently separated from the underlying tissue (f), completely removed (g) and quickly placed into the dissection medium (h) (Beaudoin *et al*., 2012).

2.4.3 Cell dissociation and seeding

The tissue was allowed to settle before the HBSS was removed and 1ml of seeding neurobasal medium (2% B27 supplement [Gibco, NY, USA], 1% L glutamine [Gibco, NY, USA] in neurobasal medium [Gibco]) was added. Tissues were dissociated by trituration using P1000 pipette. After cell dissociation cell concentration was determined by counting with a haemocytometer. Cells were seeded at $5x10^5$ cells per well in poly-l-lysine precoated 24-well plates and cultured for 7 days before infection.

2.5 Infection of Primary Neurons with *M. tuberculosis*

M. tuberculosis H37Rv stocks were thawed at RT, centrifuged at 10000rpm at 4°C for 10 minutes to remove glycerol. The pellet was resuspended in seeding neurobasal medium. To reduce clumping, the inoculum was vortexed for 1 minute with glass beads to generate a homogenous solution. Primary neurons were infected at a multiplicity of infection (MOI) of 30:1 and incubated at 37°C and 5% CO_2 for 24 and 48 hours. The infected neurons were then processed for microarray analysis, and the culture supernatant were collected for Luminex analysis or used as conditioned media (CM) for antigen presenting cell stimulation *in vitro*.

2.6 Intracerebral Infection

For intracerebral infection, the inoculum was prepared in sterile saline solution; briefly, H37Rv stocks were thawed, centrifuged at 10000rpm and then resuspended in saline. The mice were anesthetized with an intraperitoneal injection of 100mg/kg ketamine and 10mg/kg Xylazine mixture and a subcutaneous injection of 100µg/kg Buprenorphine. Eye lubrication was applied to prevent drying, and the heads of the mice were shaved before being placed onto the stereotactic device in preparation for the intracerebral infection procedure. The surgical area was sterilised with F10 skin-prep before an incision between the ears was made which exposed the skull. A burr hole was drilled (Dremel 300i, Wisconsin, USA) into the skull approximately 2mm to the left of the midline and anterior to the bregma which exposed the dura mater. Using a Hamilton syringe (Gastight no. 1701, Hamilton, Bonaduz, Switzerland), 3µl of saline solution or *M. tuberculosis* inoculum ($1x10^5$ CFUs) was injected into the cortex. Directly after withdrawal of the syringe, the burr hole was closed with sterile

bone wax (Ethicon LLC, China) and the skin was sutured with monofilament suture material (5/0 Nylon, 3/8 circle reverse cutting, 13mm needle) (Ethicon LLC, China). The effects of anaesthetic were reversed using 1mg/kg antisedan while monitoring the mice under a warm lamp until post-surgery recovery, before being returned to the cages After 24 hours of infection, brains were collected from 5 mice, homogenized and plated on Middlebrook 7H10 agar for CFU to confirm the infection dose.

For post-surgery management, the mice received Buprenorphine every 12 hours for the first 72 hours and were monitored twice a day for the duration of the experiment. Mice were humanely euthanised at set time points or after a 20% loss in weight with 5% halothane inhalation (2-bromo-2-chloro-1,1,1-trifluoro-ethane) (Safeline Pharmaceuticals Pty Ltd, South Africa) and confirmed by cervical dislocation. Mouse organs were harvested at various time points (7- and 14-days post infection for C57BL/6 mice (5 mice per timepoint and per condition), and 16- and 17-days post infection for NSG (5 mice per condition) and BLT-NSG mice (5 infected mice and 3 saline inoculated mice)) and prepared for their respective analysis.

2.7 Antigen Presenting Cell Isolation, Culture & Stimulation

2.7.1 Antigen Presenting Cell Isolation & Culture

Adult C57BL/6 mice were euthanized by halothane inhalation and blood was collected from mice by cardiac puncture and placed into heparin contained tubes. The blood was pooled in 50ml tubes and red blood cells were lysed. Lysis was stopped by adding PBS and then filtered through a 40µm filter. The sample was centrifuged at 1200rpm for 10 minutes before discarding the supernatant. The pellet containing leukocytes were resuspended and counted to identify the concentration. The leukocytes were subsequently seeded at $2x10^5$ per well in 96-well plate for stimulation.

2.7.2 Antigen Presenting Cell Stimulation

After 24 hours of *in vitro* infection in neuronal cultures, the neuronal CM was collected by filtering the culture supernatant twice through a 0.22µm filter. Thereafter, the CM was added to the wells containing the leukocytes and cultured for a further 24 hours. The 96 well plate was centrifuged at 1500rpm for 10 minutes and the

supernatant was removed. The cells were washed and transferred to v-bottom plate for flow cytometry processing.

2.8 Flow Cytometry Analysis

For *in vivo* mouse samples, single cell suspensions were generated by mechanical dissociation through a 70µm nylon cell strainer (Beckton and Dickinson) and gentle trituration of the mouse brains and 50ul of brain cells was transferred to v-bottom plates. For *in vitro* samples, the cells were transferred from their culture plates to v-bottom plates for the staining process. The v-bottom plates containing the cells were centrifuged at 1500rpm for 10 minutes and supernatants were discarded. The samples were incubated for 15 minutes with 25µl of viability dye (1:2000 dilution, BD Biosciences). Cells were washed twice by adding 100µl of FACS buffer and centrifuging at 1500rpm for 10 minutes. The cells were incubated with 25µl of the respective surface markers (Table 2.1) for 30 minutes at room temperature and washed twice. After surface staining, samples were fixed and permeabilised (BD Cytofix/Cytoperm Plus Fixation/Permeabilization Solution Kit) over night at 4°C. After fixation and permeabilization, cells were centrifuged at 1500rpm for 10 minutes and supernatant discarded. Following a wash step using Perm/Wash (BD Cytofix/Cytoperm Plus Fixation/Permeabilization Solution Kit), the cells were incubated with the respective intracellular antibody (Table 2.1) mixtures for 45 minutes. After Perm/Wash, the cells were fixed and transferred to 5ml Falcon tubes (Gilson) and analysed on BD LSRII or BD Fortessa (Beckton Dickinson) flow cytometer using FACS Diva version 6.0 (Beckton Dickinson).

Table 2-1: Antibody panel mixes.

Antigen	Fluorophore	Clone	Dilution	Manufacturer
Mouse neurons panel				
βtub	Alexa Fluor 647	EP1569Y	1:50	Abcam
MHC class I (H-2kd/H-2Dd)	PE	34-1-25	1:100	Invitrogen

TNF	PerCP-Cy5.5	MP6-XT22	1:50	BD Biosciences
IL1β	PE- Cy7	NJTEN3	1:50	eBioscience
IL6	V450	MP5-20F3	1:50	BD Biosciences
IL10	BV711	JES5-16E3	1:50	BD Biosciences
Mouse APC panel				
CD45	Alexa Fluor 700	RA3-6B2	1:100	BD Biosciences
CD11b	V450	M1/70	1:100	BD Biosciences
CD11c	PerCP-Cy5.5	HL3	1:100	BD Biosciences
Ly6G	APC	1A8	1:100	BD Biosciences
MHC class II (1A/I-E)	BV711	M5/114.15.2	1:100	BD Biosciences
IL1β	PE- Cy7	NJTEN3	1:50	eBioscience
INOS	FITC	6/iNOS/NOS Type II	1:50	BD Biosciences
IL12 (p40/p70)	PE	C15.6	1:50	BD Biosciences
Mouse lymphocyte panel				
CD3	BV421	145-2C11	1:100	BD Biosciences
CD4	Alexa Fluor 700	RM4-5	1:100	BD Biosciences
CD8	APC-Cy7	53-6.7	1:100	BD Biosciences

CD44	BV786	IM7 (RVO)	1:100	BD Biosciences
TBet	PE	O4-46	1:50	BD Biosciences
RORyT	PerCP-Cy5.5	Q31-378	1:50	BD Biosciences
GATA3	PE-Cy7	L50-823	1:50	BD Biosciences
FoxP3	Alexa Fluor 647	MF23 (RVO)	1:50	BD Biosciences
BLT-NSG panel				
hCD45	PerCP-Cy5.5	HI30	1:100	Biolegend
mCD45	BV510	30-F11	1:100	BD Biosciences
CD45RA	PE-CF594	HI100	1:100	BD Biosciences
CD45RO	Alexa Fluor 700	UCHL1	1:100	BD Biosciences
HLA-DR (L243)	PE	Cat. 347401	1:100	BD Biosciences

2.9 RNA Extraction and Microarray-based transcriptomic analysis

Following 24 hours of infection, the neurons were lysed in 1ml TRIzol (Ambion) and stored at -80°C. For RNA extraction, samples were thawed and left to stand for 5 minutes at room temperature before adding 200ul of chloroform. Samples were vigorously shaken and allowed to rest for 5 minutes at room temperature. After resting, the samples were centrifuged for 15 minutes at 14000rpm followed by the transferal of the aqueous phase to new eppendorf tubes. 500ul isopropanol, 120ul 5M ammonium acetate and 10ul glycogen was added to the aqueous phase before vortexing and resting for 30 minutes. The samples were then centrifuged (14000rpm) for 15 minutes, and the supernatant was discarded. Cold 70% ethanol (750ul) was added to each sample and vortexed. Samples were centrifuged at 14000rpm for 10

minutes, and the supernatant discarded before leaving the samples to air dry for 15 minutes. Next, the RNA pellets were dissolved in water by triturating with the pipette and allowing to rest on ice for 15 minutes. Quality control and quantification of isolated RNA was performed with an Agilent 2100 Bioanalyzer (Agilent Technologies) and a NanoDrop 1000 UV-Vis spectrophotometer (Thermo Fisher Scientific).

Samples were shipped to Max Planck Institute for Infection Biology, Berlin, Germany to perform the microarray analysis as single-color hybridizations using total RNA labeled with the Low Input Quick Amp Labeling kit (Agilent Techonologies). In brief, mRNA was reverse transcribed and amplified using an oligo-dT-T7 promoter primer and labeled with cyanine 3-CTP by T7 *in vitro* transcription. After precipitation, purification, and quantification, 0.75µg labeled cRNA was fragmented and hybridized to whole genome mouse 8 × 60K multipack microarrays according to the supplier's protocol (Agilent Technologies). After SSPE Wash (Agilent Technologies) scanning of microarrays was performed with 3-µm resolution and 20-bit image depth using a G2565CA high-resolution laser microarray scanner (Agilent Technologies). Microarray image data were processed with the Image Analysis/Feature Extraction software G2567AA v.A.11.5.1.1 (Agilent Technologies) using the protocol GE1_1105_Oct12 and recommended settings.

All microarray data analysis was conducted in R Briefly, microarrays were background corrected, normalized, and controlled for quality using the R package limma (Smyth, 2004, Ritchie *et al*., 2015). For background correction the method 'normexp' was used on the gProcessedSignal and the gProcessedBackground data. Between-array normalization was done using the 'quantile' method in limma. The gene expression values were averaged for each probe over all replicates of that probe on the microarray, using the 'avereps' function. Differences in gene expression were assessed using the linear model 'lmFit' and 'makeContrasts' in limma. Genes with corrected p-values of <0.05 were considered significant after Benjamini-Hochberg correction for multiple testing.

2.10 Luminex

After 48 hours of *in vitro* infection, the plates were centrifuged for 10 minutes at 1500rpm and the culture supernatants were collected and filtered twice through a 0.22µm filter and stored at -80°C before transporting them to the University of Stellenbosch for Luminex analysis. The Milliplex Mouse Cytokine Chemokine Panel I kit with 12 analytes was purchased from Merck (Pty) Ltd. For Luminex analysis, the supernatant samples from different experiments were pooled and added to the wells of the Milliplex plate. The Luminex experiments were performed using the Bioplex 200 system (Bio-Rad) and the Bio-Plex Manager 6.1 software (Bio-Rad). Data points that were OOR were reported as not detected.

2.11 Statistical analysis

The data are presented as the mean ± standard deviation (SD). Statistical analysis was completed using GraphPad Prism software. All Luminex data was statistically tested with the Mann-Whitney U test. Flow cytometry and gene expression box and whisker plots were analysed by two-sample Student t-tests for comparing two samples with 95% confidence. For all tests, a p-value of ≤ 0.05 was considered significant. Analysis of variance (ANOVA) was used to determine statistical significance for organ to body weight comparison between the different study groups analysis. For differential gene expression analyses R packages limma and tmod were utilized. All analyses were corrected for quality and batch influences to adjust for any variations. Principal component analysis (PCA) and Signaling Pathway Impact Analysis (SPIA) were applied to visualise the high throughput data obtained from the microarray.

Chapter 3: Neurons modulate immune responses.

3 Neurons modulate immune responses.

3.1 Analysis of differential expression.

Cerebral immunity is defined by a combination of structural and cellular responses. The BBB forms the first line of defence and provides the “immune privileged” phenomenon by tightly regulating the biological substances which enter and exit the brain via the vasculature. Cellular immunity of CNS constituted the combined responses elicited by both the resident brain cells as well as recruited leukocytes. The main immune cell type in the brain are resident microglia however other cells may also participate in CNS immune responses (Rock *et al*., 2005, Randall *et al*., 2014). Neurons contribute to CNS immunity by interacting with immune cells in response to different pathogens (Shrestha *et al*., 2003, Herrera-Rincon *et al*., 2020). However, there is limited knowledge on how neurons respond to mycobacterial infection. Hence, this study set out to elucidate the immune regulatory ability of neurons in response to *M. tuberculosis*.

Li *et al.* shared a transcriptional approach to identifying genetic differences between neuronal responses to hypoxic insult model (Li *et al*., 2013) while a gene expression study of neurodevelopmental disorder identified 13 genes that was common to other diseases such as cancer, amyotrophic lateral sclerosis and TB (Yadav and Srivastava, 2018). Using a gene expression approach to study disease development, progression and outcome provides a comprehensive interpretation of molecular changes which occur in response to infection or inflammation. Hence, in this study transcriptional analysis was employed to investigate the functional changes which occur within neurons in response to *M. tuberculosis* infection. Microarray analysis provides a response spectrum of differentially expressed genes (DEGs) which allows for interrogation of the biological functions of neurons during mycobacterial challenge. Therefore, the first objective of the current study was to perform genome wide analysis of neurons and compare the transcriptional activity between *M. tuberculosis* infected and non-infected neurons to identify neuron specific responses to infection.

Randall *et al.* demonstrated that internalisation of *M. tuberculosis* was very similar at 24 hours post infection compared to 48 hours post infection (Randall *et al*., 2014) and Cappelli and colleagues showed that gene expression of important

proinflammatory cytokines waned over time but was present at 24 hours post *M. tuberculosis* infection of human macrophages (Cappelli *et al*., 2001). In the current study primary neuronal cultures were seeded at $5x10^5$ cells per well and infected with *M. tuberculosis* H37Rv for 24 hours at a MOI of 30:1, which was subsequently followed by RNA extraction and microarray analysis. To visualise the high throughput data generated, PCA was applied to demonstrate variation in gene expression between infected and uninfected neurons. The results showed clear cluster separations in gene expression between infected and non-infected neurons (Figure 3.1 a), indicating *M. tuberculosis* infection induced specific transcriptional changes in neurons. Additional visualisation of differential expression using a volcano plot displayed multiple genes that were significantly differentially expressed. Thresholds of 0.05 and 1 were applied for the false discovery rate and $\log_2$ fold change respectively. The positive values on the x-axis is indicative of upregulation and the negative values represent downregulation. Furthermore, the horizontal cut-off displayed statistical significance less than 0.05 and the expression of all genes displayed above the line was significantly altered (Figure 3.1 b). From the volcano plot genes such as *CXCL10*, *CCL2, CCL7, CXCL5* and *CXCL2,* which are involved in chemotaxis, were shown to be upregulated. *RELB* a component of NF-κβ was upregulated which suggests priming neurons towards an inflammatory response. Interestingly, there was a reduction in expression of specific genes such as *CX3CR1* and *STAB1* which were previously reported as important for inflammation and protection against bacterial infections (Fong et al., 1998, Pombinho et al., 2021).

A heatmap was generated from the genes that were significantly differentially expressed with a $\log_2$ fold change of greater than 1 (Figure 3.1 c). The heatmap supported the outcome of the PCA plot and showed clear expression profile differences between the non-infected neurons and *M. tuberculosis* infected neurons. The results convincingly demonstrate that *M. tuberculosis* infection induces transcriptional changes within neurons.

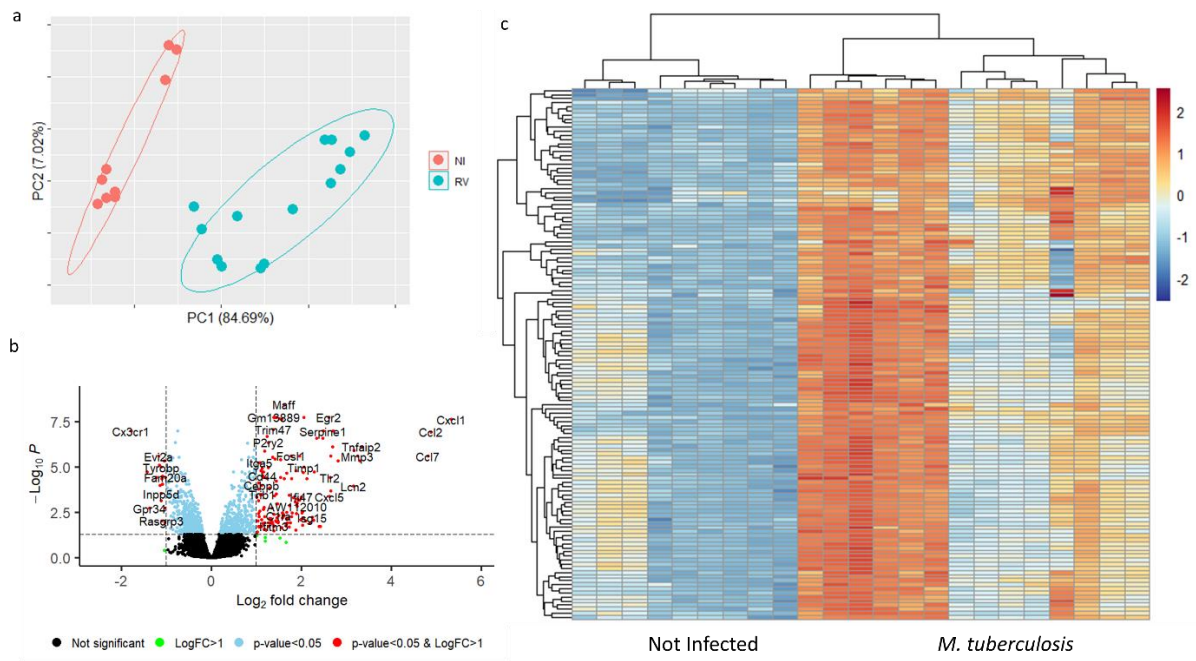

Figure 3-1: *M. tuberculosis* induces differential gene expression in neurons.
Gene expression data from microarray analysis was assessed by performing data reduction and represented in (a) a PCA plot showing separate clusters between the infected and non-infected cultures. The differential expression of genes was shown on (b) a volcano plot with the cut-offs expressing Log_2 fold changes and significance. Black points indicate non-significant genes, green points are non-significant genes that have a log_2 fold >1, blue points are genes with $p<0.05$ and log_2 fold changes <1 and red points show genes with $p<0.05$ and log_2 fold change >1. (c) The significantly differentially expressed genes from the volcano plot was represented in a heatmap that shows gene expression differences between the not infected and infected samples.

Next, the data was analysed using the SPIA method to identify the biological pathways that were affected during *M. tuberculosis* infection (Tarca *et al*., 2009). The SPIA method generates significantly perturbed pathways by combining the statistical significance of the differentially expressed genes, the pathways of those genes and the topology of the specific pathways (Tarca *et al*., 2009). There were 49 pathways considered to be significantly perturbed with a false discovery rate of less than 0.05, of which 33 were activated and 16 were inhibited (Appendix Table A-1). Three major pathway clusters were identified, with the smallest cluster being non-communicable diseases followed by the communicable diseases cluster and the biological processes cluster (Figure 3.2 a). The variation and spread of the significantly perturbed pathways suggest overlapping gene expression profiles within these pathways produced by neurons in response to *M. tuberculosis*.

The pathways within each cluster were listed according to their respective perturbations scores, which was signified by their t_A value that represents the total

net accumulated perturbation within each pathway. The Non-communicable Diseases cluster comprises of 10 pathways of which 8 were inhibited and only 2 activated. Rheumatoid arthritis and prions disease were the only activated pathways. Rheumatoid arthritis is characterised by an inflammatory response and prions disease is known to be associated with neuronal loss, which suggests a proinflammatory driven response by CNS cells. The biological processes cluster consisted of 21 significantly perturbed pathways and here 13 were activated and 8 were inhibited. The top five pathways with positive perturbation scores were “Chemokine signaling”, “Cytokine-cytokine receptor interactions”, “Apoptosis”, “Toll-like receptor signaling” and “NF-kappa B signaling”. This supported an inflammatory response induced by neurons and additionally proposed that the response was geared towards microbial infection. Within the communicable diseases cluster 17 pathways were activated while two were inhibited, which further supported a neuronal immune response to infection. This cluster was subdivided and showed diversity in the pathways that were activated. Viral, parasitic, and bacterial response pathways were perturbed but surprisingly the bacterial pathways were the fewest (Figure 3.2 b). This data suggested that different pathogens and diseases may promote common biological responses which has previously been shown by Zhou and colleagues (Zhou *et al*., 2023).

Visualization of the enriched pathways activated by *M. tuberculosis* infection in neurons was performed by mapping the current transcriptomic data to reference pathways on the Kyoto Encyclopaedia of Genes and Genomes (KEGG) database (Kanehisa, 2019, Kanehisa *et al*., 2021, Kanehisa and Goto, 2000). The KEGG database was used because it was able to visually represent communicable disease pathways unlike databases such as MetaCyc and BRENDA that mainly consist of metabolic and enzymatic pathways. The limitation of this analysis is that there is limited knowledge of neuronal responses to *M. tuberculosis* and thus reference pathways were curated using literature from peripheral professional immune cells. However, for the purpose of modelling and possibly providing a novel perspective on the molecular interactions involved in neuronal immune responses to *M. tuberculosis*, this type of analysis is not only important but necessary.

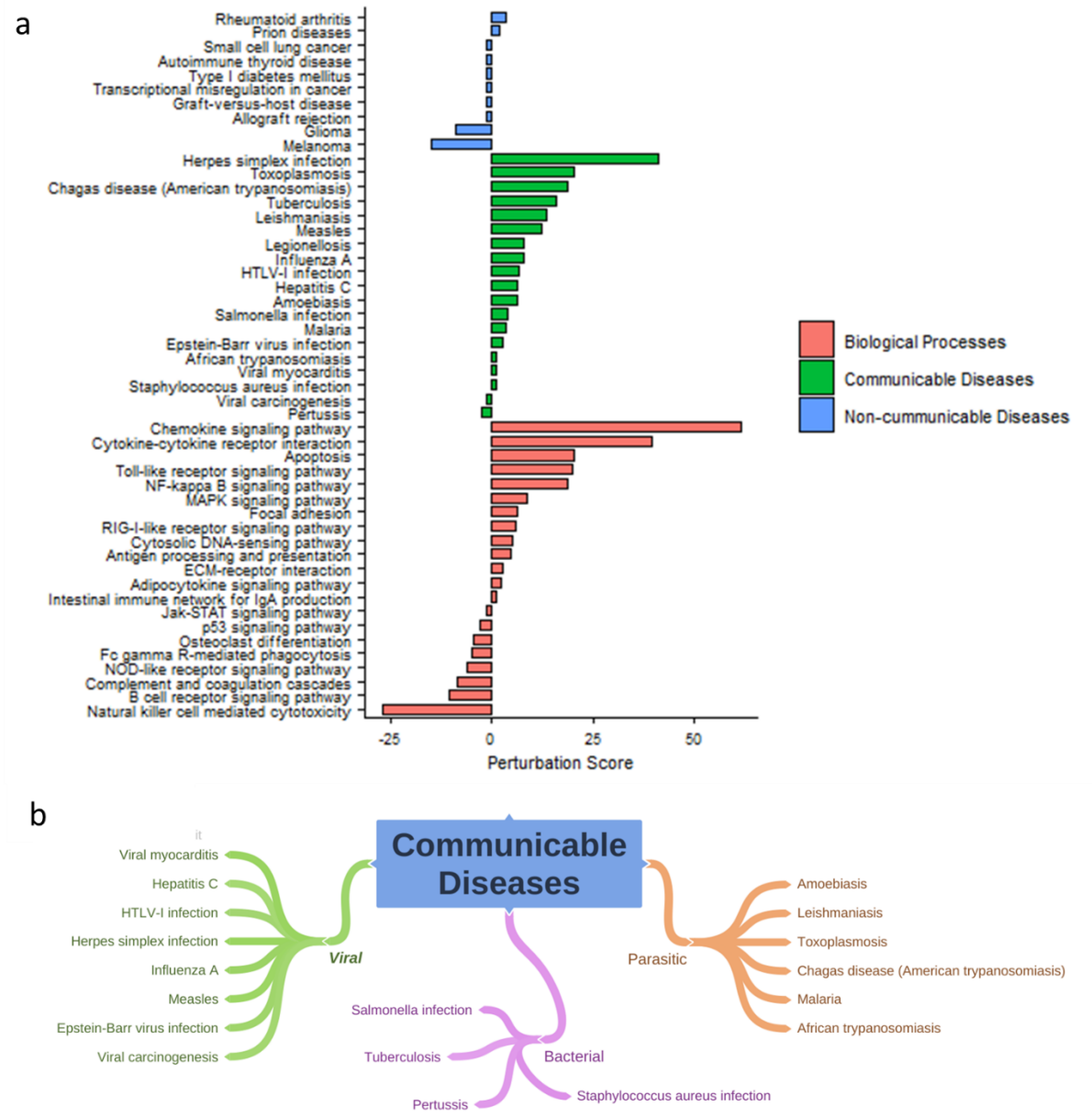

Figure 3-2: Biological pathway perturbations in neurons post *M. tuberculosis* infection.
The transcriptional data was analysed by the SPIA to identify biological pathways that were perturbed in neurons during *M. tuberculosis* infection. (a) The perturbations scores of t_A was used and identified three major groups. (b) The communicable diseases group was further studied and shows three subgroups of pathogenic pathways which were significantly altered.

Therefore, further analysis of the “Tuberculosis” enriched KEGG pathway was performed (Figure 3.3 a). The “Tuberculosis” pathway is a pre-set pathway which displays molecular interactions and relations from cell surface signals through the cytoplasm and finally into the nucleus of the cell in response to *M. tuberculosis* infection. This pathway is shown to comprise of various molecular interactions which in some cases may be a combination of several biological processes as indicated by

the white rectangular shaped boxes. “Apoptosis”, “Jak-STAT signaling pathway”, “Antigen processing and presentation”, “NOD-like receptor signaling pathway”, “Toll-like receptor signaling pathway” and “MAPK signaling pathway” are shown to contribute to the metabolic make-up of the “Tuberculosis” pathway. Analysis of the Tuberculosis pathway displayed 26 DEGs (red highlighted boxes) which are mostly associated with key *M. tuberculosis* response elements such as TLRs, MyD88, nuclear factor kappa beta (NF-κβ), type I interferon and pro-inflammatory cytokine production. Hence, the related individual pathways from the SPIA analysis were further explored with the objective of obtaining a more detailed assessment of the downstream molecular responses. “Toll-like receptor signaling pathway”, “NF-kappa B signaling pathway”, and “Cytokine-cytokine receptor interaction” consisted of 13, 23 and 43 unique DEGs respectively and only share one common gene. Four genes were shared between “Toll-like receptor signaling pathway” and “NF-kappa B signaling pathway” but only one gene between “Cytokine-cytokine receptor interaction” and the aforementioned pathways (Figure 3.3 b).

3.1.1 Toll-like receptor signaling pathway.

Toll-like receptors are pattern recognition receptors which are crucial for innate immune recognition of pathogens (Vidya *et al*., 2018). They are present throughout various stages of brain development and are prominently expressed on neurons from various regions of the brain (Kaul *et al*., 2012). Furthermore, Hoffmann and colleagues showed that TLR2 was involved in neurodegeneration in response to synthetic bacterial lipopeptide stimulation (Hoffmann *et al*., 2007). A study by Drennan *et al.* showed that TLR2 deficient mice succumb to chronic *M. tuberculosis* infection (Drennan *et al*., 2004), suggesting the importance of TLR2 in response to *M. tuberculosis* infection TLR (Gopalakrishnan and Salgame, 2016). Therefore collectively, there is precedent for TLR expression on neurons and, more broadly, for its importance against bacterial infection.

In the current study, Appendix Figure A-1 shows 18 DEGs in the TLR signaling pathway. Differential expression of genes in neurons following *M. tuberculosis* infection encoding both TLR2 and TLR6 were observed together with the gene that encodes for the extracellular adaptor protein CD14, which is important for binding gram-negative bacteria and has previously been shown to play a role in *M.*

tuberculosis immunity (Wieland *et al*., 2008). Viral recognition associated receptors TLRs 3 and 7/8 were found to be differentially expressed in neurons in response to *M. tuberculosis* infection. Internalised *M. tuberculosis* display an immune evasive nature and differential expression of these intracellular PRRs suggest a constant battle between the host and the pathogen. TLR3 has previously been identified as an IL10 production regulator in response to mycobacterial RNA and polymorphisms in TLR7/8 were shown to increase susceptibility to *M. tuberculosis* infection (Bai *et al*., 2014, Lai *et al*., 2016).

Toll like receptor signaling is conveyed via the adaptor protein MyD88 and is pivotal for the control of *M. tuberculosis.* MyD88 are expressed by different cell types including neurons (Fremond *et al*., 2004, Liu *et al*., 2017). The differential expression of MyD88 was observed in response to *M. tuberculosis* as shown in Appendix Figure A-1. Furthermore, genes that encode for downstream proteins such as Iκβα, Tpl2, AP-1 and IRF7 were similarly differentially expressed. Additionally, differential expression of *STAT1* and the gene coding for costimulatory molecule *CD40* together with several chemokines and cytokines genes namely *TNFα*, *IL6*, *RANTES*, *IFNβ*, *IP-10* and *MIG* were all differentially expressed. The results suggest innate immune recognition of PAMPs by neurons which result in molecular signaling involved in proinflammatory responses and cellular recruitment.

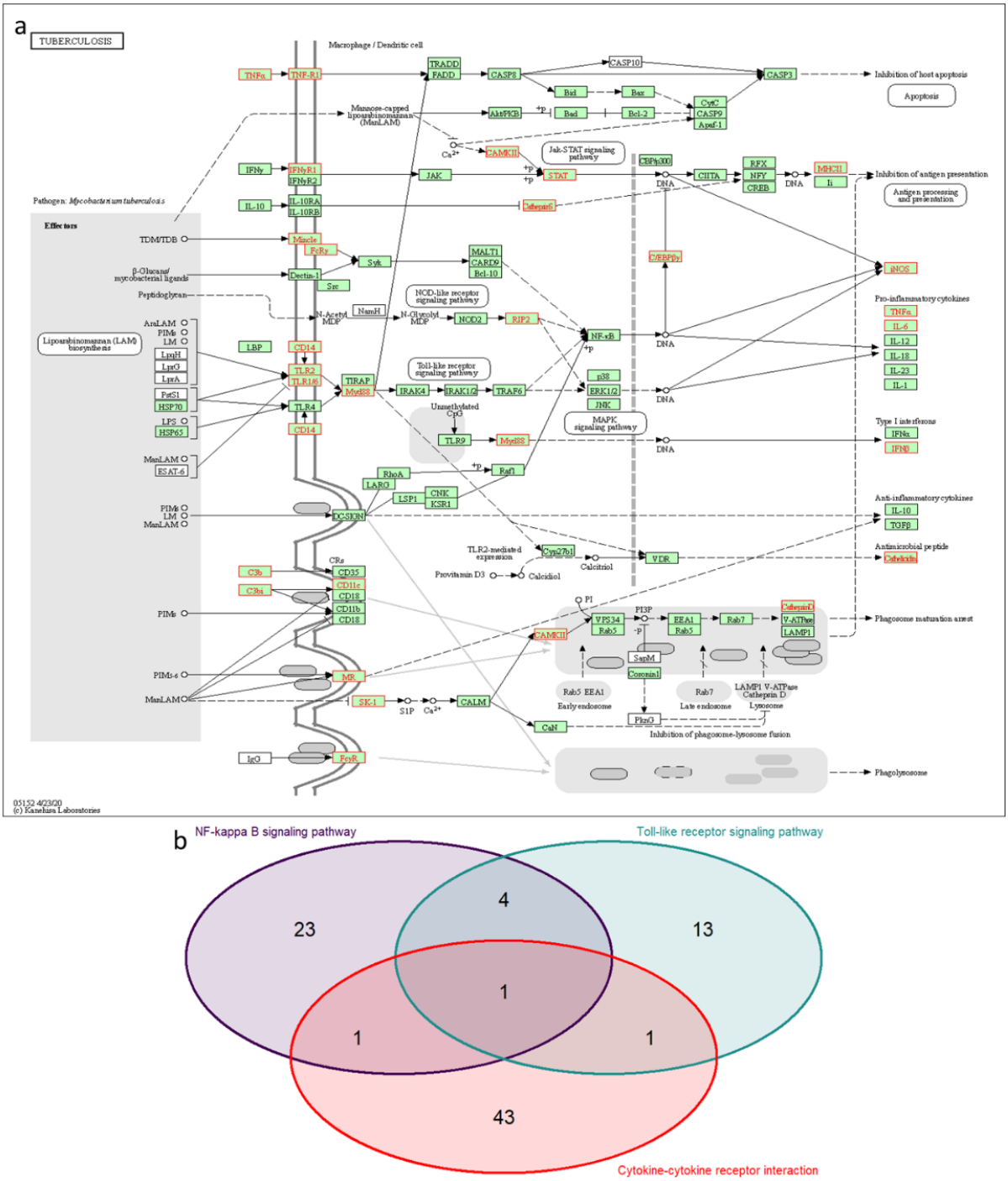

Figure 3-3: KEGG Tuberculosis pathway.
(a) The pre-set KEGG Tuberculosis pathway was produced by using the results from the SPIA method. This pathway displays the potential molecular interactions which occur within cells after *M. tuberculosis* infection. Which is achieved by combining different molecular pathways which are affected during Tuberculosis infection. Red highlighted boxes indicate differentially expressed genes and green boxes show unaltered genes. White filled rectangular shapes represent separate biological pathways which form part of the "Tuberculosis" pathway and arrows show direction of molecular signaling. (b) The Venn diagram displays the commonalities and differences in DEGs between some of the molecular pathways that are involved during neuronal *M. tuberculosis* infection.

3.1.2 NF-κβ signaling pathway.

The transcription factor NF-κβ is important for production of proinflammatory chemokines and cytokines and plays an important role in controlling the bacterial burden during *M. tuberculosis* infection (Xia *et al*., 2021). In the present study, the "NF-kappa B signaling pathway" (Appendix Figure A-2) illustrated 29 DEGs. Differential expression of genes encoding for two receptors TNFR1 and IL1R, an extracellular adaptor protein CD14 and the costimulatory molecule CD40 were observed. Intracellularly, the genes of "B-cell receptor signaling pathway" associated adaptor molecules BLNK, Btk and PLCy2 which have downstream molecular signaling through NF-κβ were significantly differentially expressed. Furthermore, significant gene alterations of MyD88, TRAF2/5, RIG-I, TRIM25, TRAF2/6 and TRAF2 were observed. Downstream from these molecules, it was shown that the NF-κβ associated molecules Iκβα, p100, RELB and p52 genes were significantly differentially expressed. Here the data suggests multiple mycobacterial recognition receptor pathways which lead to a common molecular outcome.

Phosphorylation of Iκβα and p100 releases NF-κβ transcription factor molecules which translocate into the nucleus and bind target genes resulting in transcription of several genes (Oeckinghaus and Ghosh, 2009). In Appendix Figure A-2 it is suggested that neurons differentially express gadd45β, TRAF1/2 and A/Bfl-1 which promote neuronal survival. Furthermore, positive feedback and inflammation associated genes *p100*, *TNFα*, *COX2*, *MIP-2* and *VCAM-1* as well as the negative feedback gene *A20* is shown to be significantly altered. Finally, lymphoid tissue homing gene *ELC*, lymphocyte adhesion and T cell costimulatory genes *ICAM* and *SDF-1α*, a molecule involved in myelopoiesis and B cell lymphopoiesis, are also shown to be changed. Here the data reveals that *M. tuberculosis* infection of neurons resulted in differential gene expression of genes associated with cell signaling, inflammation and cell adhesion.

3.1.3 Chemokine signaling pathway.

In previous sections, KEGG pathway analysis of the differentially expressed genes between *M. tuberculosis* infected and non-infected neurons revealed a significant number of chemokines and cytokines were involved in various signalling pathways. As shown in Appendix Figure A-3, "chemokine signalling pathway" was identified by

KEGG analysis and significantly enriched, where 49 chemokine, cytokine and receptor genes were differentially expressed. These included genes from the CC- and CXC-subfamilies of chemokines, TNF family, TGF-β family, class I and II helical cytokines, IL1-like cytokines and two unclassified cytokine members (*CSF1* and *CSFR*).

Chemokines are divided into four subgroups where the CC and CXC subfamilies are known to be responsible for the recruitment of neutrophils and monocytes respectively and collectively attract lymphocytes (Spandau *et al*., 2002). The CC subfamily had six DEGs namely *CCL2, CCL5, CCL6, CCL7, CCL12* and *CCL19*. The CXC subfamily showed differential expression for *CXCL1, CXCL2, CXCL3, CXCL4, CXCL4L1, CXCL5, CXCL6, CXCL9, CXCL10, CXCL12* and *CXCR7*. The third representative of the chemokine subgroups is the CX3C subfamily. Significant changes of *CX3CL1* and *CX3CR1* were observed, which contribute to leukocyte recruitment through mediating leukocyte migration (Fong *et al*., 1998).

The helical cytokine genes that were differentially expressed are *TSLP, IL6, IL11, IL19, CLCF1* and *LIF.* The receptor genes from this group were *CSF2R, EPOR* and *OSMR*. The interferon subfamily showed differential gene expression of *IFNB1* and *IFNGR1* while the IL1-like subfamily had expression of three receptors genes altered (*IL1R1, IL1RAP* and *IL1R2)*. The TNF family showed differential expression of three ligands (*TNF, TRAIL* and *CD70)* and eight receptors (*TNFR1, FAS, DR4, DR5, OPG, FN14, CD40* and *TACI*). Finally, the TGF-β family showed differential expression of ligands *INHBA* and *BMP2*, and receptor *BMPR1B.* This result shows activity in the pro-inflammatory responses with differential expression of *TNF, IL6* and *IFNB1* but also shows activity in the anti-inflammatory response with differential expression of *IL19*. One limitation of the KEGG pathway analysis is that it does not indicate if the differential expression refers to upregulation or downregulation of a specific gene. Therefore, in the following section a different type of analysis was applied to evaluate the extent of differential expression within the various genes.

3.2 Neuronal gene enrichment post *M. tuberculosis* infection.

The previous section revealed several pathways that were altered and numerous genes that were differentially expressed in response to *M. tuberculosis* infection. However, for better understanding of this gene expression data, gene ontology and gene enrichment were performed using the tmod R package. This type of analysis allows for comparison of different gene module expression as well as individual gene expression changes between the two conditions. Comparisons made on the gene expression data, between infected and uninfected neurons, resulted in 89 modules which were significantly different with p-values of less than 0.05 (Appendix Table A-2). The number of statistically significant modules were reduced to 45 when more stringent criteria of a p-value 0.001 was applied (Figure 3.4). The figure displays statistical significance of a specific module by the intensity of the bar colours, where low intensity is equal to a p-value of 0.001 and high intensity signifies a p-value of less than 10^{-6}. The effect sizes are shown by the size of the bars, where the effect size shows the magnitude of gene expression difference between the two groups.

Analysis of the transcriptional modules showed that the most significantly enriched module was “Cell cycle and transcription” with a p-value of $6{,}15E^{-18}$ and an effect size of $7{,}46E^{-01}$ (Appendix Table A-2). It was observed that the “RIG-1 like receptor signalling” module had the largest effect size of $9{,}87E^{-01}$ and most of the genes within the module (module members) were upregulated as indicated by the red portion of the bar in Figure 3.4. Further assessment revealed several additional viral sensing and cytosolic related enriched modules; LI.M75, LI.M111.0, LI.M111.1, LI.M13 and LI.M150. It was noted that four modules from the top 45; “complement and other receptors in DCs”, “BCR signalling”, “enriched in antigen presentation (III)” and “inflammatory response”, consisted mostly of downregulated module members as displayed by the blue portion of the bars in Figure 3.4.

The top 10 statistically significant enriched modules were examined, to further understand the neuronal immune responses to *M. tuberculosis* infection from a molecular perspective. All the modules in this selected group had a p-value of less than $1x10^{-8}$ but a limitation on the method of selection is that it only relied on the p-value, and presented a stringent cut-off which saw modules such as “Viral sensing & immunity; IRF2 targets network (II)” and “Type I interferon response” not be selected

even though their respective p-values were $1.07x10^{-8}$ and $1.14x10^{-8}$. Figure 3.5 is a schematic that shows the links between the selected modules. Here it shows which modules share genes and identify the exact genes which are shared. Furthermore, the genes that are unique to each module is also displayed. The modules that share the most genes are LI.M4.0 and LI.M11.0 which is followed by the pairing of LI.M11.0 and LI.M37.0. The modules with the most unique genes are LI.M4.0, LI.M37.0 and LI.M111.0, and LI.M20.0 is shown to have the least shared genes. The diagram depicts the overlap between the various biological expression modules and highlights the complexity of genetic engagement in response to *M. tuberculosis*. To understand the specific gene expression differences between the non-infected neurons and the *M. tuberculosis* infected neurons the modules in Figure 3.5 are discussed further in the sections to follow.

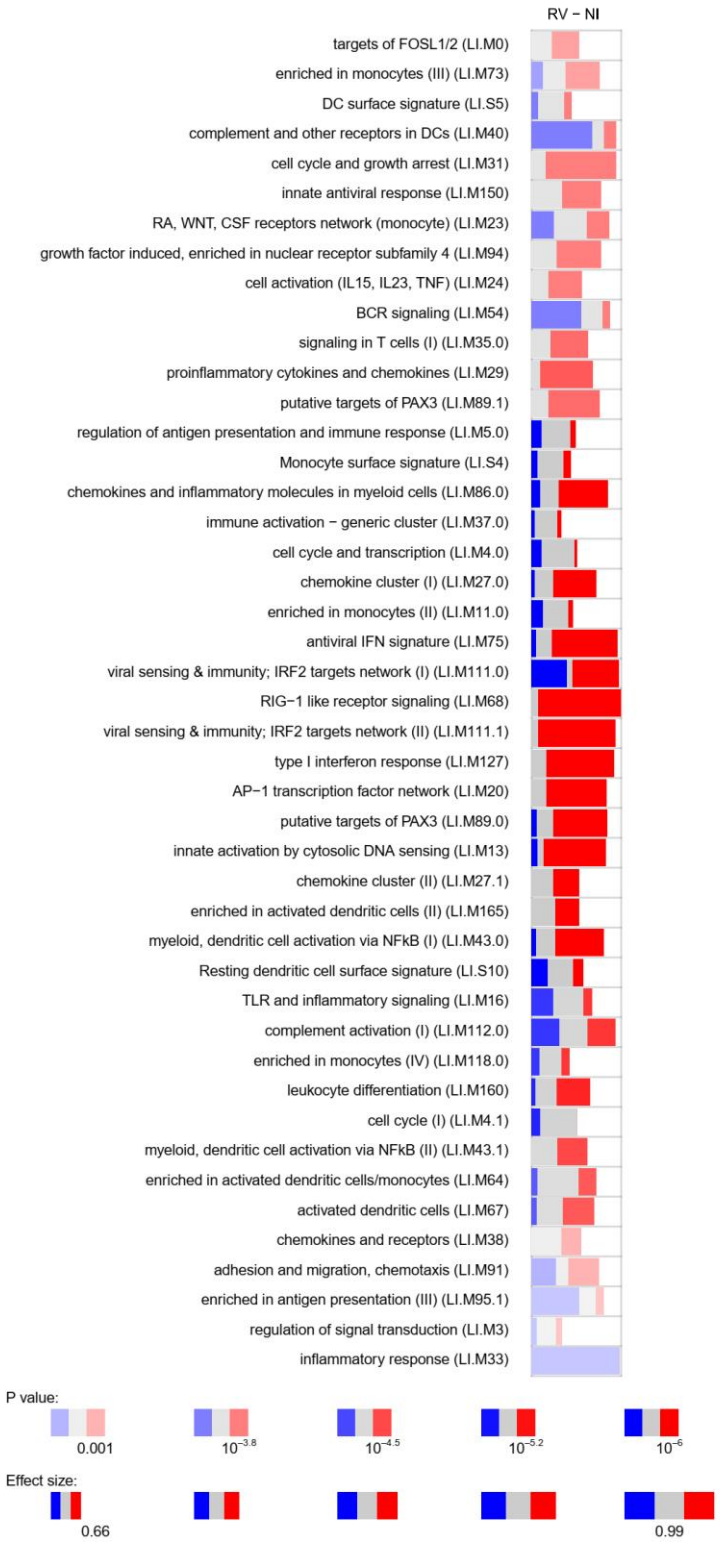

Figure 3-4: Gene module enrichment.
Decides test showing gene module enrichment of cultured primary hippocampal neurons post *M. tuberculosis* infection. The tmod R package was used with significance indicated by p<0.001. Red and blue indicates significantly upregulated and downregulated respectively and grey indicates unregulated. The p-value is displayed by the colour intensity and the effect size of the module is shown by the size of the bar.

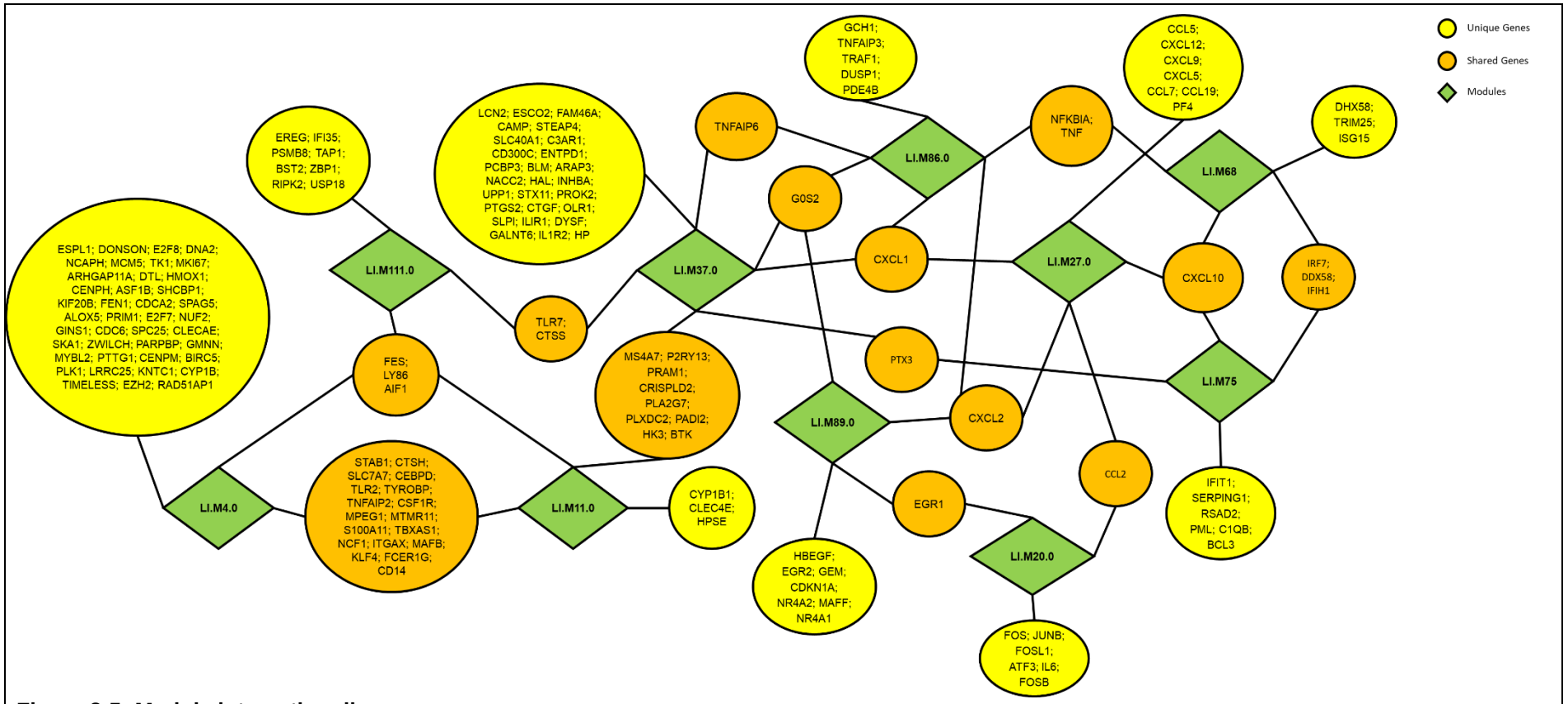

Figure 3-5: Module interaction diagram.
The top 10 most significantly enriched modules are shown in relation to one another. The diagram represents shared genes by the different modules and unique genes to specific modules.

3.2.1 Modules LI.M4.0 and LI.M11.0.

Modules LI.M4.0 and LI.M11.0 share 21 common genes which is the most within the top 10 modules. The combination of modules LI.M4.0 and LI.M11.0 resulted in 74 significantly altered genes. A total of 14 genes were upregulated and 60 genes were downregulated. Table 3.1 shows 22 DEGs with significance of less than 0.0001. In this group of 22 genes a total of 7 genes were upregulated and 15 were downregulated. The upregulation of *TLR2, CLEC4E*, *KLF4*, *CRISPLD2* and *CD14* all provide evidence for an immune response to bacterial infection. TLR2 and CLEC4E are conserved PRRs, together with CD14 are known for their recognition of *M. tuberculosis* (Drennan *et al*., 2004, Zanoni and Granucci, 2013, Ishikawa *et al*., 2009). CRISPLD2 has previously been identified as a LPS binding protein and KLF4 is a transcription factor that regulates inflammation during bacterial infections (Wang *et al*., 2009, Bhattacharyya *et al*., 2020). Furthermore, upregulation of *CEBPD* resulted in attenuation of phagocytosis of apoptotic neurons by macrophages and the upregulation of *TNFAIP2* which encodes for a TNF inhibitory protein (Ko *et al*., 2012, Thair *et al*., 2016), suggests dampening of the proinflammatory response to promote neuronal survival. The 15 downregulated genes are involved in various cellular processes from cell division to antimicrobial functionality. In Table 3.1 downregulation of *GMNN, DONSON* and *TIMELESS* were noted. These genes play a role in cell cycle and DNA replication regulation (Nishitani and Lygerou, 2004, Reynolds *et al*., 2017, Rothenfluh *et al*., 2000) and suggests that cell division of infected or distressed cells are stopped. Downregulation of *SLC7A7* has previously been shown to enhance the inflammatory response by increasing the expression of proinflammatory mediators (Rotoli *et al*., 2018) and supports the findings of a proinflammatory response mediated by neurons to *M. tuberculosis*. Surprisingly *STAB1* and *MPEG1* genes were downregulated even though previous studies have identified them to promote antibacterial immunity (Pombinho *et al*., 2021, Bayly-Jones *et al*., 2020). The downregulation of *MAFB* and *P2RY13* supported a more controlled immune response as deficiency of the *MAFB* gene results in the impairment of the type I and type II interferon responses to *M. tuberculosis*, and blocking of P2RY13 was shown to reduce LPS induced IL6 (Hikichi *et al*., 2022, Ishimaru *et al*., 2014, Malin and Molliver, 2010). Genes involved in signal transduction such as *TYROBP* and *FES* were noted to be downregulated (Campbell

and Colonna, 1999, Bouchon *et al*., 2001, Nelson *et al*., 1998, Park *et al*., 1998). Downregulation of *TBXAS1, FCER1G* and *AIF-1* was observed. These genes respectively play roles in arachidonic acid metabolism, immune response regulation and cell survival (Zhao *et al*., 2023, Sweet *et al*., 2017, Egana-Gorrono *et al*., 2019). Reduction of *NCF1* expression supported a neuroprotective function as it encodes a protein that induces ROS production (Sareila *et al*., 2013) and a decrease in *LRRC25* expression reinforced the concept of an inflammatory immune response by neurons, as this gene is known to be a negative regulator of the NF-κβ signaling pathway (Feng *et al*., 2017). Collectively the data argues strongly for a functional proinflammatory immune response by neurons which occurs in tightly regulating environment.

Table 3-1: Modules LI.M4.0 and LI.M11.0.
Shows top 22 DEGs with p-values of less than 0.0001 in a combination of modules LI.M4.0 and LI.M11.0. Columns show the gene names, protein names, fold change, adjusted p-value and the function performed by the protein.

Gene Name	Protein Name	Log FC	Adj. p-value	Function
TNFAIP2	Tumor necrosis factor alpha-induced protein 2	3,946	$5{,}91E^{-08}$	A TNF inhibitory protein involved in reduced NF-kβ signaling (Thair *et al*., 2016).
CEBPD	CCAAT/enhancer binding protein (C/EBP) delta	1,332	$7{,}84E^{-08}$	A transcription factor involved regulation of inflammation (Ko *et al*., 2012).
TLR2	Toll-like receptor 2	3,395	$9{,}51E^{-08}$	Contributes to host recognition and protection against M. tuberculosis (Drennan *et al*., 2004).
STAB1	Stabilin-1	-1,760	$2{,}12E^{-06}$	A scavenger receptor that plays a role in protection against bacterial infections (Pombinho *et al*., 2021).
MAFB	V-maf musculoaponeurotic fibrosarcoma oncogene homolog B	-1,265	$1{,}09E^{-05}$	A transcription factor that regulates type I and II interferon responses to *M. tuberculosis* (Hikichi *et al*., 2022).

TBXAS1	Thromboxane A synthase 1	-1,459	1,82E^{-05}	A downstream enzyme of arachidonic acid metabolism (Zhao *et al*., 2023).
TYROBP	TYRO protein tyrosine kinase-binding protein	-1,280	2,22E^{-05}	Adapter protein for a variety of surface receptors (Campbell and Colonna, 1999, Bouchon *et al*., 2001)
KLF4	Kruppel-like factor 4	0,844	2,65E^{-05}	A transcription factor involved in regulation of the inflammatory response to bacteria (Bhattacharyya *et al*., 2020).
CRISPLD2	Cysteine-rich secretory protein Limulus factor C-related region domain containing 2	1,343	2,96E^{-05}	An LPS binding protein that regulates endotoxin function (Wang *et al*., 2009).
FCER1G	Fc Epsilon Receptor Ig	-0,957	7,67E^{-05}	Receptor that contributes to regulation of immune cell immune responses (Sweet *et al*., 2017).
CD14	Cluster of differentiation 14	1,300	9,25E^{-05}	TLR co-receptor and pattern recognition receptor (Zanoni and Granucci, 2013).
LRRC25	Leucine Rich Repeat Containing 25	-0,731	9,92E^{-05}	A negative regulator in the NF-κβ signaling pathway (Feng *et al*., 2017).
FES	Tyrosine-protein kinase Fes/Fps	-1,051	1,18E^{-04}	Important for STAT3 activation (Nelson *et al*., 1998, Park *et al*., 1998)
CLEC4E	C-Type Lectin Domain Family 4 Member E	1,285	1,23E^{-04}	A pathogen recognition receptor which recognises mycobacterial glycolipids (Ishikawa *et al*., 2009).
P2RY13	P2Y purinoceptor 13	-0.892	2.14E^{-04}	A Gi-coupled receptor activated by ADP (Malin and Molliver, 2010, Ishimaru *et al*., 2014)
SLC7A7	Solute Carrier Family 7	-0,733	2,80E^{-04}	Important for cationic amino acid

	Member 7			transport (Rotoli *et al*., 2018).
NCF1	Neutrophil Cytosolic Factor 1	-0,554	$3{,}54E^{-04}$	A key regulatory component of NOX2 (Sareila *et al*., 2013).
MPEG1	Macrophage-expressed gene 1 protein	-0,907	$4{,}19E^{-04}$	Plays a role in antibacterial immunity (Bayly-Jones *et al*., 2020).
AIF1	Allograft inflammatory factor 1	-0,909	$4{,}28E^{-04}$	A protein important for macrophage survival and function (Egana-Gorrono *et al*., 2019).
GMNN	Geminin	-0,814	$6{,}70E^{-04}$	A protein important for the regulation of the cell cycle (Nishitani and Lygerou, 2004).
DONSON	Downstream neighbour of Son	-0,511	$7{,}03E^{-04}$	A protein involved in DNA replication (Reynolds *et al*., 2017).
TIMELESS	Timeless Circadian Regulator	-0,507	$7{,}39E^{-04}$	A protein important for the circadian molecular cycle (Rothenfluh *et al*., 2000).

3.2.2 LI.M27.0 Chemokine cluster (I).

Neuronal expression of chemokines has been described in physiological and pathological conditions (de Haas *et al*., 2007). This immune class of molecules is known to promote cellular recruitment, more specifically (Spandau *et al*., 2002, Fong *et al*., 1998) leukocyte migration to sites of infection to contain infection. The production of chemokines and cytokines by neurons was assessed by analysing the significantly differentially expressed genes in the “chemokine cluster (I)” module (Figure 3.6). The upregulation of chemokine transcripts *CCL2, CCL5, CCL7, CCL19* and *CXCL12* provided a strong case for regulation of both an innate and adaptive immune response by neurons in response to *M. tuberculosis*. These chemokines are responsible for the recruitment of both innate monocytes/macrophages and neutrophils, and adaptive T cells (Cedile *et al*., 2017, Araujo *et al*., 2018, Zhang *et al*., 2020b, Yan *et al*., 2019, Isles *et al*., 2019). Furthermore, *CXCL1, CXCL2* and

CXCL5 were upregulated and are involved in early innate immune responses (Sawant *et al*., 2016, Sawant *et al*., 2021, Disteldorf *et al*., 2015). The concentration of CXCL9 and CXCL10 at the site of infection was suggested to be possible markers for identifying TB-meningitis (Yang *et al*., 2014), therefore the upregulation of *CXCL9* and *CXCL10* in this study is particularly interesting and suggests that neurons may contribute to pro-inflammatory immune responses as well as assist in chemotaxis. Unexpectedly, the platelet factor 4 gene (*PF4*), which is known to be increased in response to infection was down regulated (Cai *et al*., 2020). Overall, the data indicates that neuronal regulation of leukocyte recruitment is made possible by the cytokine/chemokine milieu priming and actively participating in proinflammatory responses.

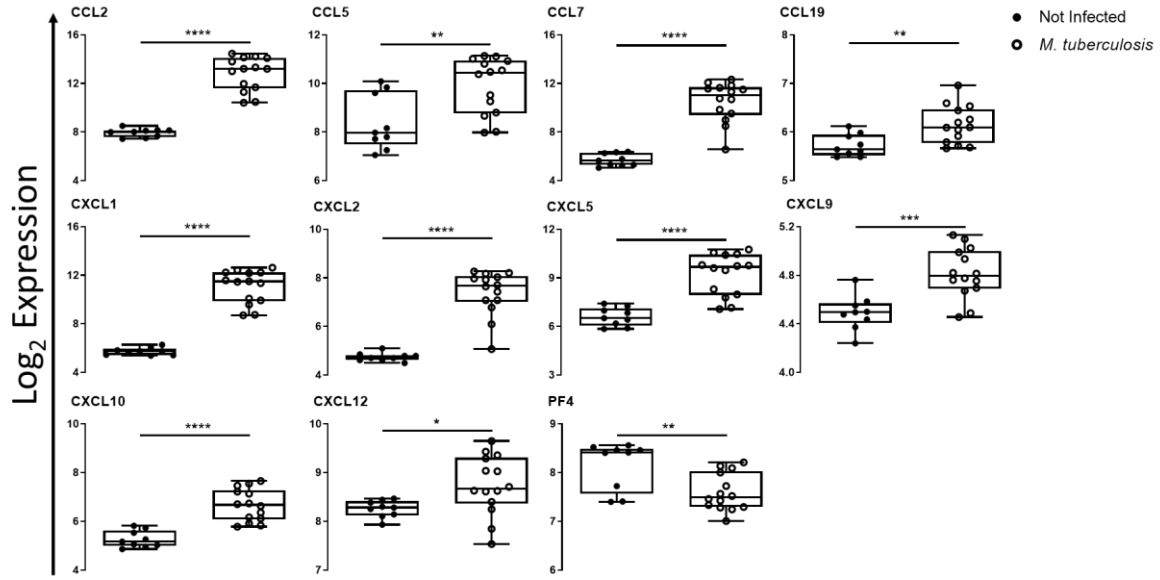

Figure 3-6: LI.M27.0 Chemokine cluster (I).
Differentially expressed module members from the combination of modules LI.M68 and LI.M75 after 24 hours of neuronal infection with *M. tuberculosis*. The figure represents pooled data from 3 experiments and statistical significance (*p<0.05; **p<0.01; ***p<0.001; ****p<0.0001) was determined by the Student's t-test.

3.2.3 Modules LI.M68 and LI.M75.

Modules LI.M68 and LI.M75 share 4 common genes and together consist of 16 DEGs (Figure 3.7). The only downregulated module member was *C1QB*. This complement subcomponent subunit forms part of the recognition molecule C1q. The absence of C1qB results in reduced classical complement pathway function which causes recurrent infection and illness that may lead to lupus (van Schaarenburg *et*

al., 2015). However, a study has shown that neutralizing C1q results in lower chronic inflammation and reduced neuron loss (Cho *et al*., 2013). Additionally *Serping1*, a C1 inhibitor, was shown to be important in cortical development and promote neuronal stem cell proliferation (Gorelik *et al*., 2017). In the current study *Serping1* was upregulated in neurons post *M. tuberculosis* infection, therefore presenting a compelling argument for neuronal survival during *M. tuberculosis* infection. *IFIH1* is an innate immunity viral sensing receptor which promotes proinflammatory signaling and was found to be enriched in neurons during a study of positive-stranded RNA viruses (Holden *et al*., 2021). Furthermore, PBMCs from healthy donors induced *IFIH1* after 24 hours of infection with *C. Albicans* and heat-killed *M. tuberculosis* (Jaeger *et al*., 2015). Therefore, the significant induction of *IFIH1* in neurons after *M. tuberculosis* infection is in line with current reports. The finding of significant induction of *IFIT1* is supported by Qiao *et al.*, as they suggested that IFIT1, which is known to participate in anti-pathogenic innate immunity, plays an important role in CNS-TB and can possibly be a biomarker for CNS-TB (Qiao *et al*., 2022, Pichlmair *et al*., 2011). *RSAD2* gene was upregulated after *M. tuberculosis* infection even though it is a known antiviral protein which restricts viral release from infected cells (Kurokawa *et al*., 2019). *DDX58* and *DHX58* encodes for cytoplasmic viral RNA sensing proteins which ultimately contribute to cytokine production while *ISG15* which encodes for a protein involved in viral replication disruption (Brisse and Ly, 2019, Perng and Lenschow, 2018) was upregulated in the current study. Furthermore, significant upregulation of proinflammatory cytokines *TNF* and *CXCL10* was observed. Surprisingly, *NFKBIA*, the gene that encodes IκBα and *BCL3* were shown to be upregulated, however both genes have previously been identified as negative regulators of NF-κβ activity (Tan *et al*., 2020, Ali *et al*., 2010).

In contrast, the upregulation of *Trim25*, a positive regulator of NF-κβ (Liu *et al*., 2020d) was observed in neurons after *M. tuberculosis* infection. In addition to this, *PML* and *PTX3* which play roles in cell cycle and inflammatory response regulation were significantly increased (Guan and Kao, 2015, Magrini *et al*., 2016). Collectively the results support an argument for an anti-pathogenic response by increasing proinflammatory gene expression and tightly regulating homeostatic conditions.

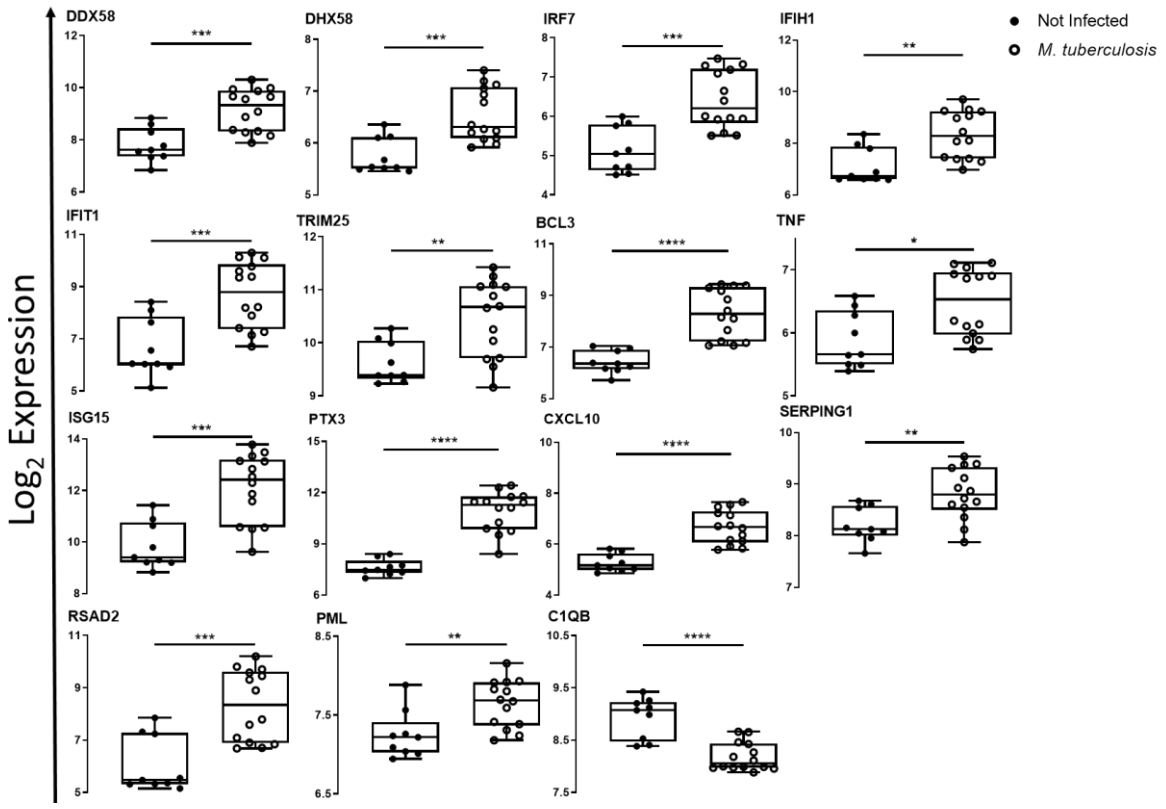

Figure 3-7: LI.M68 RIG-1 like receptor signaling and LI.M75 Antiviral IFN signature.
Gene expression profiles of module members from the combination of modules LI.M68 and LI.M75 after 24 hours of neuronal infection with *M. tuberculosis* is displayed. Statistical significance (*p<0.05; **p<0.01; ***p<0.001; ****p<0.0001) was determined by the Student's t-test and the figure represents pooled data from 3 experiments.

3.2.4 LI.M37.0 Immune activation - generic cluster.

The immune activation-genetic cluster module had 42 DEGs of which 21 were upregulated and 21 downregulated. Figure 3.8 a, show the top 10 most significantly upregulated DEGs in this module. Of the 10 genes 7 were identified as being unique and 3 were shared with modules LI.M11.0, LI.M27 and LI.M75.0. This module showed contrasting results with the upregulation of both *LCN2* and *IL1R1*. LCN2 induces neurodegeneration (Bi *et al*., 2013) and IL1R1 is known for its role in neurogenesis and immune cellular recruitment to the CNS (Liu *et al*., 2019). The expression of *INHBA*, which correlated with immune cell recruitment in a cancer model (Zhao *et al*., 2021), contributes to the findings of neuronal immune regulation through leukocyte recruitment. Furthermore, the upregulation of *STX11* and *CRISPLD2*, which are associated with cytotoxic lymphocyte function and LPS binding respectively (Muller *et al*., 2014, Wang *et al*., 2009), was observed. There was an increased expression observed in the chemokine *CXCL1*, *PTX3* and

FAM46A which is a nucleotidyltransferase, in response to *M. tuberculosis* (Kuchta *et al.*, 2009). Other intracellular and enzymatic response related genes such as *Steap4* which is involved in iron and copper homeostasis and the arachidonic acid converting enzyme *PTGS2* were upregulated (Scarl *et al.*, 2017, Rumzhum and Ammit, 2016).

The top 10 downregulated genes in this module are shown in Figure 3.8 b. The majority of these downregulated genes are shared with other modules; only 4 of the top 10 being unique. These DEGs are known to form part of a number of biological processes. The downregulation of the transcription repressor *NACC2*, known to have an influence on the p53 pathway, was observed (Xuan *et al*., 2013). The surface receptor *CD300c* gene was surprisingly downregulated, as this gene is involved in the inflammatory response (Simhadri *et al*., 2013). The pathogen recognition receptor *TLR7* and the protease *CTSS* were also down regulated (Farooq *et al*., 2021, Smyth *et al*., 2022). Additionally, the downregulation of compliment receptor *C3AR1* was observed which is controversial as this protein is known to be important for survival in response to bacterial infections (Coulthard and Woodruff, 2015). The Gi-coupled receptor *P2RY13* and G0S2 which plays a role in inflammation regulation was significantly decreased (Malin and Molliver, 2010, Okabe *et al*., 2022). A significant reduction observed in *GALNT6* gene expression was observed with high protein expression associated with shorter survival of breast cancer patients due to increased metastasis (Liu *et al*., 2020a). Lastly, significant downregulation of the genes coding for the metabolic proteins involved in inflammation *PLA2G7* and *PADI2* which plays a role in cell proliferation was observed (Huang *et al*., 2020, Liu *et al*., 2020b). Generally, the data from this module shows neurons display a transcriptional response that does not follow dogma and presents a unique profile reflective of neuronal involvement in immune regulation.

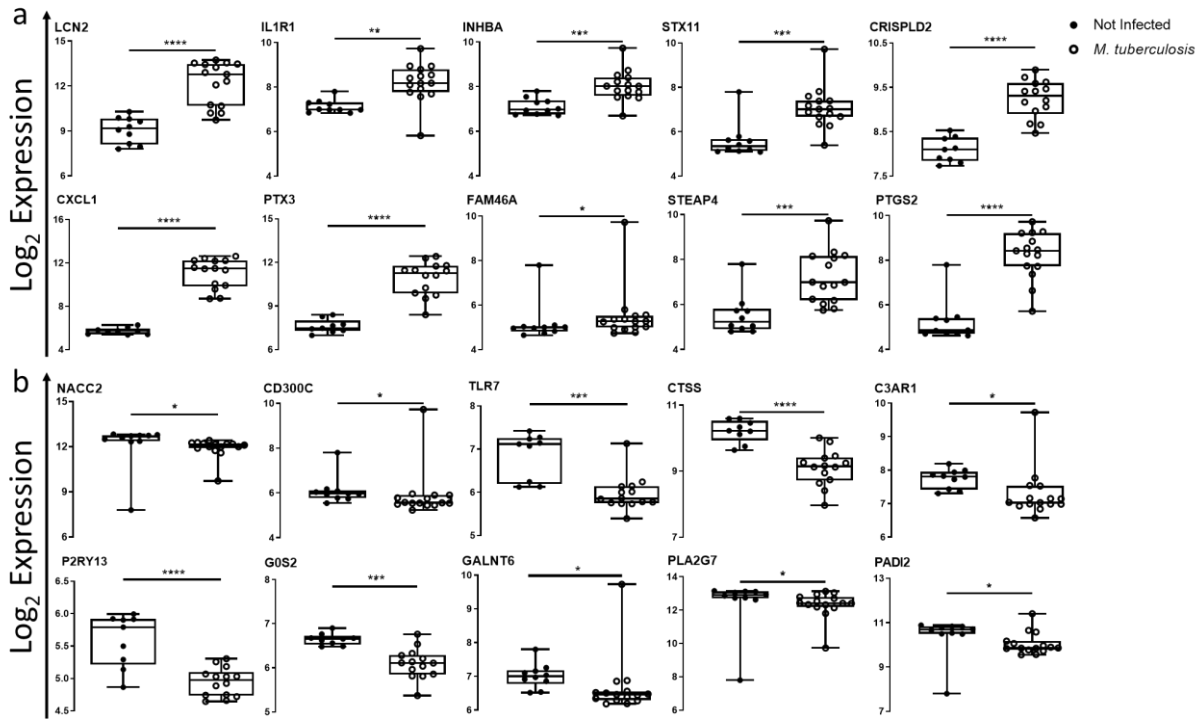

Figure 3-8: LI.M37.0 Immune activation - generic cluster.
The figure shows the (a) top 10 upregulated and (b) top 10 downregulated module members from the LI.M37.0 module. The data is presented as box and whisker plots with statistical significance (*p<0.05; **p<0.01; ***p<0.001; ****p<0.0001) calculated by the Student's t-test. The figure represents pooled data from 3 experiments.

3.2.5 LI.M86.0 Chemokines and inflammatory molecules in myeloid cells.

The module "Chemokines and inflammatory molecules in myeloid cells" presented with 9 upregulated genes and 2 downregulated genes (Figure 3.9). Three of the genes were cytokines namely *CXCL1, CXCL2, TNF* and *TNFAIP6*, which are known to be associated with immune cellular recruitment and inflammation. There were notable upregulations of *TNFAIP3* and *NFKBIA* which are inhibitors of NF-κβ activity (Giordano *et al*., 2014, Tan *et al*., 2020, Ali *et al*., 2010) suggesting a possible attempt to maintain homeostatic conditions to reduce the risk of neuropathology. This was supported by the downregulation of *TRAF1* and *G0S2* which are respectively known for their contributions in NF-κβ and TNF regulation during inflammation (Edilova *et al*., 2018, Okabe *et al*., 2022). The significant induction of *GCH1* was observed and suggested a nitric oxide (NO) dependent manner of mycobacterial infection control. Previously the absence of this gene resulted in the loss of nitric oxide production which was shown to be protective against mycobacterial infection via NO-independent mechanism (McNeill *et al*., 2018). In this study McNeill and colleagues showed that the loss of *GCH1* gene expression

resulted in beneficial *M. tuberculosis* control. Additionally, the upregulation of *DUSP1* and *PDE4B* genes were observed, which supported neuronal proinflammatory responses to *M. tuberculosis* infection, as both these genes have been identified as promotors of inflammation (Hammer *et al*., 2010, Komatsu *et al*., 2013).

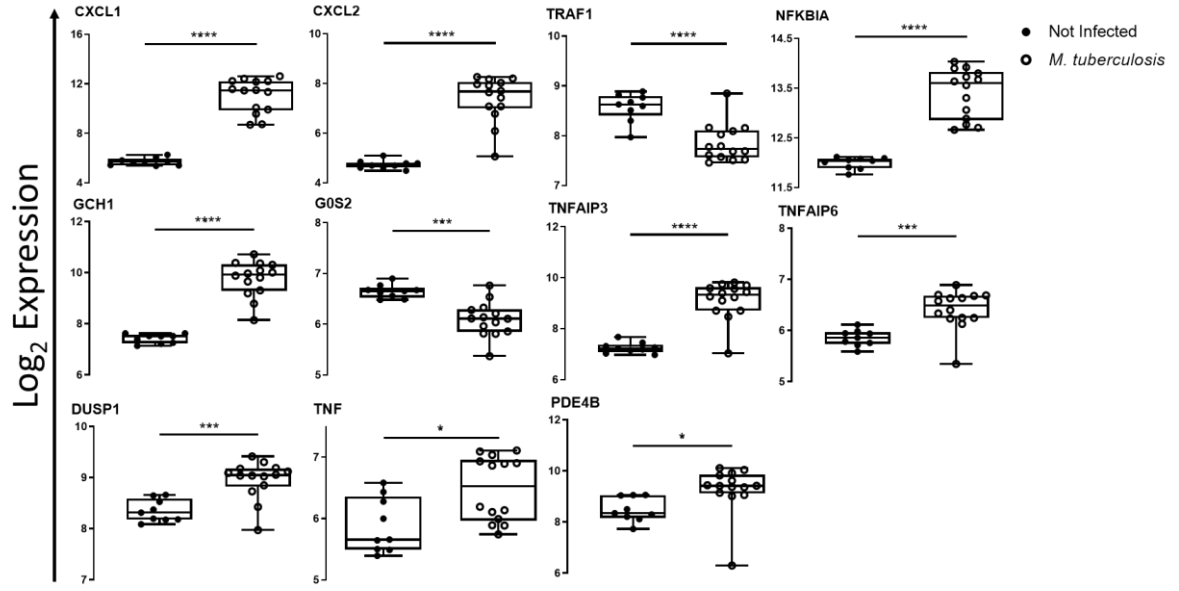

Figure 3-9: LI.M86.0 Chemokines and inflammatory molecules in myeloid cells.
Individual differentially expressed genes from the "Chemokines and inflammatory molecules in myeloid cells" module is shown after a 24-hour infection of neurons with *M. tuberculosis*. The figure represents pooled data from 3 experiments. Significance (*p<0.05; **p<0.01; ***p<0.001; ****p<0.0001) was determined using the Student's t-test.

3.2.6 LI.M111.0 Viral sensing & immunity; IRF2 targets network (I).

The IRF2 protein is a transcriptional repressor that reduces M1 microglial activity while increasing M2 microglia activity (Chen and Stewart, 2017). In this module, 13 IRF2 targets were differentially expressed (Figure 3.10). *TLR7*, *CTSS, AIF1* were the only downregulated genes. TLR7 is a pathogen recognition receptor that senses ssRNA and generates a MyD88 dependent immune response to viral infections whereas CTSS is a protease which has several functions mostly reported for autoimmune and allergy related inflammatory responses (Farooq *et al*., 2021, Smyth *et al*., 2022). *AIF1* encodes for the protein IBA1, a surface maker used to identify microglia. This protein is suggested to be involved in phagocytosis but though neurons were reported to have phagocytic capabilities (Bowen *et al*., 2007), no evidence was found that neurons engulf *M. tuberculosis* (Lituma *et al*., 2021, Randall *et al*., 2014). There were significant increases in the expression of *TAP1, ZBP1,*

IFI35 and *LY86*. The TAP1 protein is facilitates antigen processing and loading of MHC class I molecules. TAP1 expression is increased in macrophages when stimulated with LPS (Schiffer *et al*., 2002). The upregulation of TAP1 together with MHC class I suggest the potential of neurons to present antigen during M. tuberculosis infection. The upregulation of *ZBP1*, an innate anti-viral sensor, *IFI35* a damage associated molecular pattern and *LY86* a glycoprotein, which all participate in the inflammatory response was observed (Kuriakose and Kanneganti, 2018, De Masi and Orlando, 2020, Su *et al*., 2014, Xiahou *et al*., 2017). Furthermore, *PSMB8* coding for the subunit of a proteasome involved in protein degradation and peptide generation for MHC class I loading, *BTS2* which encodes for an innate immune transmembrane anti-viral protein and *USP18* a protease coding gene which is involved in regulating the inflammatory response was significantly upregulated (Kitamura *et al*., 2011, Tokarev *et al*., 2009, Santin *et al*., 2012). The gene *EREG* was upregulated and previously found to be important for protection against *M. tuberculosis* infection (Cao *et al*., 2019). Moreover, this protein contributes to innate immunity by generating signals for cell survival and cytokine production (Strachan *et al*., 2001). Additionally, *RIPK2* a major participant in the NOD signaling pathway and *FES* which is an activator of STAT3, and promotor of cell survival was upregulated (Ashton *et al*., 2022, Nelson *et al*., 1998, Park *et al*., 1998). Here the data again supports the hypothesis that neurons promote an inflammatory response against *M. tuberculosis* and generates responses to assist its survival.

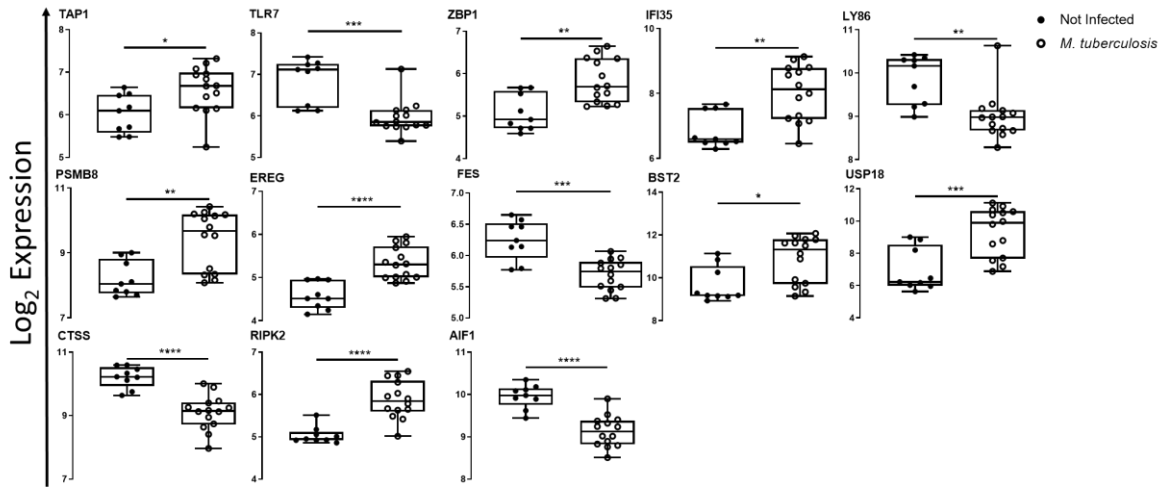

Figure 3-10: LI.M111.0 Viral sensing & immunity; IRF2 targets network (I).
Individual significantly DEGs from module LI.M111.0 are shown after a 24-hour infection of neurons with *M. tuberculosis*. Statistical significance (*p<0.05; **p<0.01; ***p<0.001; ****p<0.0001) was observed by using the Student's t-test and the figure is representative of pooled data from 3 separate experiments.

3.2.7 LI.M20 AP-1 transcription factor network.

The AP-1 transcription factor network is made up of four families of proteins: Jun, Fos, Creb and Maf families. Jun family members form homodimers or heterodimerize with Fos whereas Fos family members can only heterodimerize with Jun family members, and together modulate activity of the transcription factor complex AP-1 (Jochum *et al*., 2001). Some of these genes are significantly expressed in bone marrow derived macrophages in response to *M. tuberculosis* infection with the most significant being *JunB* (Denisenko *et al*., 2019). The neuronal response to *M. tuberculosis* produced a similar response, with significant induction of *JunB* (Figure 3.11). Concomitant increased expression of *fos, fosb* and *fosl1* was observed and is known to interact with JUN proteins. The significant induction of *ATF3*, a known stress-responsive gene (Cui *et al*., 2015), was upregulated in response to *M. tuberculosis* infection in neurons and was previously reported to supress inflammation in response to *M. tuberculosis* infection (Zhang *et al*., 2022). Furthermore, *EGR1* is ubiquitously expressed and is induced in response to bacterial infection. EGR1 regulates neural plasticity and play a major role in long term memory (de Klerk *et al*., 2017, Mo *et al*., 2015). Previously, EGR1 transcription was shown to affect downstream regulation of IL6 (Pang *et al*., 2019). In the present study, significant upregulation of the proinflammatory cytokines IL*6* and *CCL2* were observed. The findings in this module follows observations from previous modules

with clear proinflammatory response contributions by neurons to *M. tuberculosis* infection. Furthermore, biological stress responses are activated as well as cell survival supporting the previous outcomes.

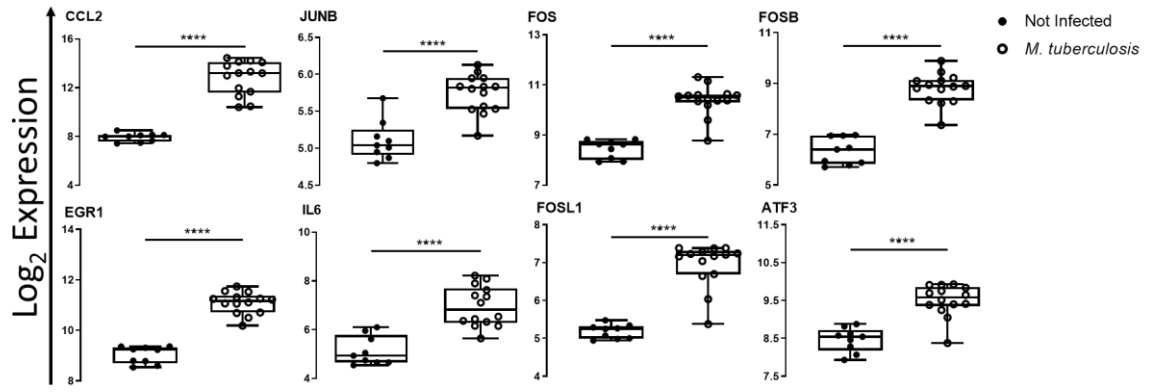

Figure 3-11: LI.M20 AP-1 transcription factor network.
All the significantly expressed genes from the LI.M20 module are shown after neuronal infection for 24 hours with *M. tuberculosis*. The figure represents pooled data from 3 experiments. The Student's t-test was used to observe statistical significance (****p<0.0001).

3.2.8 LI.M89.0 Putative targets of PAX3.

The putative targets of PAX3 module are one of the top 10 most significantly enriched modules. This module has an effect size of $9{,}11x10^{-1}$ and a p-value of $7{,}79x10^{-9}$. PAX3 is a transcriptional regulator which is important for embryonic neural development and reduces neuron viability and proliferation after infection (Boudjadi *et al*., 2018, Huo *et al*., 2021). In the current study 12 genes suggested to be targets of PAX3 have been differentially expressed (Figure 3.12). Only one gene in this module was downregulated, the *G0S2* gene involved in cell metabolism and differentiation (Heckmann *et al*., 2013). The 11 genes that were upregulated included chemotactic gene *CXCL2* and *HBEGF* important for neuronal survival (Oyagi and Hara, 2012). The IL6 related transcription factor *EGR1* was a significantly upregulated member of this module (Pang *et al*., 2019) while the upregulation of the transcriptional regulator *EGR2* is involved in M1- M2- macrophage differentiation (Veremeyko *et al*., 2018). *EGR1* and *EGR2* are induced by opposing stimuli; proinflammatory stimuli upregulates *ERG1* while anti-inflammatory stimuli upregulates *ERG2* (Veremeyko *et al*., 2018). The upregulation of *NR4A1* which is involved in inflammation, cell cycle control and apoptosis (Pei *et al*., 2006) supports a proinflammatory response by neurons against *M. tuberculosis* infection while

significant induction of *NR4A2* transcription factor, important for dopaminergic neuron development (Sacchetti *et al*., 2006), is also displayed by Figure 3.12. Moreover, there were significant increased expression of the anti-viral transcription factor *MAFF,* the cell cycle regulatory gene *CDKN1A* and *GEM* which encodes for a GTP-binding protein involved in T cell chemotaxis (Ibrahim *et al*., 2021, Engeland, 2022, Chevalier *et al*., 2014). This module again suggested coercion neurons towards a proinflammatory response against *M. tuberculosis* infection.

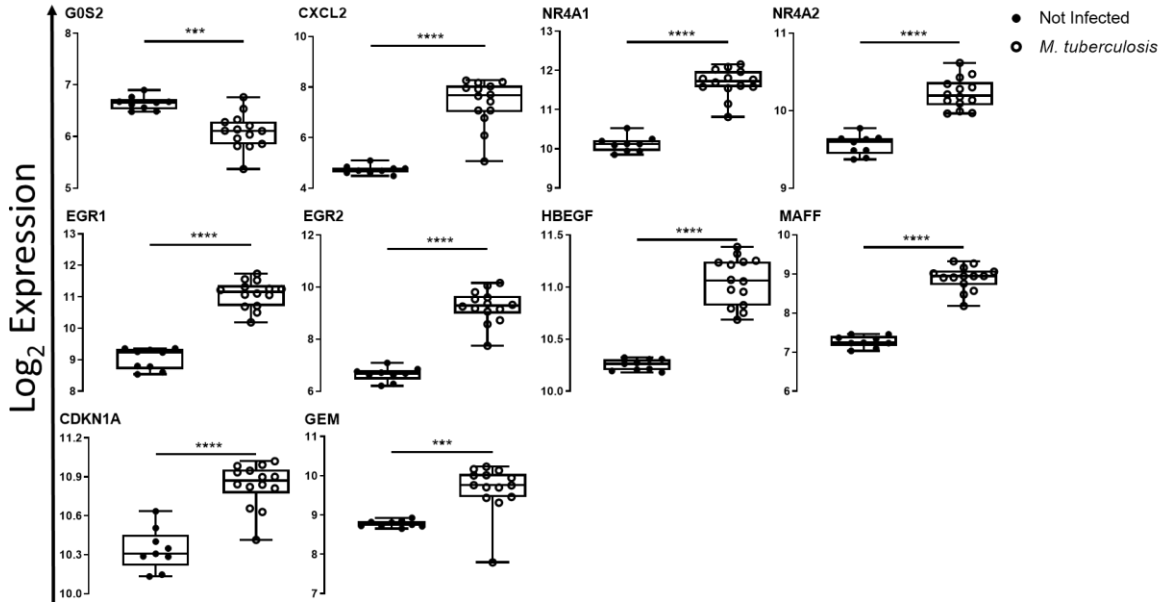

Figure 3-12: LI.M89.0 Putative targets of PAX3.
The individual module members from the LI.M89.0 module that were significantly upregulated or downregulated in neurons after *M. tuberculosis* infection. The figure represents pooled data from 3 experiments. Statistical significance (***p<0.001; ****p<0.0001) was determined by the Student's t-test.

3.2.9 TLR-MyD88- NF-κβ associated genes in response to M. tb infection.

The selection of the top 10 modules based on significance as a criterium had substantial limitations as stated in section 3.2 which resulted in the exclusion of modules related to immune responses to *M. tuberculosis* infection. Modules LI.M16, LI.M43 and LI.M43.1 consist of genes involved in pathogen recognition, signal transduction and gene transcription in response to *M. tuberculosis* infection. Toll-like receptors as a class of PRR's are expressed by neurons (Kaul *et al*., 2012) with TLR 2, 4, 8 and 9 expressed in various cell types that interact with *M. tuberculosis* (Faridgohar and Nikoueinejad, 2017). Here modules LI.M16, LI.M43 and LI.M43.1 were assessed in combination because of their sequential involvement in

inflammatory signaling via TLR and NF-κβ. The significantly upregulated module members (Table 3.3) post *M. tuberculosis* infection consisted of *TLR2*, *MYD88*, *RELB*, *NFKBIA*, *NFKB2* and *BCL3*. The upregulation of these genes indicates the possible recognition activation of neurons by *M. tuberculosis*. Furthermore, the upregulation of *MAP3K8* which is important for TNF production, and adhesion molecules *ICAM1* and *VCAM1* expression which both contribute to the translocation of leukocytes was observed (McNab *et al*., 2013, Okada *et al*., 2003, Koni *et al*., 2001, Park *et al*., 2013). *DYSF* an important calcium ion sensor for synaptic vesicle and plasma membrane fusion, and pro-inflammatory chemokines *TNF* and *CCL5* were also upregulated (Zhang *et al*., 2020a, Hsu *et al*., 2017, Liou *et al*., 2012). This data shows an *M. tuberculosis* specific pro-inflammatory neuronal response which includes recognition of the pathogen, signal transduction and possible contribution to the translocation of leukocytes.

Next, the significantly down regulated module members (Table 3.4) were examined, which included *TLR6* and *TLR7*. TLR6 is known to recognise bacterial lipoprotein in conjunction with TLR2 while TLR7 is a ssRNA sensor (Takeuchi *et al*., 2001, Bao *et al*., 2017). Downregulation of *SAMSN1* which is involved in cell proliferation regulation, *CTGF* which is involved in wound healing, *C5AR1* a component of the complement system and *FES* was reported (Noll *et al*., 2014, Igarashi *et al*., 1993, Farkas *et al*., 1998). Additionally, *ITGAX* a component of complement receptor 4*, ALOX5* an enzyme involved in neuroinflammation*, TYROBP* an adaptor protein and the Gi-coupled receptor *P2RY13* were all found to be downregulated (Holers, 2014, Joshi *et al*., 2014, Campbell and Colonna, 1999, Bouchon *et al*., 2001, Malin and Molliver, 2010). The data revealed a possible TLR-MyD88- NF-κβ pathway response to *M. tuberculosis* infection combined with neuronal isolation and neuronal inflammation.

Table 3-2: Upregulated module members associated with signaling through TLR and NF-κβ. The upregulated genes associated with TLR and NF-kβ signaling are shown. Columns show the gene names, protein names, fold change adjusted p-value and the function performed by the protein.

Gene Name	Protein Name	Log FC	Adj. p-Value	Function
TLR2	Toll-like receptor 2	3.394673867	$9.51E^{-08}$	Contributes to host recognition and protection against M. tuberculosis (Drennan *et al*., 2004).
MyD88	Myeloid differentiation primary response protein	1.079819234	$6.43E^{-04}$	An intracellular adapter protein critical for innate immunity during *M. tuberculosis* (Fremond *et al*., 2004)
RELB	Transcription factor RelB	2.181128578	$1.75E^{-10}$	A subunit of the NF-κβ transcription factor complex and promotes the generation of a T_H1 immune response (Corn *et al*., 2005)
NFkBIA	NF-kappa-B inhibitor alpha	1.605641523	$7.03E^{-09}$	Inhibits NF-κβ translocation to the nucleus (Lopez-Granados *et al*., 2008)
NFkB2	Nuclear factor NF-kappa-B p100/p52 subunit	1.428710487	$3.86E^{-07}$	Subunit of NF-κβ responsible for the alternative NF-κβ pathway (Bonizzi and Karin, 2004)
BCL3	B-cell lymphoma 3	2.597335099	$3.68E^{-06}$	Contributes to the generation of a T_H2 immune response and regulates transcription of NF-κβ target genes (Corn *et al*., 2005)
MAP3K8	Mitogen-activated protein kinase kinase kinase 8	0.7019535576	$2.97E^{-03}$	Important for the regulation of chemokines and cytokines (McNab *et al*., 2013)
ICAM1	Intercellular adhesion molecule	1.062235621	$9.72E^{-05}$	Important for leukocyte translocation (Okada *et al*.,

	1			2003)
VCAM1	Vascular cell adhesion protein 1	1.260864051	$2.36E^{-05}$	Key protein involved in leukocyte translocation (Koni *et al*., 2001, Park *et al*., 2013)
DYSF	Dysferlin	0.5984600127	$2.80E^{-03}$	Mutations in this gene leads to muscular dystrophies which can be diagnosed through the levels in blood monocytes (Zhang *et al*., 2020a)
TNF	Tumor necrosis factor	0.9346706133	$3.92E^{-03}$	Crucial for a protective immune response during CNS-TB (Hsu *et al*., 2017)
CCL5	C-C motif chemokine 5	1.990507424	$4.46E^{-03}$	Plays an immune modulatory role during inflammation (Liou *et al*., 2012)

Table 3-3: Down regulated genes associated with TLR and NF-κβ signaling.
The downregulated genes associated with TLR and NF-κβ signaling are shown. Columns show the gene names, protein names, fold change adjusted p-value and the function performed by the protein.

Gene Name	Protein Name	Log FC	Adj. p-Value	Function
TLR6	Toll-like receptor 6	-0.4331627318	$1.87E^{-02}$	Important for the recognition of bacterial lipoproteins in combination with TLR2 (Takeuchi *et al*., 2001)
TLR7	Toll-like receptor 7	-1.090500216	$2.31E^{-05}$	Plays a role in innate immunity by sensing ssRNA (Bao *et al*., 2017)
SAMSN 1	SAM domain-containing protein SAMSN-1	-0.4377714175	$2.38E^{-02}$	Implicated in the regulation of cell proliferation (Noll *et al*., 2014)

CTGF	Connective tissue growth factor	-0.6833968459	$4.21E^{-03}$	Associated with angiogenesis and wound healing (Igarashi *et al*., 1993)
C5AR 1	C5a anaphylatoxin chemotactic receptor 1	-0.4632232355	$2.08E^{-02}$	An important component of the complement system (Farkas *et al*., 1998)
FES	Tyrosine-protein kinase Fes/Fps	-1,051	$1,18E^{-04}$	Important for STAT3 activation (Nelson *et al*., 1998, Park *et al*., 1998)
ITGAX	Integrin alpha-X	-0.6575774067	$6.94E^{-03}$	Forms part of complement receptor 4 (Holers, 2014)
ALOX5	Polyunsaturated fatty acid 5-lipoxygenase	-0.565802399	$4.24E^{-04}$	A proinflammatory enzyme involved in neuroinflammation (Joshi *et al*., 2014).
TYROBP	TYRO protein tyrosine kinase-binding protein	-1.279763361	$2.22E^{-05}$	Adapter protein for a variety of surface receptors (Campbell and Colonna, 1999, Bouchon *et al*., 2001)
P2RY13	P2Y purinoceptor 13	-0.8922713193	$2.14E^{-04}$	Gi-coupled receptor activated by ADP (Malin and Molliver, 2010)

3.3 Validation of neuronal gene expression by assessing cytokine production.

3.3.1 Neurons produce chemokines and cytokine proteins in response to *M. tuberculosis* infection.

Randall *et al.* 2014 for the first time showed that neurons can be host cells for *M. tuberculosis* (Randall *et al*., 2014). Furthermore, the authors provided evidence that neurons can potentially participate in immune regulation by producing cytokines. They found significant increases in the expression of IL1β, IL6 and IL10 after 48 hours of infection. Additionally, neurons have been shown to express CXC and CC chemokines (de Haas *et al*., 2007). The CXC and CC families of chemokines are important for their chemoattractant functions, regulation of angiogenesis and vascular remodelling (Cabrero-de Las Heras and Martinez-Balibrea, 2018, Strieter *et al*., 2007, Korbecki *et al*., 2020b, Korbecki *et al*., 2020a). These proteins have been named based on the position of conserved cysteines in the N-terminus. The CXC chemokines have one amino acid separating the cysteines whereas the CC cysteines are not separated. The previous sections revealed that neurons undergo transcriptional changes in response to *M. tuberculosis* infection, which can contribute to immune regulation and possibly host protection. This section aimed to validate the transcriptomic data by assessing protein expression by neurons in response to *M. tuberculosis*.

To further explore and expand on neuronal immune regulatory properties, primary hippocampal derived neuronal cultures were infected for 48 hours with *M. tuberculosis*. The culture media was collected and processed for analysis by Luminex Multiplex. Similarly, to Randall and colleagues the present study showed a significant ($p<0.01$) increase in the expression of IL6 for the infected cells compared to the uninfected cells (Figure 3.13 a). In contrast to Randall and colleagues, the expression of the proinflammatory cytokine IL1β was not significantly altered (Figure 3.13 b). Although, TNF was increased in the *M. tuberculosis* infected cultures, this difference was not statistically significant and the anti-inflammatory cytokine IL10 did not present with any differences between the infected and uninfected cells either (Figure 3.13 c-d). This data indicates that neurons are immunologically active and promotes proinflammatory conditions in response to *M. tuberculosis*.

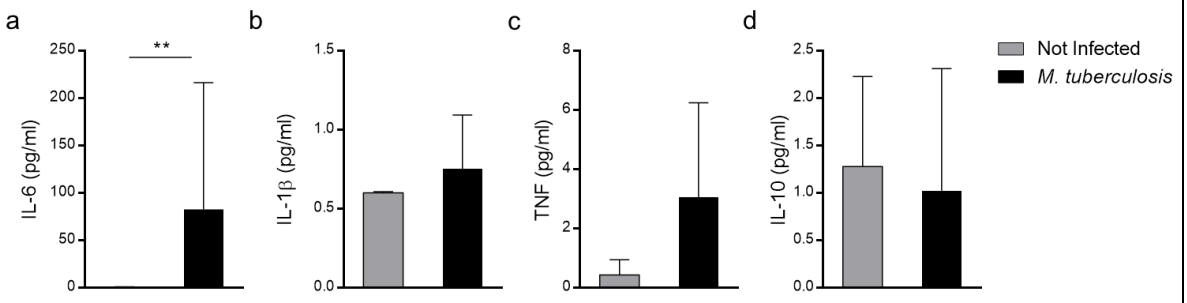

Figure 3-13: Cytokine analysis of neuronal culture media.
Neuronal culture media was collected after 48 hours of infection and analysed for (a) IL6, (b) IL1β, (c) TNF and (d) IL10 using Luminex Multiplex. The data is representative of 3 experiments with 3 to 5 wells per experiment. The data shown is expressed as mean ± SD. Statistical significance (**p<0.01) was determined by the Mann-Whitney U test.

This study investigated the profile of four CXC and three CC neuron secreted chemokines in response to *M. tuberculosis* infection. A study of HSV-1 previously implicated CXCL1 in neutrophil transmigration across the blood brain barrier. This same study identified neurons together with astrocytes as being the source of CXCL1 but showed that neurons did not produce CXCL1 *in vitro* in response to HSV-1 infection (Michael *et al*., 2020). However, in response to *M. tuberculosis*, the culture media from the infected neurons revealed significant ($p<0.01$) upregulation of CXCL1 compared to the non-infected group (Figure 3.13 a). It was previously shown that CXCL2 is significantly upregulated in the brains of mice infected with equine herpes type 1 (Mesquita *et al*., 2021), and Stoolman *et al.* found that recruited neutrophils, macrophages/monocytes and resident microglia were the main contributors of CXCL2 during experimental autoimmune encephalomyelitis resulting in an autocrine/paracrine feedback loop (Stoolman *et al*., 2018). However, in the present study *M. tuberculosis* infected neurons produced significantly ($p<0.01$) higher concentrations of CXCL2 than non-infected neurons (Figure 3.13 b), suggesting neurons are unexpected contributors to CXCL2 expression in the CNS during mycobacterial challenge.

A study of hypoxic ischemia encephalopathy by Wang *et al.* showed that most CXCL5 positive cells in the cortex of 2 days postpartum rats were neurons (Wang *et al*., 2016). Furthermore, Merabova *et al*. showed that CXCL5 is important for neuronal survival in response to JC virus protein stimulation (Mesquita *et al*., 2021). In response to *M. tuberculosis*, cultured neurons increased the expression of CXCL5

in comparison to the uninfected neurons, but this increase was not statistically significant (Figure 3.13 c). The expression of CXCL10 from neurons infected with *M. tuberculosis* was significantly ($p<0.05$) upregulated compared to the non-infected neuronal culture media (Figure 3.13 d). This finding was supported by a previous study that showed neuronal production of CXCL10 in response to Dengue virus infection (Ip and Liao, 2010). Apart from CXCL5, all the other CXC chemokines were significantly induced which suggests a strong proinflammatory response by neurons with a focus on immune regulation of the cellular environment.

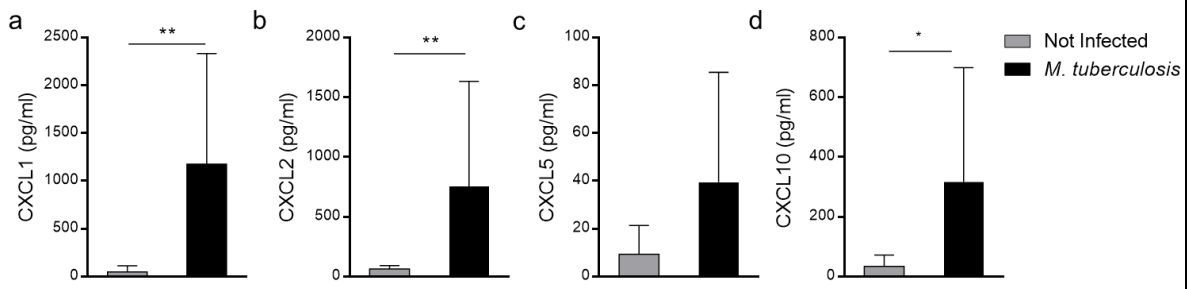

Figure 3-14: CXC-chemokine analysis of neuronal culture media.
Neurons were infected with *M. tuberculosis* H37Rv for 48 hours and the culture medium was processed and analysed by Luminex Multiplex. The concentration of CXC-chemokines (a) CXCL1, (b) CXCL2, (c) CXCL5 and (d) CXCL10 were assessed between the infected and non-infected cultures. The data is representative of 3 experiments with 3 to 5 wells per experiment. The data shown is expressed as mean ± SD. Statistical significance (*$p<0.05$; **$p<0.01$) was determined by the Mann-Whitney U test.

After neuronal infection with *M. tuberculosis*, the concentration of CCL2 in the culture media was significantly (**$p<0.01$) increased compared to the CCL2 produced by the non-infected neurons (Figure 3.14 a). The neuronal expression of CCL2 was previously implicated in the activation and recruitment of microglia and monocytes/macrophages (Howe *et al*., 2017, Zhang *et al*., 2017), suggesting a possible immune regulatory role for neurons during *M. tuberculosis* infection. A study showed that LPS stimulation of rat cerebral neuron-enriched preparations significantly increased CCL3 mRNA (Hattermann *et al*., 2015) but analysis in the present study did not find any differences in CCL3 production between the *M. tuberculosis* infected and non-infected neurons (Figure 3.14 b), signifying that neuronal CCL3 is not affected by *M. tuberculosis* infection. A previous study of the rat brain showed hippocampal neuronal expression of CCL5 (Lanfranco *et al*., 2017). For this study very low levels of CCL5 were detected in the culture medium of non-

infected neurons but *M. tuberculosis* infection significantly increased expression (Figure 3.14 c). The results show that neurons actively contribute to recruitment of peripheral immune cells by producing chemoattractant molecules.

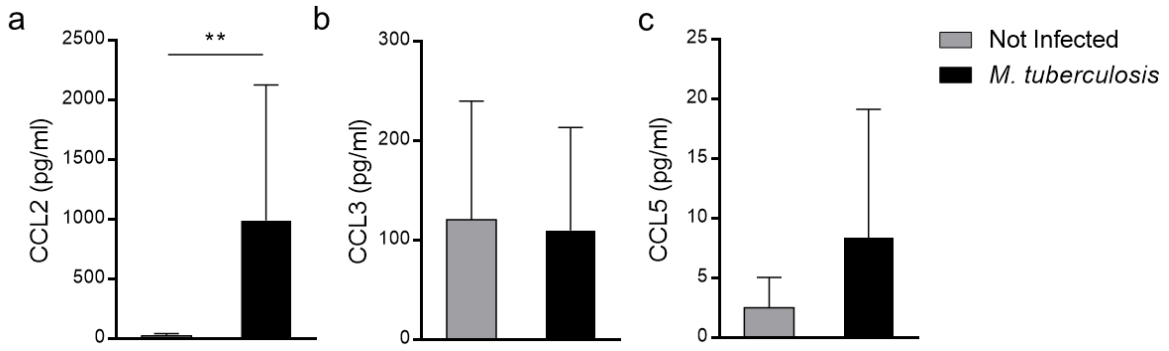

Figure 3-15: CCL-chemokine analysis of neuronal culture media.
Neuronal culture medium was processed and analysed by Luminex Multiplex after a 48-hour infection with *M. tuberculosis* H37Rv. The following CCL-chemokines (a) CCL2, (b) CCL3 and (c) CCL5 were assessed for differences between the infected and NI groups. The data is representative of 3 experiments with 3 to 5 wells per experiment. The data shown is expressed as mean ± SD. Statistical significance (**p<0.01) was determined by the Mann-Whitney U test.

3.3.2 Neurons activate leukocytes *in vitro*.

A variety of studies have shown that neurons can communicate with leukocytes via the release of soluble molecules. For example, the CCL2 secreted by neurons in a co-culture system can induce pro-regenerative macrophage activation and mediate the release of important factors for neurite outgrowth (Yun *et al*., 2018). The present study, following the observations where neurons expressed various immune modulatory genes and produced chemokines and cytokines in response to *M. tuberculosis*, suggested neurons contribute to cellular interaction and immune regulation under pathological conditions, and thus important to assess the direct impact of neurons on leukocytes. Primary neuronal cultures were infected at an MOI of 30:1 for 24 hours and the conditioned media were filtered twice to remove all bacterial and neuronal cells. Leukocytes were obtained from whole blood after red blood cells lysis and were seeded at $2x10^5$ per well. The leukocytes were stimulated with the filtered neuronal conditioned media for 24 hours after which the cells were processed for flow cytometry analysis.

Antigen presenting cells were identified according to specific lineage markers as follows: $CD45^+CD11c^+$ representing dendritic cells, $CD45^+CD11b^+Ly6G^-$ as

monocytes and $CD45^+CD11b^+Ly6G^+$ signifying neutrophils (Figure 3.16 a) (Keeton *et al*., 2014, Walters *et al*., 2021, Burfeind *et al*., 2020). Flow cytometric analysis revealed that mouse whole blood contained 30% of neutrophils, 20% of macrophages and 5% of dendritic cells when treated with the non-infected neuronal conditioned medium; however, no significant differences were observed in the percentages of each cell type between the *M. tuberculosis* H37Rv infected and the uninfected conditioned media (Figure 3.16 b). This data revealed that leukocyte stimulation with neuronal conditioned media had no effect on cellular proliferation or expansion.

To evaluate the efficiency of leukocyte activation by the neurons, the immunological profiles of the $CD45^+$ leukocytes were analysed by flow cytometry. A significant ($p<0.05$) increase in the percentage of $CD45^+$ cells expressing MHC class II stimulated with the *M. tuberculosis* infected CM as compared to the leukocytes cultured in the uninfected conditioned media was observed (Figure 3.16 c). The percentage of leukocytes expressing IL1β (Figure 3.16 d) significantly ($p<0.01$) increased in the infected samples, but there were no statistically significant differences observed in the percentage of APCs expressing IL12 (Figure 3.16 e) and inducible nitric oxide synthase (INOS) (Figure 3.16 f). These findings demonstrate that neurons produce immune modulatory factors which activate immune cells in response to *M. tuberculosis* infection.

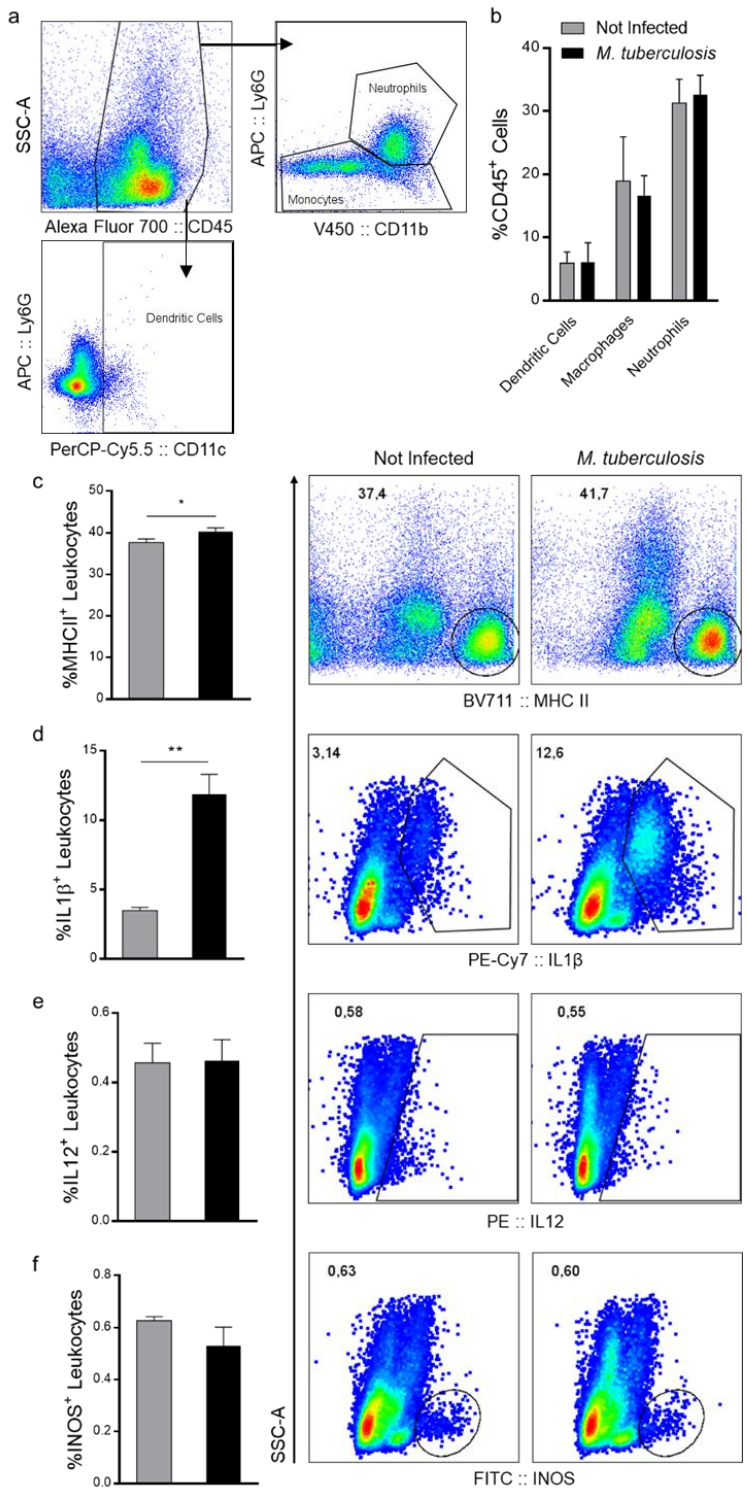

Figure 3-16: The effect of neuron-conditioned medium on leukocyte activation.
Primary hippocampal neurons were infected for 24 hours, then the supernatants were used to stimulate leukocytes from mouse blood. (a) The gating strategy was used to identify the (b) cellular composition of blood leukocytes. The percentage of $CD45^+$ blood leukocytes expressing (c) MHC class II, (d) IL1β, (e) IL12 and (f) INOS was assessed. The data shown is expressed as mean ± SD. Statistical significance (*$p<0.05$; **$p<0.01$) was determined by Student's t-tests.

Chapter 4: Investigating cellular immune responses during CNS-TB

4 Investigating cellular immune responses during CNS-TB.

4.1 CNS-TB disease progression in response to acute intracerebral inoculation.

Central nervous system tuberculosis is one of the most severe forms of extra-pulmonary tuberculosis and has been studied by using *in vivo* animal models (Tsenova *et al*., 2005, van Well *et al*., 2007). Tsenova *et. al.* described CNS-TB in a rabbit model where the outcomes were human-like (Tsenova *et al*., 1998, Tsenova *et al*., 2005, Tsenova *et al*., 1999). In this model, bacilli were injected into the cisterna magna where it disseminated into the brain causing TB-meningitis. Others performed intracerebral mycobacterial challenge studies in mice (Mazzolla *et al*., 2002, van Well *et al*., 2007), and while these murine models did not mimic human pathology, the use of genetically modified mice revealed important biological functions and mechanisms for understanding host defence against *M. tuberculosis* (Olin *et al*., 2008, Francisco *et al*., 2015, Hsu *et al*., 2017). The CNS has always been regarded to be an immune privileged site. However, the findings of a functional lymphatic system within the brain (Louveau *et al*., 2015) has shown immune cells can traffic from the brain to the lymph nodes essentially performing immune surveillance (Mohammad *et al*., 2014). Furthermore, DCs are able to traffic antigen from the brain to the lymphoid organs where they educated T cells on the specific antigens (Karman *et al*., 2006). Although, tuberculosis is a chronic disease, leukocytes are recruited to the site of infection during acute infection (Walters *et al*., 2021) supported by a previous study which reported equivalent numbers of antigen specific T cell accumulation in the brain and cervical lymph nodes 3 days post intracerebral inoculation with ovalbumin (Ling *et al*., 2006). Others have shown dissemination of *M. tuberculosis* from the brain to the spleen after intracerebral infection (Hsu *et al*., 2017). Here the aim was to establish a successful intracerebral infection similar to previous studies. Therefore, in the present study a murine infection model was used where C57BL/6 mice were intracerebrally inoculated with ~1x10^5 CFUs of *M. tuberculosis*. Bacterial burden and dissemination were assessed by harvesting the brains and spleens. The bacterial burden in the brains increased from day 1 post infection and plateaued at day 7. There was no further increase at day 14 post infection (Figure 4.1 a). Furthermore, dissemination to the spleens occurred as early

as 1 day post infection (Figure 4.1 a), possibly due to bacilli access to damaged vasculature. The bacterial burden in the spleens followed a similar trend to that of the brains, increasing from day 1 post infection and reaching the highest burden by day 14 post infection. The possibility of bacilli trafficking to the cervical lymph nodes via the CNS lymphatics may have occurred as bacilli were detected in the lymph nodes (Figure 4.1 b). This data revealed the potential for early control of acute CNS-TB infection and highlighted the probable routes of *M. tuberculosis* dissemination from the brain.

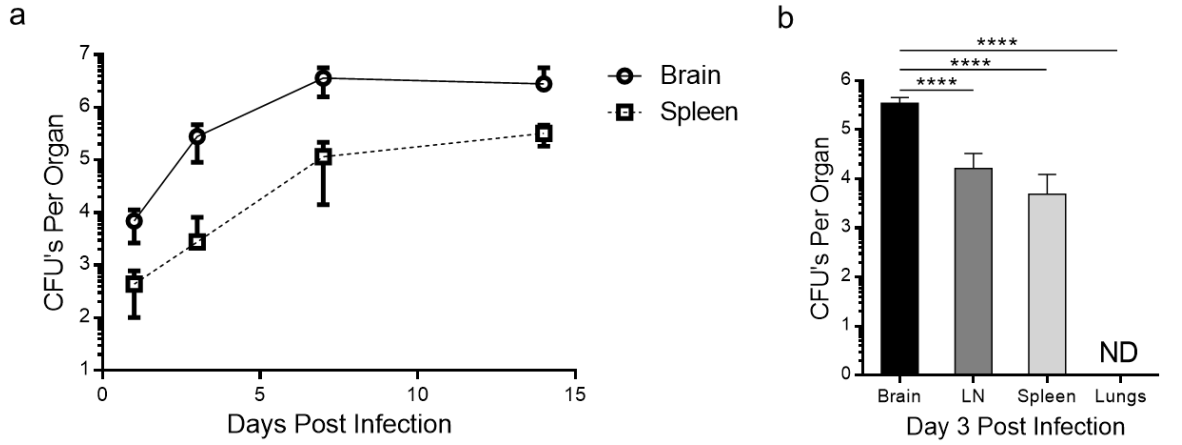

Figure 4-1: Bacterial burden analysis of *M. tuberculosis* infected C57Bl/6 mice.
C57BL/6 mice were intracerebrally infected with 1x10^5 CFUs of *M. tuberculosis*. Organs were harvested at various timepoints and prepared for CFU enumeration. Bacterial burden of the brain and spleen were determined at 1-, 3-, 7- and 14-days post infection (a). The brain is depicted by open circles and solid line and the spleen is represented by open squares connected by a dotted line. At day 3 post infection dissemination to other organs were compared to the bacterial burden of the brain (b). The black bar symbolizes brain CFUs, the dark grey is for the lymph nodes, the spleen is represented by light grey and no CFUs were detected in the lungs at day 3 post infection. Data is shown as mean ±SD and the Student's t-test was used for significance (****p<0.0001).

4.2 Innate immune responses to CNS-TB.

4.2.1 Neuronal responses to *M. tuberculosis* infection.

M. tuberculosis bacilli infect various cell types in the CNS including neurons (Randall *et al*., 2014, Randall *et al*., 2015). The previous chapter confirmed that neurons can generate an immune response to *M. tuberculosis* infection in culture. Next, neuronal responses to *M. tuberculosis* infection was investigated *in vivo* to provide physiological context, in mice which were intracerebrally challenged, and data analysed by flow cytometry. In this study, Beta-III-tubulin^{+} neurons (Appendix Figure A-4) were assessed for MHC class I expression as a determinant of cell activation. Although contentious, MHC class I expression by neurons was previously reported (Neumann *et al*., 1995, Liblau *et al*., 2013). Furthermore, neuronal expression of MHC class I has been directly linked to T cells activation (Chevalier et al., 2011, Cebrian et al., 2014), despite not being professional APCs. Significant increases in the percentage of neurons expressing MHC class I was observed at both 7- ($p<0.01$) and 14-days ($p<0.0001$) post infection in *M. tuberculosis* infected mice compared to saline inoculated mice (Figure 4.2 a). The data indicates a significant increase in immunologically active neurons during bacterial infection. Expression of MHC class I suggests a direct neuro-immune cross reactivity and the potential to activate cytotoxic CD8^{+} T cells and NK cells.

The contributions of lL1β, TNF, IL6 and IL10 in host immunity to CNS-TB have been extensively studied and has been suggested to be an indication of a functional immune response (Randall et al., 2014, Francisco et al., 2015, Hsu et al., 2017). Production of neuronal cytokines IL1β, TNF, IL6 and IL10 in response to *M. tuberculosis* infection *in vivo* was measured. The comparison between control mice and infected mice at 7- and 14- days post infection showed no significant differences in percentage of neurons expressing IL1β, TNF, IL6 and IL10 (Figure 4.2). The data indicates that neurons do not produce a *M. tuberculosis* specific pro-inflammatory response during acute CNS-TB infection.

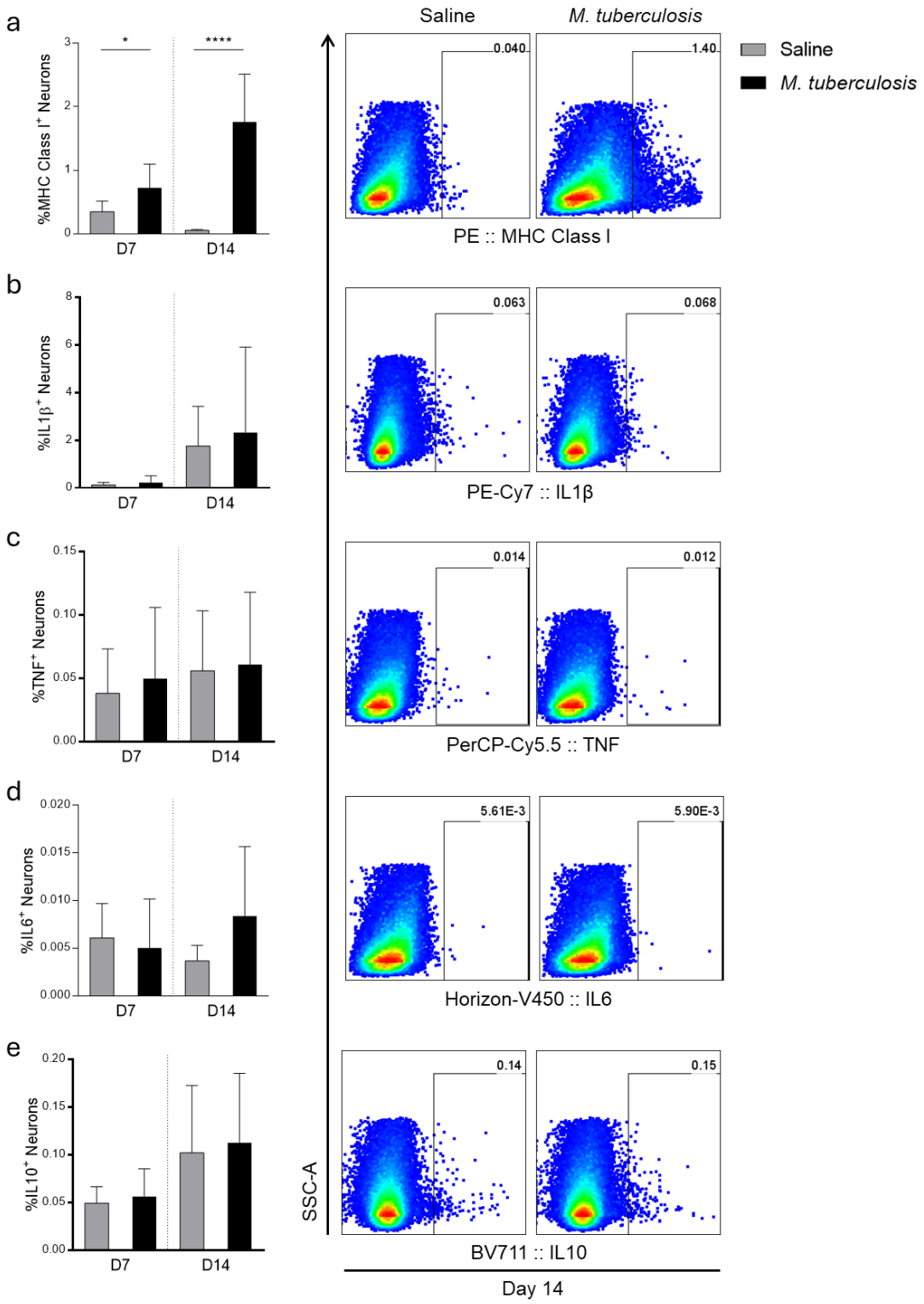

Figure 4-2: Neuronal responses to CNS-TB infection.
C57BL/6 mice were intracerebrally infected, and the neuronal responses were analysed by flow cytometry at 7- and 14- days post infection. Percentages of β-III-tubulin⁺ neurons expressing (a) MHC class I, (b) IL1β (c) TNF (d) IL6 and (e) IL10 were evaluated. The results are expressed as mean ± SD and are representative of pooled samples from two similar experiments (n = 3-5 mice/group per time point). The grey bars represent saline inoculated mice, and the black bars represent *M. tuberculosis* infected mice. Significant differences (*p<0.05; ****p<0.0001) were determined by Student's t-tests.

4.2.2 Microglial responses to *M. tuberculosis* infection.

Microglia are critical immune effector cells and the first line of defence in response to CNS-TB (Spanos *et al*., 2015). Microglia were analysed by flow cytometry as $CD45^{lo}CD11b^{+}$ cells (Appendix Figure A-5) and no significant differences were observed in the percentage of microglia at 7- and 14- days post infection between saline inoculated mice and *M. tuberculosis* infected mice (Figure 4.3 a). Next immune functionality of microglia was determined by measuring the expression of MHC class II, IL1β, INOS and IL12. As a resident antigen presenting cell within the CNS, activated microglia can initiate a crosstalk with infiltrated T cells by increasing surface expression of MHC class II for antigen presentation. A study by Djukic *et. al.* 2006 showed that microglia change morphology and upregulate MHC class II in response to bacterial infection in the brain (Djukic *et al*., 2006). The percentage of microglia expressing MHC class II in *M. tuberculosis* infected mice was significantly increased from 14 days ($p<0.0001$) post infection compared to the saline inoculated groups (Figure 4.3 b).

Microglia actively produce pro-inflammatory cytokines in response to bacterial infection (Rock *et al*., 2004, Mariani and Kielian, 2009). IL1β was previously shown to be upregulated in macrophages in response to *M. tuberculosis* (Krishnan *et al*., 2013). It was therefore surprising to note equivalent IL1β levels between infected mice and the saline group (Figure 4.3 c). Macrophages infected with *M. tuberculosis* were found to increase INOS production (Landes *et al*., 2015). Furthermore, microglia were shown to be major producers of INOS in response to viral infection (Marques *et al*., 2008). In the current study there were no differences observed in the specific induction of INOS because of *M. tuberculosis* infection at these time points (Figure 4.3 d).

IL12 deficient mice showed uncontrollable mycobacterial growth (Cooper *et al*., 1997), demonstrating its importance for immune protection during tuberculosis. Microglia have also been shown to produce IL12 after stimulation (Aloisi *et al*., 1997). Therefore, this study investigated IL12 production by microglia post *M. tuberculosis* infection. There were however no statistically significant differences observed between *M. tuberculosis* infected and saline challenged mice (Figure 4.3 e). The data shows functional differentiation based on MHC class II expression and

suggests equivalent acute microglial cytokine responses to infection and inflammation.

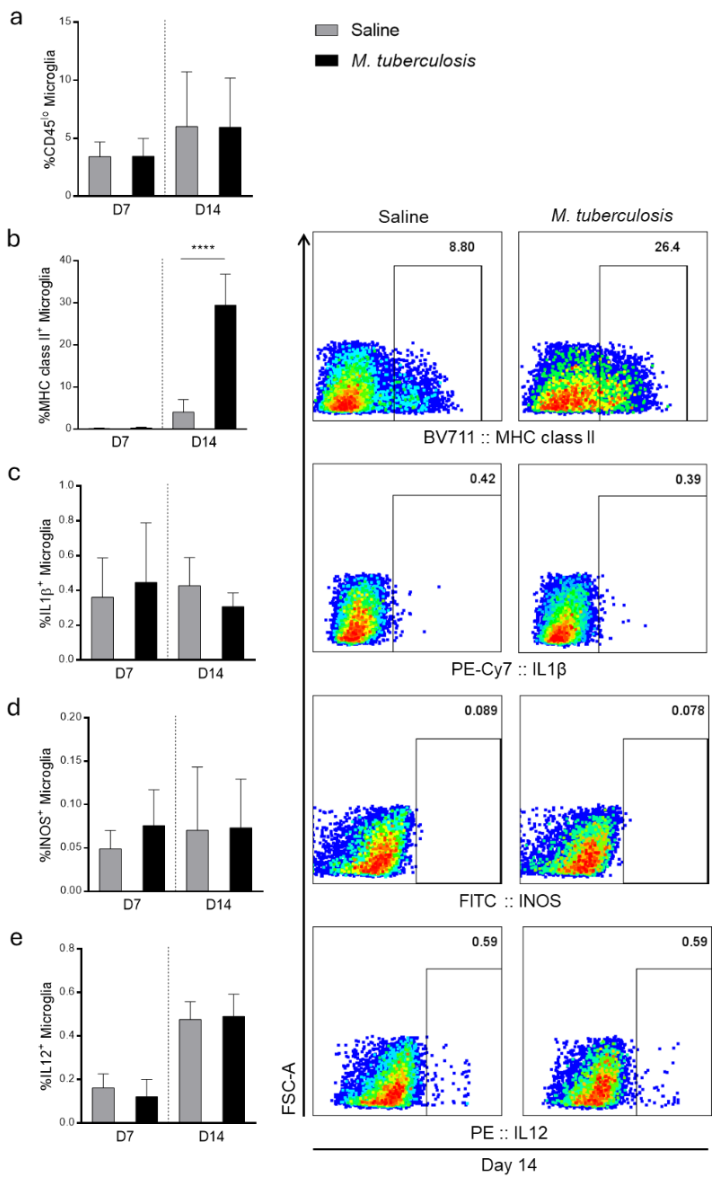

Figure 4-3: *M. tuberculosis* infection increases the potential of antigen presentation by microglia.
The percentage of $CD45^{lo}CD11b^{+}$ microglia were analysed (a), followed by determining the activation status through examining the percentage of MHC class II^{+} microglia (b) and microglia expressing IL1β (c), INOS (d) and IL12 (e). The grey bars represent saline inoculated mice, and the black bars represent *M. tuberculosis* infected mice. The data is representative of pooled samples from two separate experiments and is displayed as mean ±SD (n= 3-5 mice/group). The student T-test was used to determine significance (****p<0.0001).

4.2.3 Leukocyte recruitment and activity.

Trafficking of peripheral immune cells to the CNS is strictly controlled, however lymphocytes can transverse the blood brain barrier for surveillance under normal and pathological conditions. In previous studies, authors have shown the recruitment of $CD45^{hi}$ cells to the mouse brain after 2 weeks of intracerebral infection which is regulated by TNF during cerebral *M. tuberculosis* infection (Francisco *et al*., 2015, Hsu *et al*., 2017). In this study cellular recruitment was assessed in the brains of *M. tuberculosis* infected and saline inoculated mice by flow cytometry where recruited leukocytes were identified as $CD45^{hi}$ cells (Appendix Figure A-5). The data shows no significant difference in recruitment of peripheral leukocytes (Figure 4.4 a) between infected and saline challenged mice at both 7- and 14- days post infection and suggests an equivalent potential for cellular recruitment to the brain during both sterile inflammation and microbial infection at these early time points.

Although, the number of leukocytes recruited to the brain under infectious and non-infectious conditions were equivalent, it was important to investigate whether cell functionality differed under the respective conditions. Evaluation of the percentage of leukocytes expressing IL1β indicated a significant difference at day 7 ($p<0.05$) in *M. tuberculosis* infected mice as compared to saline challenged mice (Figure 4.4 b). However, this difference did not persist to day 14 post infection. $CD45^{hi}$ cells expressing IL12 did not show any differences between the two groups of mice were observed at both 7- and 14- days post infection (Figure 4.4 c). Furthermore, INOS expression by leukocytes also did not provide statistically significant differences between infected and saline control mice (Figure 4.4 d). Finally, the percentage of leukocytes expressing MHC class II in *M. tuberculosis* infected mouse brains was significantly higher than saline challenged mice at 14 days ($p<0.0001$) post infection (Figure 4.4 e). Collectively the data indicated that *M. tuberculosis* directly induces cellular antigen presentation potential and highlighted differences in recruitment of cells under physiological and pathological conditions. The data supports a robust proinflammatory response which is essential for protective immunity against *M. tuberculosis* infection in the brain.

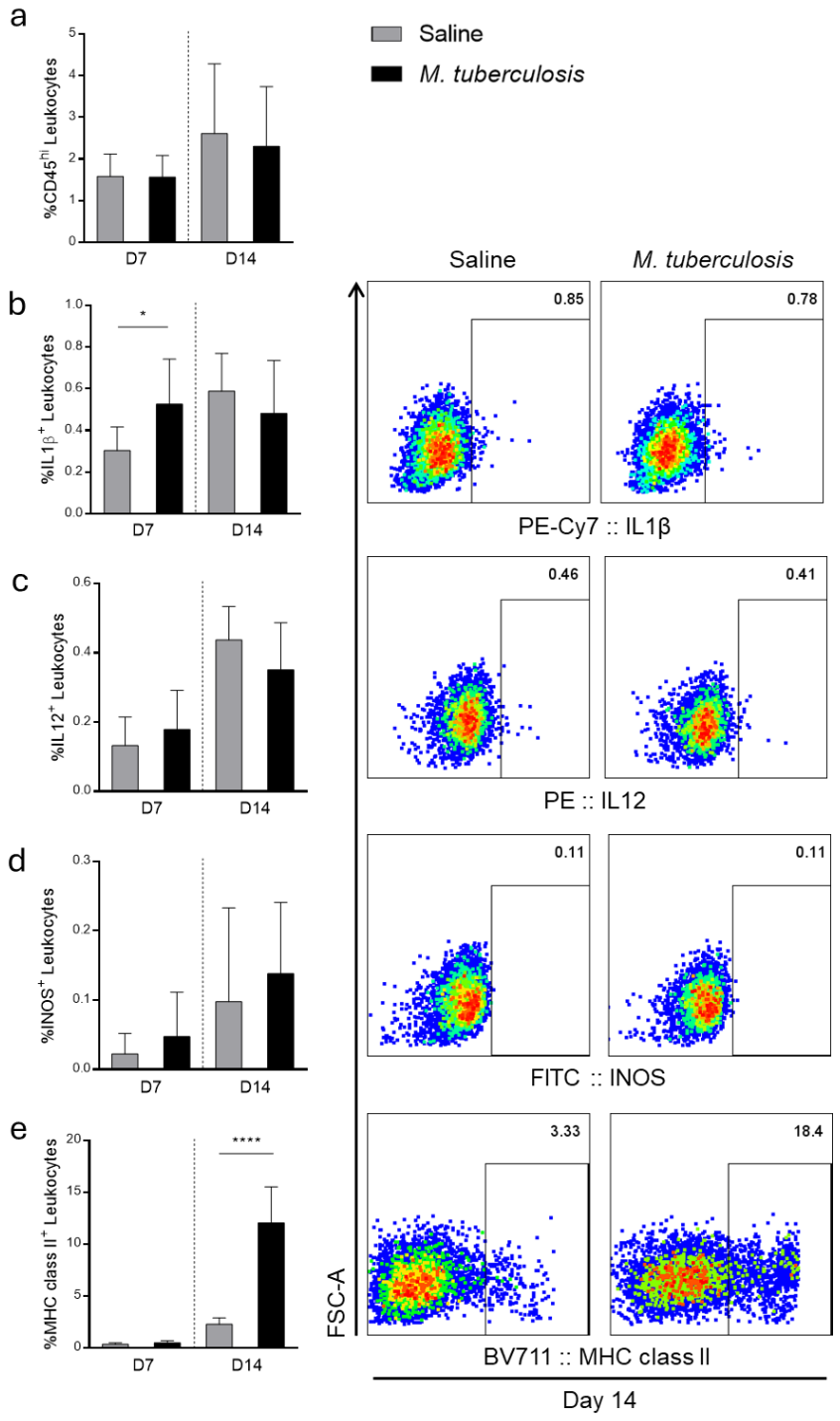

Figure 4-4: Leukocyte recruitment and cytokine responses.
Mouse brains were processed for flow cytometric analysis and the percentage of CD45^{hi} recruited cells were isolated at day 7 and day 14 post infection (a). The cells were further analysed for IL1β (b), IL12 (c) and INOS (d) production. The data shown is expressed as mean ± SD (n= 3-5 mice/group) and is representative of pooled samples from two separate experiments. Statistical significance (*p<0.05; ****p<0.0001) was determined by Student's t-tests. The grey bars represent saline inoculated mice, and the black bars represent *M. tuberculosis* infected mice.

4.3 Early adaptive immune responses in the brain of *M. tuberculosis* infected mice.

T cells generate “immune memory” as part of their function and go through 3 basic stages during an immune response namely expansion after being primed by APCs for a specific pathogen, followed by contraction when the infection is resolved and finally the generation of short term effector memory or long term central memory T cells, which occurs after infection (Ahmed and Gray, 1996). Education of T cells occur within the primary and secondary lymphoid organs and after activation and expansion the T cells migrate to the site of infection where they produce specific immune regulatory cytokines which drive specific immune response (Saenz *et al*., 2013).

T cells have previously been identified as critical for immune protection during pulmonary mycobacterial infection (Xing *et al*., 1998), however the manner in which T cells contribute to immunity during CNS-TB are limited. In this study, T cell phenotypes and functionality were investigated to gain insight into its potential functionality. Brain samples from mice infected with *M. tuberculosis* for 7- and 14-days were processed for flow cytometric analysis, using the gating outlined in Appendix Figure A-6, in which $CD3^+CD4^+$ T cells were identified and analysed. The percentage of $CD4^+$ T cells recruited to the brains were equivalent at both 7- and 14-days post infection for both the conditions (Figure 4.5 a).

T cell activation is associated with CD44 expression (Huet *et al*., 1989). Evaluation of $CD4^+$ T cells expressing CD44 showed no difference between the *M. tuberculosis* infected and non-infected groups at day 7 (Figure 4.5 b). However, at day 14 there were significantly ($p<0.0001$) more $CD4^+CD44^+$ T cells detected in infected brains compared to saline inoculated brains. The data therefore indicates *M. tuberculosis* specific activation of $CD4^+$ T cells in the brain, which is consistent with the results of previous studies (Hsu et al., 2017).

T cells can differentiate into various effector types, driven by the upregulation of specific transcription factors which control proinflammatory, anti-inflammatory and regulatory responses (Zhu and Zhu, 2020). In this study, the $CD4^+$ T cells were analysed for TBet, FoxP3, Gata3 and RorγT transcription factor expression to assess priming of specific cell-type responses. The percentage of proinflammatory

$CD4^+$ T cells expressing the T_H1 transcription factor TBet was significantly increased at 14 days ($p<0.001$) post infection compared to control mice (Figure 4.5 c). The percentage of $CD4^+$ T cells expressing the T-regulatory transcription factor FoxP3 showed a significant ($p<0.01$) increase 14 days after infection (Figure 4.5 d) and a surprising significant increase in T_H2 Gata3 at day 14 post infection (Figure 4.5 e). While the T_H17 RorγT expressing $CD4^+$ T cells (Figure 4.5 f) did not show any differences between the two groups. Therefore, the data reveals an early T_H1 mediated protective proinflammatory immune response to CNS-TB. The findings are consistent with a previous study where TBet deficient mice were unable to control *M. tuberculosis* growth and eventually succumb to infection (Sullivan *et al*., 2005). The induction of FoxP3 T cells suggests concomitant but delayed initiation of regulatory mechanisms which was complimented with T_H2 mediated processes to maintain homeostatic conditions within the CNS in response to *M. tuberculosis* infection. The data further indicates that T_H17 T cells are redundant for resolution of infection.

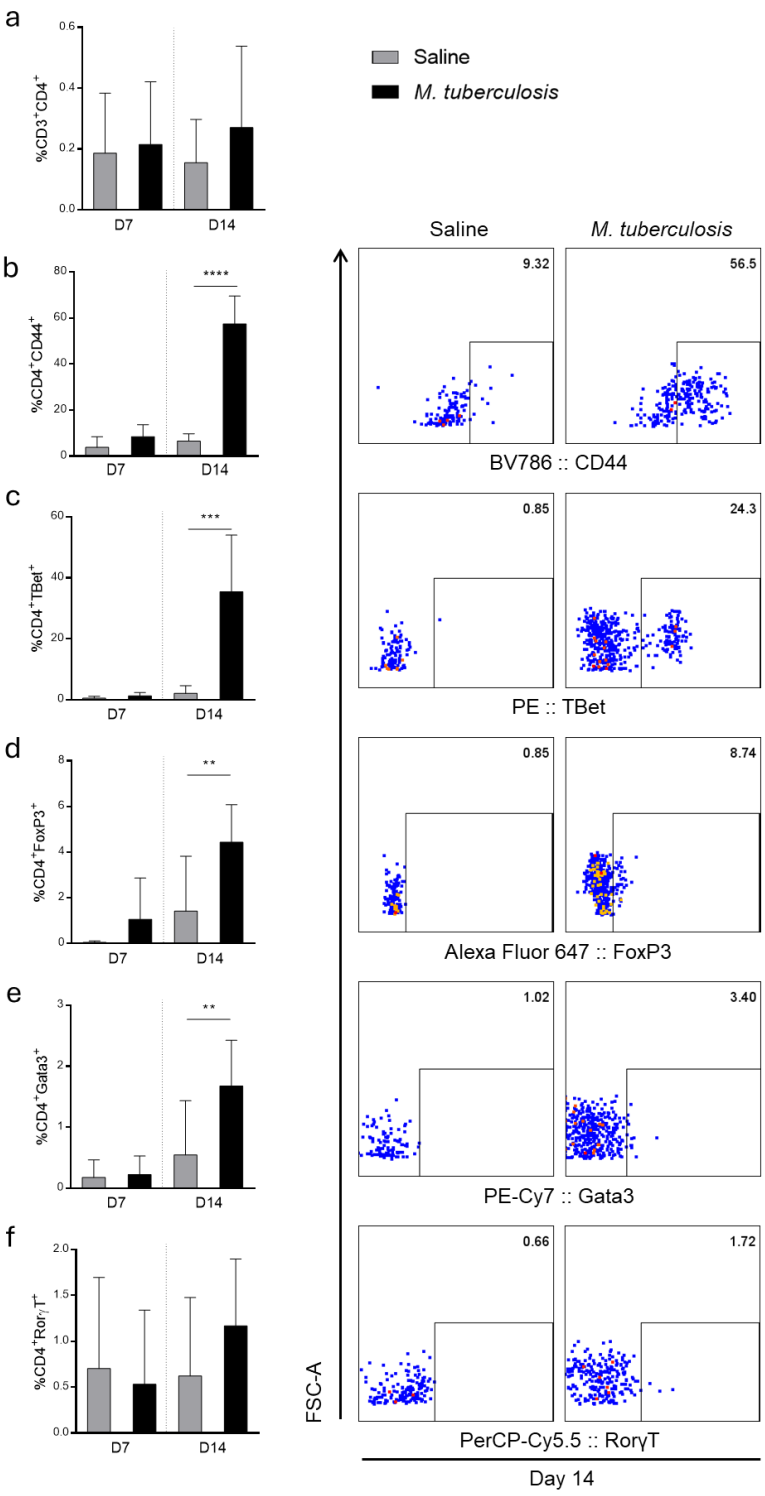

Figure 4-5: CD3⁺CD4⁺ recruitment and activation in the brains of *M. tuberculosis* infected mice.

Mice intracerebrally infected with *M. tuberculosis* H37Rv for 7- and 14- days were sacrificed and the brains were harvested for flow cytometry analysis preparation. The percentage of CD3⁺CD4⁺ T cells (a) were assessed for the activation maker CD44 (b) and transcription factors TBet (c), FoxP3 (d), Gata3 (e) and RorγT (f). The respective representative flow cytometry plots for day 14 post infection are displayed as well. Significance (*p<0.05; **p<0.01; ***p<0.001) was determined by using the student T-test. The data is representative of pooled samples from two separate experiments and is displayed as mean ±SD (n= 3-5 mice/group).

$CD3^+CD8^+$ T cells analysis was conducted using the gating strategy in Appendix Figure A-6. No significant differences were found in the recruitment of $CD8^+$ T cells to the brain between saline inoculated and *M. tuberculosis* infected mice at both 7- and 14- days post-infection (Figure 4.6 a). The analysis of $CD8^+CD44^+$ T cell showed significant ($p<0.0001$) increases in $CD8^+$ T cell activation at 14 days post infection in the *M. tuberculosis* infected mice compared to the saline inoculated mice (Figure 4.6 b). Furthermore, $CD8^+$ T cells expressing the pro-inflammatory TBet ($p<0.0001$) and regulatory FoxP3 ($p<0.05$) transcription factors, significantly increased in infected mice compared to saline inoculated mice at 14 days post infection (Figure 4.6 c-d). No significant differences were observed in $CD8^+$ T cells which expressed Gata3 (Figure 4.6 e) or RorγT (Figure 4.6 g) transcription factors. This data shows that the overall recruitment of $CD8^+$ T cells was equivalent during *M. tuberculosis* infection and saline challenge, but the overall T cell profiles were directed towards infection control and maintenance of homeostasis in the infected mice.

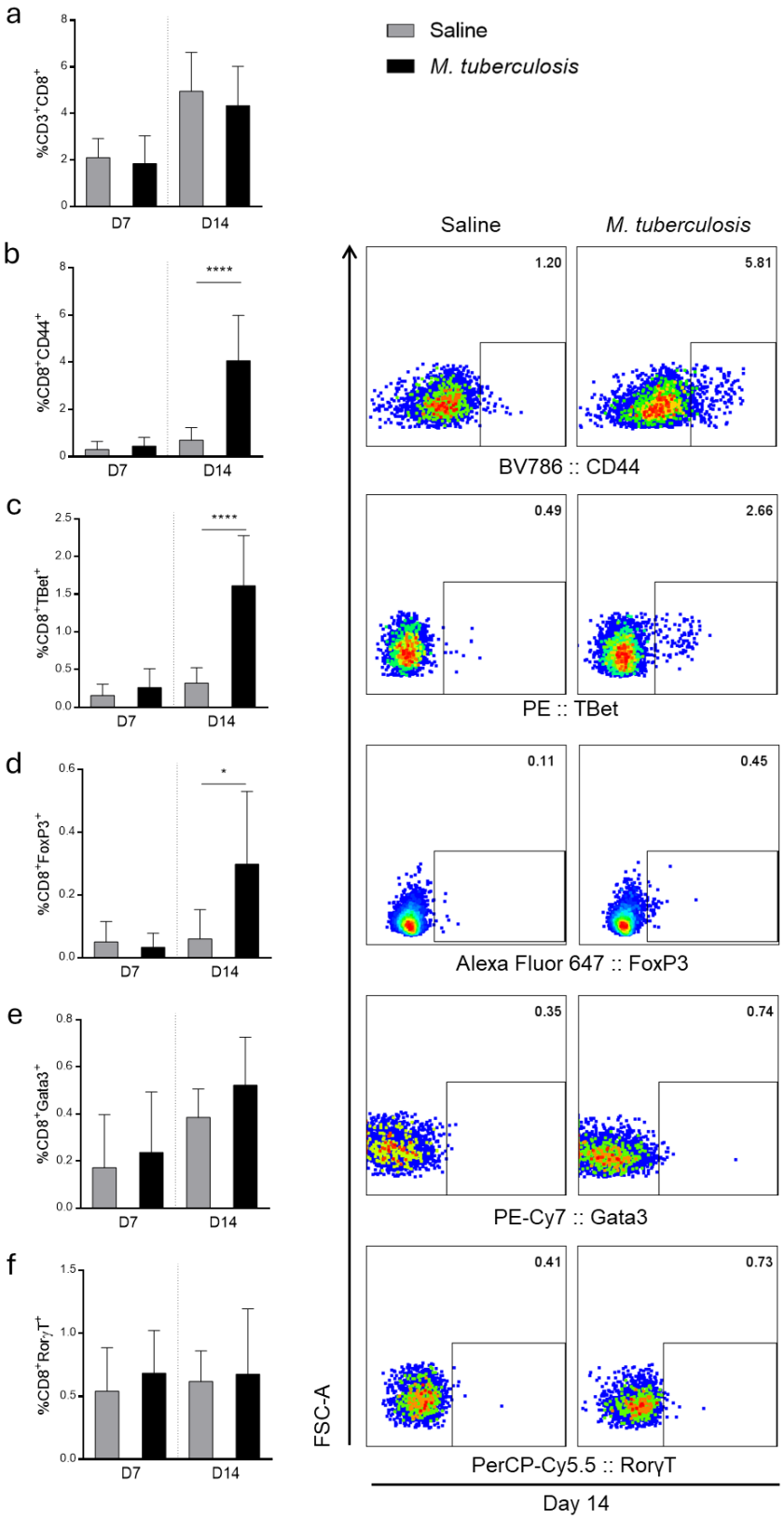

Figure 4-6: CD3⁺CD8⁺ recruitment and activation.
The percentage of CD3⁺CD8⁺ T cells (a) was analysed for CD44 (b), TBet (c), FoxP3 (d), Gata3 (e) and RorγT (e). The results are expressed as mean ± SD and are representative of pooled samples from two similar experiments (n = 3-5 mice/group per time point).

4.4 Investigating lymphocytic contributions in resolving CNS-TB.

4.4.1 Comparison of CNS-TB infection in NSG and C57BL/6 mice.

To understand the contribution of recruited lymphocytes to immune protection during CNS-TB, the immune competent C57BL/6 mice and immune compromised NSG mice were intracerebrally infected with $1x10^5$ CFUs *M. tuberculosis* or challenged with saline. NSG mice are highly immune compromised and have a severe deficiency in lymphocytes. Comparative outcomes between NSG and C57Bl/6 mice are therefore focussed on lymphocytic contributions to resolving mycobacterial infection. The body condition of *M. tuberculosis* infected C57BL/6, *M. tuberculosis* infected NSG, saline C57BL/6 and NSG saline inoculated groups were monitored for 14 days and assessed for their physical conditions which included body condition, grimace scale and clinical scoring. All groups presented with a normal clinical condition score of 1 (Figure 4.7) except for *M. tuberculosis* infected NSG mice. With a score of 1, mice did not show any signs of infection or injury and were well groomed, maintained good mobility and showed good activity and alertness. There were no visible signs of orbital tightening, nose bulge, cheek bulge, ear drooping and whisker changes (grimace scale score - 1). Moreover, these mice all presented with normal posture and breathing and no visible signs of neurological trauma. In contrast, *M. tuberculosis* infected NSG mice had poor body conditioning and showed poor grooming, low mobility and reduced activity (body condition score - 2). *M. tuberculosis* NSG mice also presented with orbital tightening, cheek bulging and ear drooping producing a grimace scale score of 3. Furthermore, some mice developed neurological conditions such as staggering, incoordination and circling, and had a hunched posture. This data suggests that immune deficient mice can recover from sterile surgery but develop clinical signs of health deterioration when intracerebrally infected with *M. tuberculosis*.

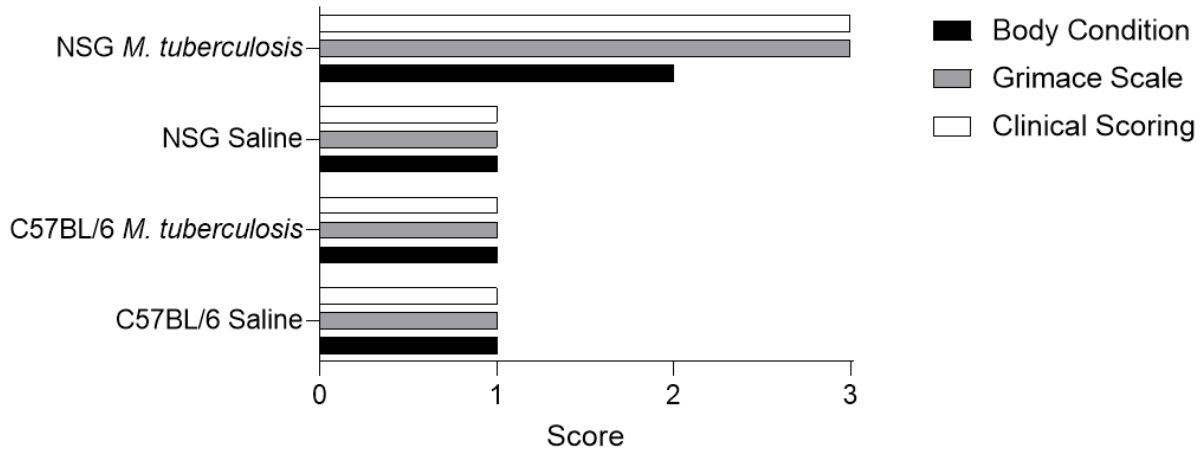

Figure 4-7: Comparison of physical condition between C57BL/6 and NSG mice post M. tuberculosis infection.
Assessment of the physical conditioning of the mice was performed after 14 days of *M. tuberculosis* infection and saline challenge. Body condition, grimace scale and clinical scoring were assessed. Body condition (grooming and nourishment): 1- Normal body condition, 2- under conditioned. Grimace Scale (orbital tightening, nose bulge, cheek bulge, ear drooping and whisker): 1- None present, 2- one or two signs present, 3- more than two signs present. Clinical scoring (staggering, incoordination and circling producing and had hunched posture): 1- None present, 2- one or two signs present, 3- more than two signs present.

Body weight change is considered a reliable indicator of health status and was measured over the 14 days period after intracerebral challenge. A decrease in body weight measured after 24 hours indicated that all the mice presented with post-operative weight loss (Figure 4.8 a), an observation consistent with previous studies (Weiergraber *et al*., 2005, Kirby *et al*., 2012, Francisco *et al*., 2015). By day 7 all the mice recovered to their initial baseline weight. There was a significant decline in the bodyweights of *M. tuberculosis* infected NSG mice at day 14 post infection with an average bodyweight loss of 25% while all other groups maintained their body weights.

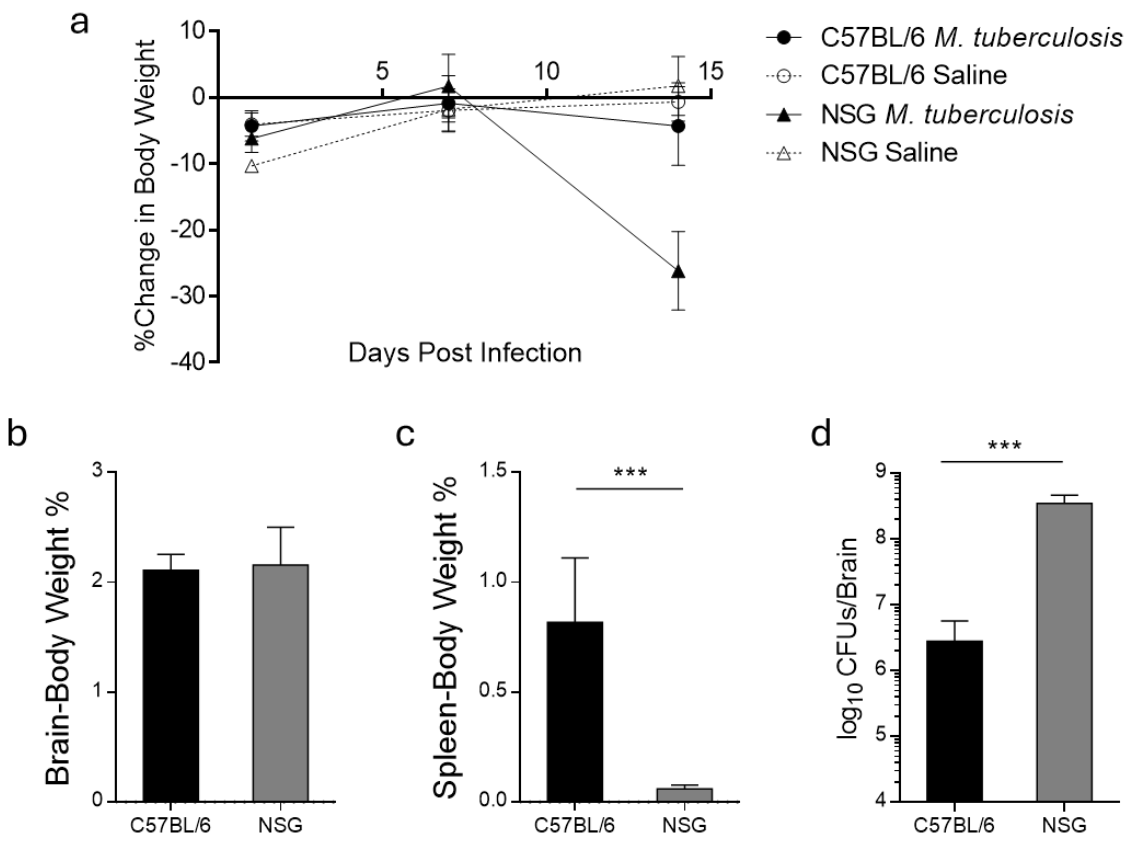

Figure 4-8: Body weight changes in infected C57BL/6 vs NSG mice.
Intracerebrally infected C57BL/6 and NSG mice were monitored for two weeks post infection. The change in body weight was recorded showing the over a 14-day period (a). Filled circle and triangle represents *M. tuberculosis* infected C57BL/6 and NSG mice. Empty circle and triangle indicate saline inoculated control C57BL/6 and NSG mice. The brain (b) and spleen (c) to body weight ratios were assessed. The differences in bacterial burdens were analysed (e). The data is expressed as mean ± SD and significant differences (***p<0.001) were determined by Student's t-tests.

The brain and the spleen weights of infected mice were calculated as a percentage of the total mouse body weight at day 14 post infection as a representation of disease progression. The brain to body weight ratio showed no difference between the C57BL/6 and the NSG infected mice (Figure 4.8 b), while the spleen to body weight ratio showed a statistically significant percentage differences because of the lack of lymphocytes in the spleen (Figure 4.8 c). Comparative bacterial burdens within the brains revealed that NSG mice were unable to control *M. tuberculosis* proliferation (Figure 4.8 d). Increase bacilli burden and ultimately death was therefore associated with the absence of functional lymphocytes required to control CNS mycobacterial infection. The study aligns with a previous report by Hsu *et al.*, which showed that immune competent T cells are essential for protection against CNS-TB (Hsu *et al*., 2017).

4.4.2 Neuronal immune responses to *M.* tuberculosis in immune deficient mice.

Neurons are immunologically responsive to *M. tuberculosis* infection *in vitro* (Randall *et al*., 2014). The ability of neurons to produce immune responses to *M. tuberculosis* infection was further shown *in vivo* in the current study (Figure 4.2). Neuronal crosstalk with immune cells can result in altered neuronal and/or immune cell activity depending on the response (Tian *et al*., 2012). In the current study, the culture medium from infected neurons were able to stimulate and activate leukocytes (Figure 3.16). To further explore the contribution of the peripheral immune system to neuronal activation *in vivo*, the immunodeficient NSG mice were intra-cerebrally infected with *M. tuberculosis* for 17 days, after which single cell suspensions of brains were generated and processed for flow cytometric analysis to study neuronal immune activity in the absence of functional lymphocyte recruitment to the CNS.

Active neurons in *M. tuberculosis* infected NSG mice were assessed by measuring cell surface expression of MHC class I, intracellular expression of IL1β, TNF, IL6 and IL10, and comparing outcomes to saline challenged NSG mice. The data showed that the percentage of neurons expressing MHC class I from infected NSG mice were significantly higher ($p<0.01$) compared to the percentage of neurons from the saline challenged mice (Figure 4.9 a). However, there was no differences detected in the percentage of neurons expressing IL1β (Figure 4.9 b), TNF (Figure 4.9 c), IL6 (Figure 4.9 d) and IL10 (Figure 4.9 e). This data shows that *M. tuberculosis* activated neurons have the potential to present antigen.

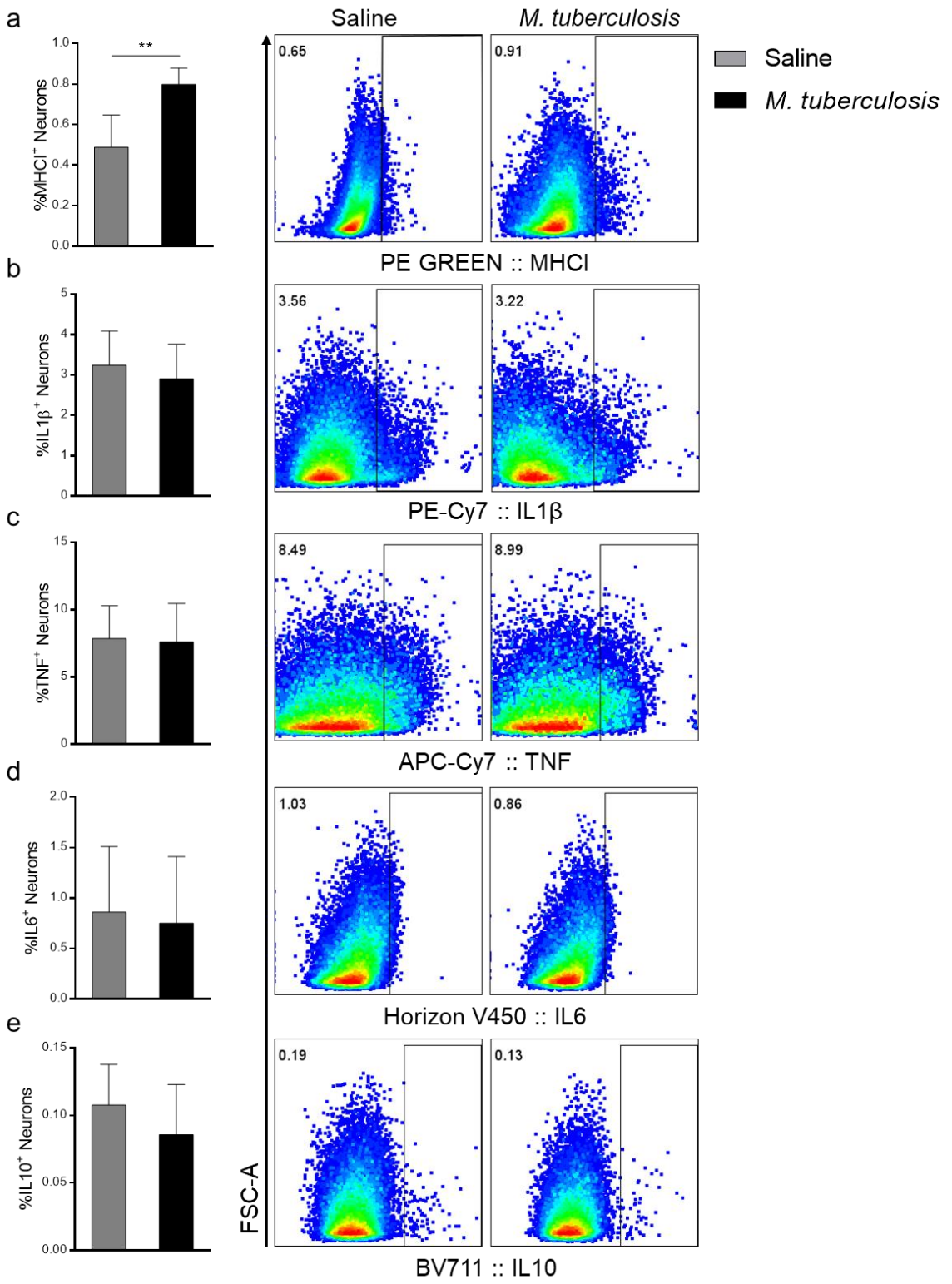

Figure 4-9: Neuronal responses to CNS-TB infection in immune deficient mice.
NSG mice were intracerebrally infected, and the brains were harvested for analysis of neuronal responses by flow cytometry 16 days post infection. β-III-tubulin$^+$ neurons expressing MHC class I (a), IL1β (b), TNF (c), IL6 (d) and IL10 (e) were isolated. The results are expressed as mean ± SD and the Student's t-tests was used to calculate statistical significance (**p<0.01).

4.5 *M. tuberculosis* infection of the CNS in reconstituted humanised BLT-NSG mice.

4.5.1 *In vivo* Analysis of Neuronal Immune Responses to *M.* tuberculosis Infection.

A previous model of tuberculosis in humanised mice revealed similar pathologies to human disease (Calderon *et al*., 2013). Furthermore, human leukocytes were recruited to the lungs and were responsive to *M. tuberculosis* infection. In this study, humanised mice (BLT-NSG) were generated to investigate if reconstituted human leukocytes could rescue immune deficient NSG mice from CNS-TB infection. BLT-NSG mice were generated by surgical engraftment of human foetal liver and thymus fragments, and intravenous injection of human $CD34^+$ stem cells into NSG mice as previously described (Karpel *et al*., 2015). NSG and BLT-NSG mice were intracerebrally infected with $1x10^5$ CFUs *M. tuberculosis* or challenged with saline and monitored for 17 days.

Evaluation of the body-conditioning and clinical score showed that both the saline challenged NSG and BLT-NSG presented with body conditions, grimace scales and clinical scores of 1 (Figure 4.10 a) indicative of good health with no signs of physical and neurological deterioration. In contrast, infected NSG and BLT-NSG mice were emaciated and ungroomed with a body condition score of 3, indicative of progressive disease. Both groups were scored at 3 on the grimace scales and had visible signs of orbital tightening, nose and cheek bulging, ear drooping and whisker changes. Lastly, both groups had severe clinical scores of 3 defined by hunched postures, neurological conditions of staggering and circling, and tended to be isolated and anti-social. Visual depiction of these outcomes is displayed in Figure 4.10 b where both the *M. tuberculosis* infected NSG and BLT-NSG groups are shown to have physical deterioration.

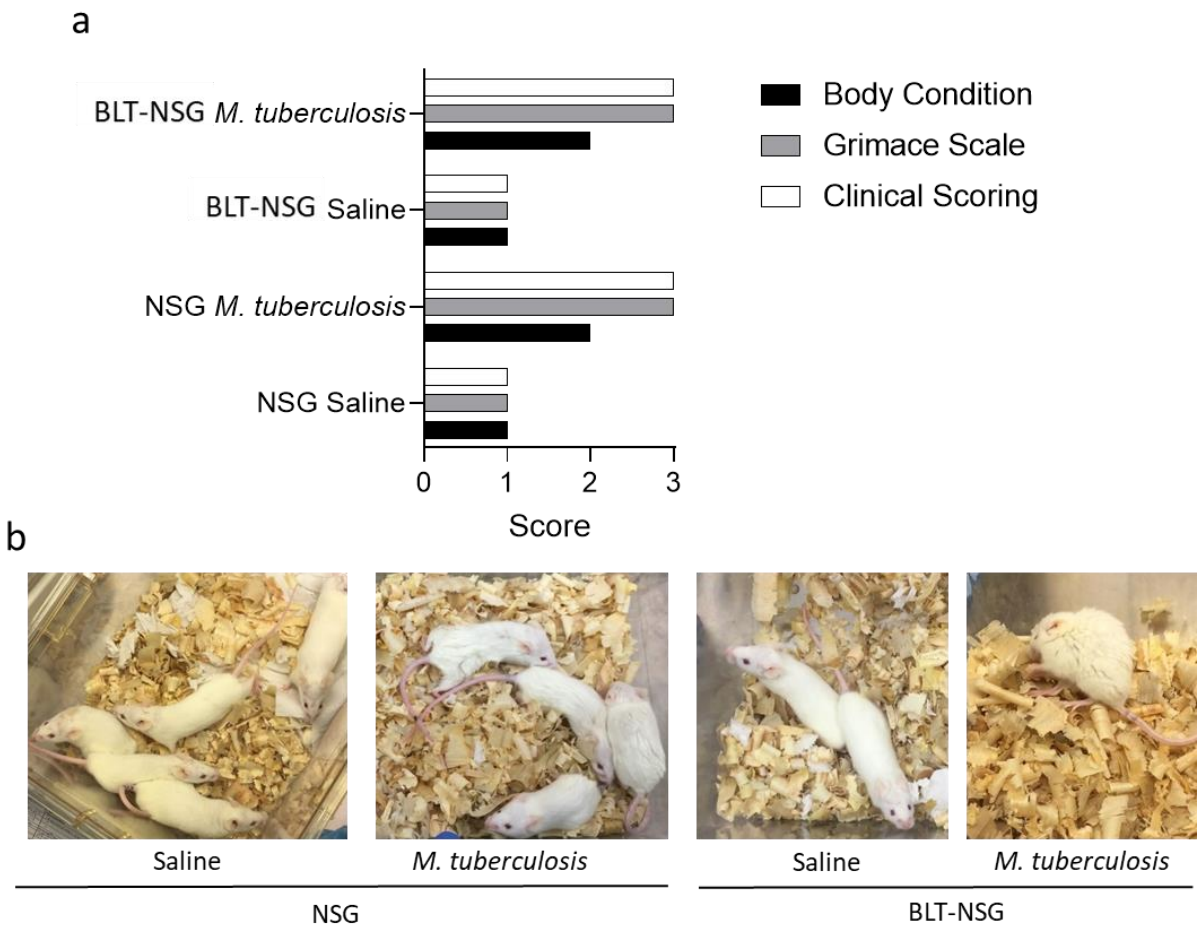

Figure 4-10: Comparison of physical condition between NSG and BLT-NSG mice post *M. tuberculosis* infection.
Mice were assessed and scored on their physical condition after 16 days of *M. tuberculosis* infection. Scores were given based on body condition, grimace scale and clinical scoring (a). Body condition (grooming and nourishment): 1- Normal body condition, 2- under conditioned. Grimace Scale (orbital tightening, nose bulge, cheek bulge, ear drooping and whisker): 1- None present, 2- one or two signs present, 3- more than two signs present. Clinical scoring (staggering, incoordination and circling producing and had hunched posture): 1- None present, 2- one or two signs present, 3- more than two signs present. Photographs of the corresponding mice are provided to visually support the scoring analysis (b).

As part of the animal welfare monitoring, the change in body weights was measured as an indicator of disease progression in the respective groups. All mice displayed post-operative weight loss of less than eight percent three days after surgery (Figure 4.11 a). All groups maintained their body weight through to nine days post infection and both saline inoculated NSG and BLT-NSG mice maintained their bodyweight and recovered fully by day 17. In contrast the *M. tuberculosis* infected NSG as well as *M. tuberculosis* infected BLT-NSG mice displayed substantial weight loss by day 17.

When assessing the organ to body weight ratios *M. tuberculosis* infected NSG mice and *M. tuberculosis* infected BLT-NSG mice showed significantly higher brain to body weight ratios compared to their respective saline inoculated groups (Figure 4.11 b). The spleen to bodyweight ratio was not significantly different in saline challenge NSG, saline challenged BLT-NSG or *M. tuberculosis* infected NSG mice. However, the spleen-body weight ratio of *M. tuberculosis* infected BLT-NSG mice was statistically significant compared to all other groups (Figure 4.11 c). This data suggests that spleen enlargement occurred due to cellular proliferation of the reconstituted human cell in response to *M. tuberculosis* infection.

Next, the potential of humanised BLT-NSG mice to induce a protective cerebral immune response was investigated. There were no significant differences between *M. tuberculosis* infected NSG and BLT-NSG mice with both groups having equivalent brain bacterial burdens (Figure 4.11 d). Similarly, no difference in the bacterial burdens of the spleens were detected (Figure 4.11 e). The data showed that reconstitution of NSG mice with human cells did not improve control of the CNS-TB infection and was incapable of rescue which resulted in mortality of infected BLT-NSG.

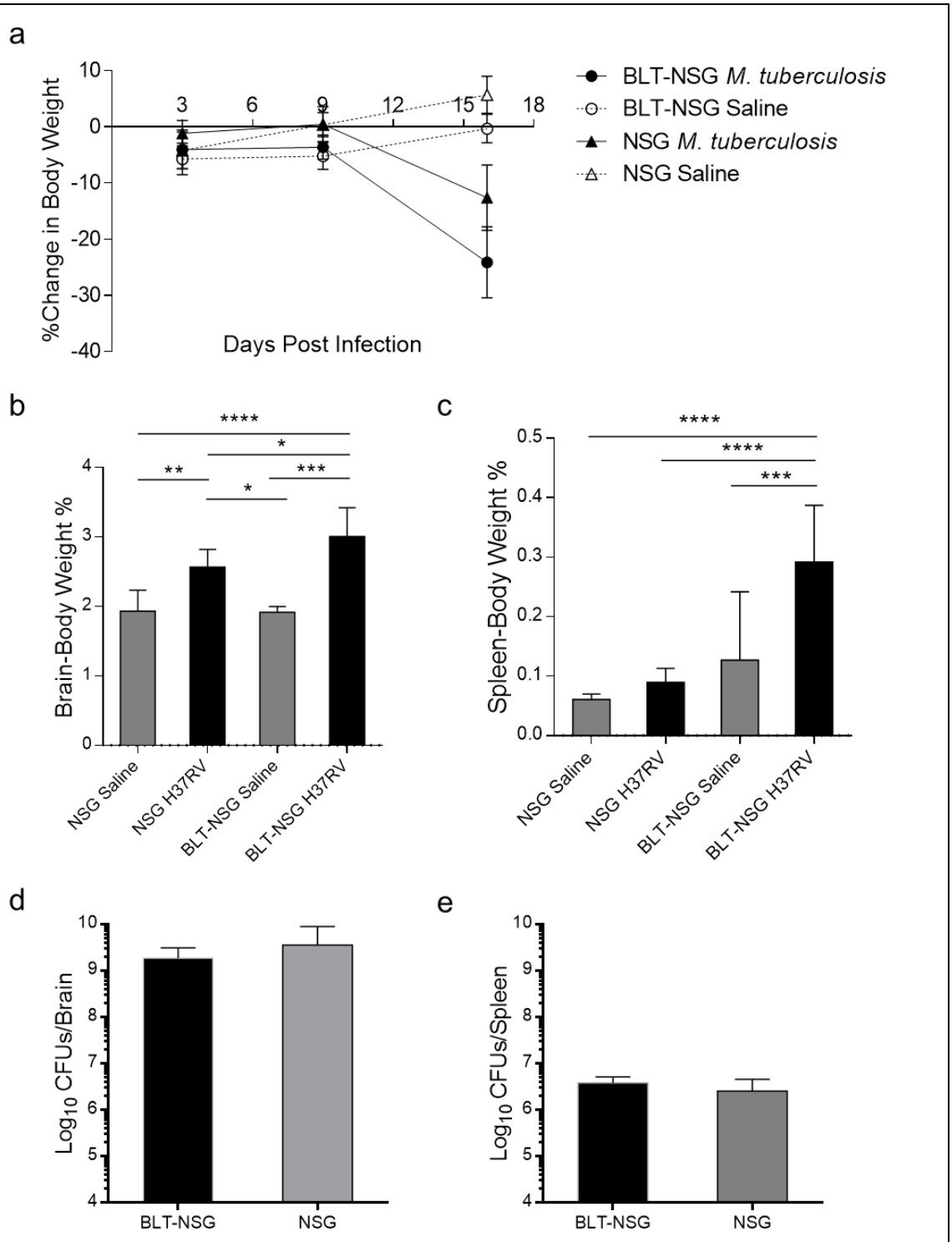

Figure 4-11: Comparison of NSG vs BLT-NSG mice intracerebrally infected with *M. tuberculosis*.
Intracerebrally infected NSG and BLT-NSG mice were monitored for 17 days post infection and the change in body weight was recorded (a). Filled circle and triangle symbols represents *M. tuberculosis* infected NSG and BLT-NSG mice respectively. Empty circle and triangle symbols indicate saline inoculated control NSG and BLT-NSG mice respectively. Thereafter the brain (b) and spleen (c) to body weight ratios were evaluated. The differences in bacterial burdens in the brains (d) and the spleens (e) were determined. The data shown as mean ± SD and significant differences (*p<0.05; **p<0.01; ***p<0.001; ****p<0.0001) were determined by ANOVA.

4.5.2 Human leukocyte cells are recruited to the brain but failed to rescue NSG mice from *M. tuberculosis* infection.

The humanised mouse model of pulmonary *M. tuberculosis* infection reveals successful recruitment of human leukocytes to the lungs (Calderon *et al*., 2013). Work reported in Chapter 4.2 showed that recruitment and activation of peripheral cells was important to control mycobacterial replication in the brains of immunocompetent C57BL/6 mice. Therefore, it was hypothesised that peripheral cells failed to be recruited to the brain during *M. tuberculosis* infection of BLT-NSG mice. To understand the potential mechanisms associated with susceptibility of BLT-NSG mice, the cellular recruitment profile in the brains of infected mice was investigated. Humanised mice were infected with *M. tuberculosis*-GFP or saline inoculated, and the brains were harvested for flow cytometric analysis at 16 days post infection. Appendix Figure A-7 shows the gating strategy used to identify and analyse recruited human leukocytes ($hCD45^+$ cells) after removing debris, doublets, and finally non-functional mouse leukocytes ($CD45^+$ cells) together with dead cells. The data showed that $hCD45^+$ cells were found in the brains of the BLT-NSG mice in response to both saline challenge and *M. tuberculosis* infection (Figure 4.12 a) indicating effective cellular trafficking of human leukocytes to the brain. The lack of bacterial control was therefore not due to failure of cell recruitment and hence did not support the initial hypothesis.

Next, the functionality of $hCD45^+$ leukocyte was assessed in the BLT-NSG mouse brains. Phagocytosis is an important mechanism for pathogen control and maintenance of homeostasis (Uribe-Querol and Rosales, 2017), which when compromised, leads to protection failure. Therefore, to analyse bacilli uptake, the percentage of $hCD45^+$ leukocytes with *M. tuberculosis*-GFP bacilli was measured by flow cytometry (Figure 4.12 b). The presence of internalised bacilli within human leukocytes implied that such cells may process antigen and present mycobacterial peptides. To investigate if the recruited $hCD45^+$ leukocytes were activated, the percentage of cells expressing HLA-DR was measured. The percentage of leukocytes expressing HLA-DR was significantly ($p<0.05$) higher in the *M. tuberculosis* infected mice as compared to the saline challenge group (Figure 4.12 c), confirming that the recruited leukocytes were indeed immunologically active.

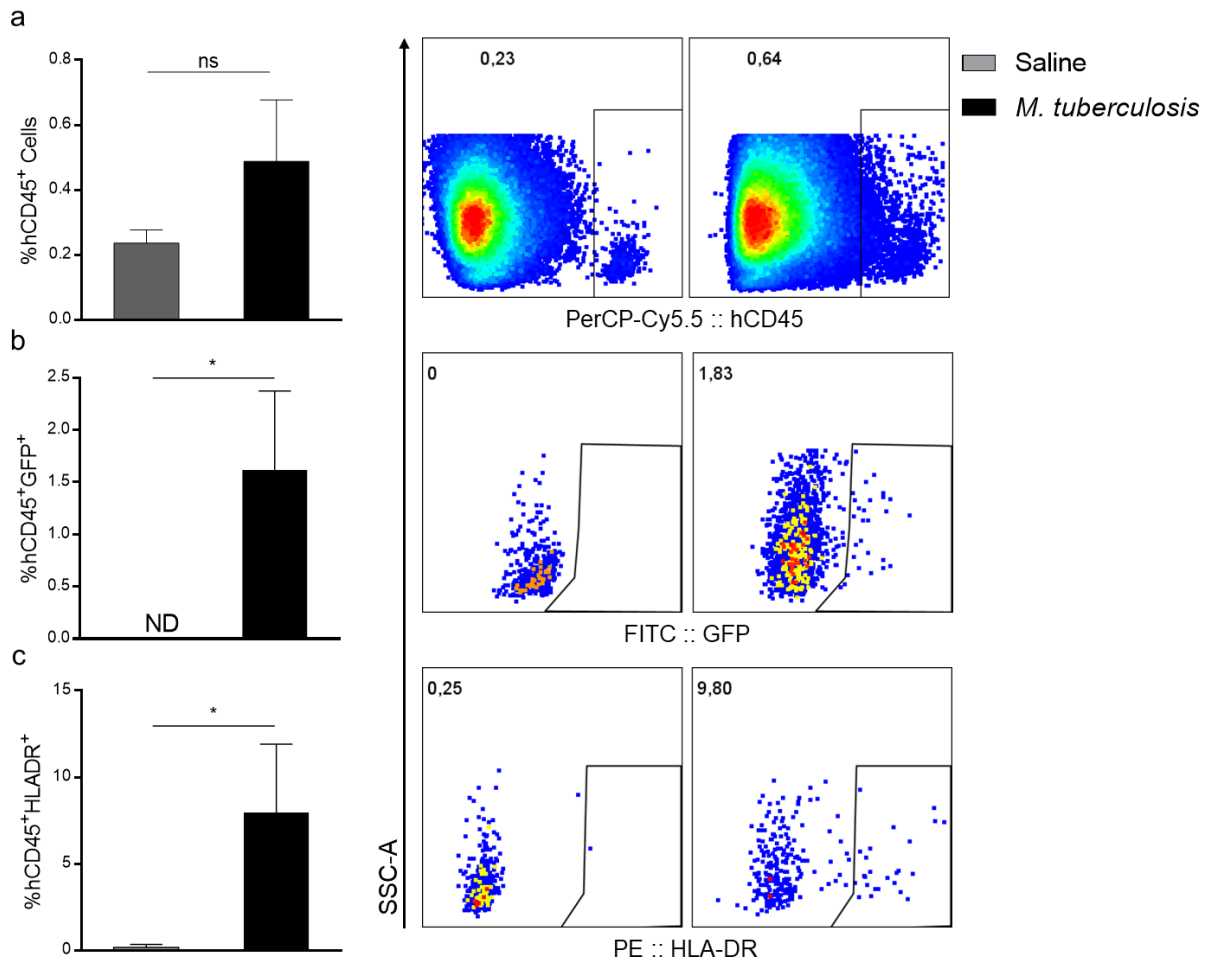

Figure 4-12: Human leukocyte recruitment to the brain.
Humanised NSG mice were infected with *M. tuberculosis*-GFP or inoculated with saline for 16 days. The brains were harvested and prepared for flow cytometry analysis. The percentage of recruited human CD45⁺ cells (a) was assessed. The recruited leukocytes were analysed for internalised *M. tuberculosis* (b) and HLA-DR (c). The data is expressed as mean ± SD and significant differences (*p<0.05) were determined by Student's t-tests.

T cell recruitment to the site of infection is imperative for mounting an effective immune response against mycobacterial infection (Xing *et al*., 1998) and require both CD4⁺ and CD8⁺ T cells subsets (Ellis *et al*., 2017, Lin and Flynn, 2015). The results from this study showed that the percentage of hCD45⁺CD3⁺ T cells were significantly ($p<0.05$) more in the *M. tuberculosis* infected mice compared to saline challenged mice (Figure 4.13 a). Furthermore, it was found that the majority of the human T cells recruited to the infected mouse brain were CD4⁺ T cells (Figure 4.13 b). CD4 T cells are known to orchestrate and regulate immune responses (Luckheeram *et al*., 2012). This data suggested that the recruitment of both human CD4 and CD8 T cells were unable to protect the BLT-NSG mice from *M. tuberculosis*

infection. Further inspection of the memory profiles of recruited human T cells showed that a significantly ($p<0.01$) larger proportion of these T cells were of the $CD3^+CD45RA^+$ phenotype compared to the $CD3^+CD45RO^+$ phenotype (Figure 4.13 c). This data was unexpected and showed that the majority of recruited T cells were of the naïve phenotype and failed to mature. Furthermore, although there was successful recruitment of immunologically active leukocytes, the percentage of recruited cells were substantially low and possibly not sufficiently effective to mediate protective immunity.

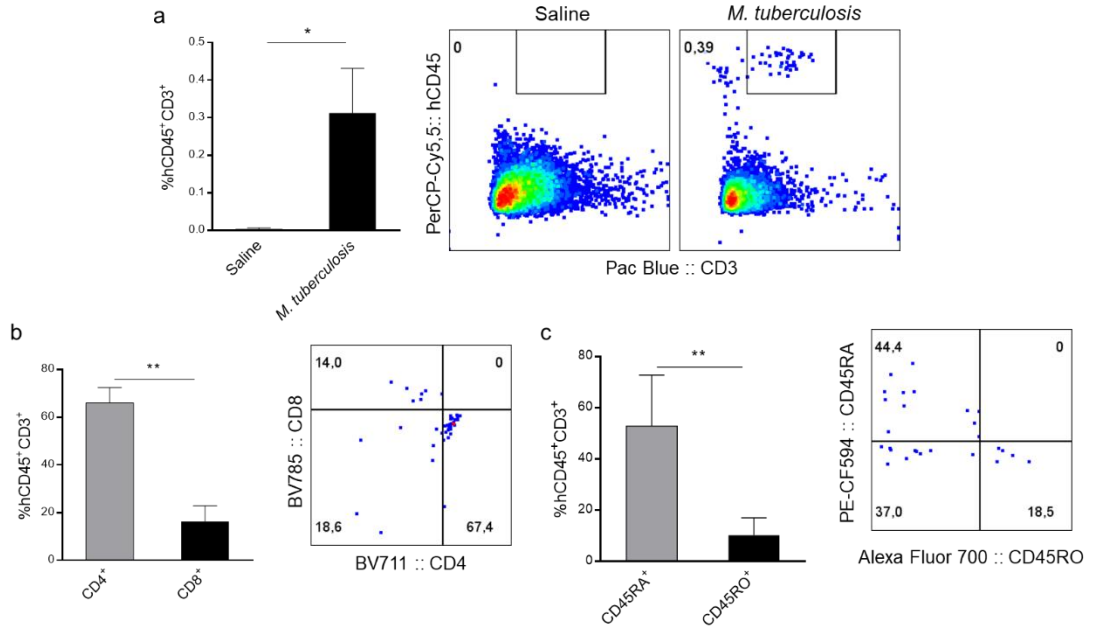

Figure 4-13: Human T cell recruitment to the infected brain.
The percentage of human $hCD45^+CD3^+$ T cells were analysed (a). Characterisation of the recruited T cell subtypes (b) and the memory phenotype was assessed (c). The Student's t-test was used to determine significance (*$p<0.05$; **$p<0.01$) and the data is shown as mean ± SD.

Chapter 5: Discussion, Conclusion & Future Studies

5 Discussion

Tuberculosis continues to be one of the leading causes of death globally and CNS-TB is one of the most extreme forms of EPTB (WHO, 2022). Much of the research which investigated host immunity of the brain against mycobacterial infection has focussed on microglial and astrocytic activity with few studies investigating neuronal immune activity. Of the limited studies, neurons have demonstrated their potential to participate in a tightly regulated neuro-immune network. The major aim of this study was to investigate the immune modulatory abilities of neurons during CNS-TB. In the current study, neurons were for the first time identified as potential immune modulatory cells in response to *M. tuberculosis* infection; novel transcriptional data revealed that neurons undergo significant gene expression changes and produce chemokines and cytokines that are capable of influencing leukocyte activation. Previously, a meta-analysis study demonstrated the importance of a functional adequate systemic immune response to protect against CNS-TB, in instances where immune-compromised individuals are at higher risk of bacteria dissemination and developing CNS-TB with high mortality rates (Navarro-Flores *et al*., 2022). Leukocyte recruitment to the site of infection is critical to mount a successful defence against *M. tuberculosis* infection (Flynn *et al*., 2011). Others have described how neurons and peripheral immune cells can communicate and contribute to CNS immunity (Tian *et al*., 2012). It was therefore important to understand how recruited immune cells can contribute to the neuro-immune network and shape a protective response against CNS-TB infection. Using a humanised mouse model of CNS-TB, this study characterized peripheral immune responses to CNS-TB and showed human immune cell recruitment to *M. tuberculosis* infected brains.

Inhalation of *M. tuberculosis* bacilli followed by dissemination to the brain is the natural route for CNS-TB infection (Hernandez Pando *et al*., 2010, Donald *et al*., 2005). Although the CNS is isolated from the periphery by the BBB to protect against neuronal pathology (Persidsky *et al*., 2006), CNS-TB occurs because of the rupturing of tuberculosis foci resulting in meningeal infection (Rock *et al*., 2008). A guinea pig model of aerosol challenge showed successful dissemination of bacilli to the CNS mimicking the natural path observed in humans (Be *et al*., 2011). Intracisternal infection of rabbits however, resulted in the most human-like outcome characterised

by increased cytokine production, protein presence and immune cell recruitment to the cerebrospinal fluid (Tsenova *et al*., 1998, Tsenova *et al*., 2005, Tsenova *et al*., 1999). Others opted for more controlled, direct intracerebral infection and while this approach did not follow the natural progression of disease it provided a platform from which important mechanistic concepts could be studied (Olin *et al*., 2008, Francisco *et al*., 2015, Hsu *et al*., 2017, Mazzolla *et al*., 2002, van Well *et al*., 2007). Many of these studies showed bacterial dissemination from the CNS to the spleen and lungs which is consistent with the present study. The use of inoculation of the brain may cause vascular damage, leading to bacilli dissemination. This study was able to successfully reproduce the direct intracerebral *M. tuberculosis* infection model which permitted the investigation of immune responses by various cell types.

Neurons are the largest population of nonprofessional immune cells within the brain and has been reported to produce proinflammatory responses to bacteria, fungi and other biological stressors (Randall *et al*., 2014, Dramsi *et al*., 1998, Aung *et al*., 2007, Lim *et al*., 2016, Alonso *et al*., 2017). In 2014 Randall and colleagues for the first time showed that neurons can be host cells for *M. tuberculosis* which manifested in functional immune responses characterised by increased cytokine expression (Randall et al., 2014). The authors showed that neurons were capable of inducing cytokines such as IL6, IL1β and IL10 after *M. tuberculosis* infection of primary neuron cultures. Additionally, a meta-analysis reported increases in IL6, IL1β, IL10 and TNF in patients with TB meningitis compared to patients without CNS infection and meningitis (Saghazadeh and Rezaei, 2022). The current study found a significant increase in IL6 in *M. tuberculosis* infected neuronal cultures. Furthermore, increasing trends of IL1β, IL6 and IL10 by *in vivo* neurons in response to infection were observed. The increasing trend in IL10 production suggested that neurons potentially generated an immune regulatory response at an early infection stage to dampen the proinflammatory responses because IL10 is a known inhibitor of IL1β (Sun *et al*., 2019). Nonetheless, the increase in IL1β highlighted and supported the possibility of neurons to activate the inflammasome pathway (Kaushal *et al*., 2015) even though they are not professional immune cells. Furthermore, the inability of neurons to generate significant TNF responses to *M. tuberculosis* infection was not surprising because TNF was previously shown to be redundant for protection against during CNS-TB (Francisco *et al*., 2015). Although neurons are not generally

considered to participate in immune responses, the ability to produce immune factors suggests a potential role in immune modulation or regulation.

To further expand on the observed neuronal cytokine expression in response to *M. tuberculosis* infection, a gene expression approach was employed. This approach was successful for studies on hypoxic insult and neurodevelopment disorder (Li et al., 2013, Yadav and Srivastava, 2018). The gene expression profiles observed in the present study identified clear distinctions between infected and uninfected neurons and like the reports by Yadav and Srivastava multiple biological pathways were invoked. This suggested that responses to *M. tuberculosis* infection by neurons are not mutually exclusive but may overlap with other biological processes that involve both communicable and non-communicable diseases. Furthermore, the results showed that viral, parasitic and other bacterial pathways were induced in response to *M. tuberculosis* infection, which implies that there are conserved aspects within these pathways.

One major conserved characteristic is pathogen recognition, which forms a fundamental part of the immune system (Vidya *et al*., 2018). Recognition of pathogens occurs through PRRs such as TLRs and neuronal expression during mouse brain development has shown the expression of TLRs 1-9, while it is known that TLRs 2, 4, 8 and 9 are responsible for *M. tuberculosis* recognition (Kaul et al., 2012, Faridgohar and Nikoueinejad, 2017). Although the exact mechanism of *M. tuberculosis* recognition by neurons is unclear, the current study found that the gene expression of TLR2 was significantly upregulated in infected neurons and a significant downregulation of TLRs 6 and 7 were observed. TLR2 proved to be very important during chronic *M. tuberculosis* infection and was shown to potentially be involved in neurodegeneration (Drennan et al., 2004, Hoffmann et al., 2007). Additionally, TLR2 forms heterodimers with TLR1 and TLR6 which increases the diversity of pathogens that can be recognised (Triantafilou et al., 2006, Takeuchi et al., 2001).

The downstream signaling of TLR2 occurs through the adaptor protein MyD88 is expressed in neurons (Liu *et al*., 2017) and is critical for survival after *M. tuberculosis* infection (Fremond *et al*., 2004). This in turn leads to activate the transcription factor NF-κβ required for bacterial control and promoting proinflammatory responses (Xia

et al., 2021). Neurons were found to express RELB (Engelmann *et al*., 2020) and together with the upregulation of NFkB2 suggested that, in the current study, infected neurons activated the non-canonical NF-κβ pathway (Mockenhaupt *et al*., 2021). Although very little is known about the non-canonical pathway within the CNS, RELB has previously been shown to promote Th1 immune responses (Corn *et al*., 2005). Therefore, the TLR-MyD88-NF-κβ pathway provides a potential mechanism for neuronal recognition of *M. tuberculosis* and subsequent downstream signalling. There are however several other gene expression changes which provide more insight into how these nonprofessional immune cells respond to *M. tuberculosis* infection.

Further investigation of the gene expression profile by gene enrichment analysis revealed the top 10 enriched modules. Numerous genes within these modules were shared and again displayed the complexity and interlinking nature of genetic expression during infection. Upregulation of genes such as *CLEC4E*, *KLF4*, *CRISPLD2*, *CD14* and *LRRC25* supported the hypothesis that a bacterial specific immune response is elicited by neurons (Ishikawa *et al*., 2009, Bhattacharyya *et al*., 2020, Wang *et al*., 2009, Zanoni and Granucci, 2013, Feng *et al*., 2017). However contrasting outcomes, for example as indicated by the downregulation of *STAB1* and *MPEG1* suggest that neuron specific immune responses may be tempered as these genes are induced during bacterial infection (Pombinho *et al*., 2021, Bayly-Jones *et al*., 2020). Other genes such as *IFIH1* and *IFIT1* are induced in CNS-TB and supported by the findings of the present study (Jaeger *et al*., 2015, Qiao *et al*., 2022).

A strong argument for neuronal mediated protection could be drawn from the data. In the current study, *CEBPD, TNFAIP2* and *SERPING1*, genes known to be involved in neuroinflammatory regulation were upregulated (Ko *et al*., 2012, Thair *et al*., 2016, Gorelik *et al*., 2017) while genes such as *NCF1* and *C1QB* were downregulated, lending further support of neuronal mediated protection. *NCF1* translation contributes to ROS production and the subcomponent C1qB a component of the complement pathway, which when inhibited reduces neuronal loss (Sareila *et al*., 2013, Cho *et al*., 2013). The C1qB result was further validated by the downregulation of *C3AR1, C5AR1* and *ITGAX*, which participate in complement responses downstream of

C1qB (Farkas et al., 1998, Holers, 2014, Coulthard and Woodruff, 2015). Additionally, the upregulation of the TNF inhibitor *TNFAIP2* and the inflammation regulating transcription factor *KLF4* genes, together with the downregulation of the inflammatory response enhancing gene *SLC7A7* further suggest neuronal specific protection by reducing inflammation (Thair et al., 2016, Bhattacharyya et al., 2020, Rotoli et al., 2018).

Although neuronal protection was highlighted in the current study, inflammation and a proinflammatory response was a dominant outcome for this study. Here, contrasting results were obtained by the downregulation of genes such as *CD300c* and *ALOX5*, which all play a role in the inflammatory response (Simhadri et al., 2013, Joshi et al., 2014). But this response was opposed by the upregulation of *DUSP1, PDE4B* and *STEAP4* which have all been shown to be increased during inflammation (Hammer *et al*., 2010, Komatsu *et al*., 2013, Scarl *et al*., 2017). Furthermore, neuronal specific expression of known antiviral genes was observed. Here, cytoplasmic viral sensing genes *ZBP1, DDX58* and *DHX58* (Kuriakose and Kanneganti, 2018, Brisse and Ly, 2019), and genes involved in viral replication (*ISG15*) and release (*RSAD2*) were found to be upregulated (Perng and Lenschow, 2018, Kurokawa et al., 2019). Moreover, the antiviral transcription factor *MAFF* and transmembrane antiviral protein *BTS2* were also significantly increased (Ibrahim et al., 2021, Tokarev et al., 2009). These outcomes suggest that neurons use antiviral associated genes to respond to *M. tuberculosis* and lends support to the complexity of immune responses especially from nonimmune cells.

In addition to neuronal specific inflammatory responses, neurons continuously communicate with other cells to maintain homeostasis within the CNS and can produce soluble factors which influence cellular activity (Szepesi *et al*., 2018). The current study showed that culture medium from *M. tuberculosis* infected neuronal cultures activated leukocytes which increased IL1β and MHC class II expression. Suggesting that cellular communication is important for neuroinflammation (Tian *et al*., 2012) and neurons may produce chemotactic molecules to assist in the recruitment of professional immune cells in the context of CNS-TB.

Gene expression of cytokines in infected neurons were found to be one of the major outcomes in the present study. The integrity of the BBB is important for separating

the CNS from the circulatory system and for maintaining optimal conditions within the CNS (Persidsky *et al*., 2006, Sweeney *et al*., 2019). Disruption of the BBB results in the infiltration of peripheral immune cells and has been linked to neuronal secretion of CXCL10 (Chai *et al*., 2015). Furthermore, neurons were identified to be the main source of CXCL1 *in vivo* but did not produce this cytokine in culture in response to HSV-1 infection. Neurons were further implicated in increased BBB permeability and neutrophil recruitment (Michael *et al*., 2020). In addition, neurons were also identified as contributors to the CXCL2 milieu, which is mainly generated by professional immune cells in the brain and were identified as producers of the chemoattractant molecule CCL2 in response to infection (Klein *et al*., 2005, Ip and Liao, 2010, Howe *et al*., 2017, Zhang *et al*., 2017, Stoolman *et al*., 2018). The current study showed the upregulation of *CXCL1, CXCL2* and *CXCL10* gene expression, which translated into increased protein secretion in culture in response to *M. tuberculosis* infection. Significant increases in *CCL5*, *CCL7*, *CCL19*, *CXCL5*, *CXCL9* and *CXCL12* genes were observed in the present study supporting a possible immune modulatory role for neurons in response to infection, by actively producing cytokines and reducing BBB permeability.

Recruitment of functional immune cells to the site of infection is important for protection during disease progression (Russo and McGavern, 2015). Successful cellular recruitment is fundamentally distinguished by the influx of leukocytes and resident immune cells to the site of infection (Marshall et al., 2018, Francisco et al., 2015, Walters et al., 2021, Giordana et al., 1994, Carbonell et al., 2005). In this study $CD45^{+}$ leukocytes were successfully recruited and presented with proinflammatory phenotypes, which were characterised by the expression of IL1β, IL12 and INOS in response to *M. tuberculosis* infection. Additionally, microglia as the main immune effector cells in the CNS (Rock *et al*., 2004), were shown to significantly increase in numbers during CNS-TB which could possibly be due to a process known as microgliosis or supplementation by recruited peripheral macrophages (Manjally and Tay, 2022, Lund et al., 2018). An increasing number of recruited APCs and resident microglia expressed MHC class II. This suggests that pathogen containment was achieved by the dominant influx of proinflammatory innate immune cells during the acute phase of CNS-TB.

Antigen presentation is a critical function during infection that requires intracellular processing of pathogens and loading of pathogen specific peptides onto MHC molecules (Pishesha *et al*., 2022). Findings of increased numbers of neurons which express MHC class I in response to *M. tuberculosis* in the present study suggested pathogen internalisation. *M. tuberculosis* antigens have previously been shown to access the cytosol and are presented on MHC class I after cytosolic processing (Grotzke et al., 2009, Hewitt, 2003). Gene expression of *M. tuberculosis* infected neurons showed significant increases in the expression of *TAP1*, a protein involved in antigen processing and MHC class I loading, and *PSMB8* a proteasome subunit (Schiffer et al., 2002, Kitamura et al., 2011). This suggests that *M. tuberculosis* is internalized by neurons before being processed by the proteasome. Randall *et al.* have elegantly demonstrated internalization of *M. tuberculosis* bacilli by neurons (Randall *et al*., 2014) and although neurons are capable of phagocytosis (Bowen *et al*., 2007), the manner in which internalisation occurs is unclear. Randall and colleagues showed limited association between the lysosomes and internalised bacilli indicating a probable alternative pathway for bacilli uptake.

Optimal functionality of MHC presentation is important for the induction of the adaptive arm of the immune system. Recruitment of lymphocytes to the site of infection is characteristic of the adaptive immune system (Wolf et al., 2008). $CD4^+$ and $CD8^+$ T cells are the most predominant subtypes and have been identified as crucial for protection against *M. tuberculosis* infection (Ellis et al., 2017, Lin and Flynn, 2015). The current study showed progressive and significant $CD4^+$ and $CD8^+$ T cell recruitment. $CD4^+$ T cells were identified as being early CD44 positive, T_H1 TBet expressing, $FoxP3^+$ expressing T-regulatory and T_H2 Gata3 phenotype T cells. This suggested a *M. tuberculosis* specific immune response (Sullivan et al., 2005) which was accompanied by an immune suppressive response to maintain homeostasis. The increase in T_{reg} T cell recruitment to the site of infection has previously been suggested as an immune evading mechanism used by *M. tuberculosis* to supress and delay protective immune responses against *M. tuberculosis* (Shafiani et al., 2010, Sharma et al., 2009). However, considering the “immune privileged” nature of the CNS and concerted effort for neuronal protection and prevention of neurological sequelae, it is highly likely that these cells have an immune regulatory function which is supported by the findings of marginal

recruitment of immunologically active $CD8^+$ cytotoxic T-lymphocytes. Thus, functional T cell recruitment is important for protection against *M. tuberculosis* and a progressive significant number of cells are required for containment of the pathogen.

Studies like the present one are only possible because of the ethical use of mouse models and the generation of transgenic mouse models further expanded the ability to study gene specific functions and mechanisms. These murine models however have fundamental clinical translational limitations but to ethically study the human immune system *in vivo* and overcome these limitations, humanised mouse models were developed. In the current study NSG mice known to be deficient in lymphocytes were engrafted with human foetal liver and thymus and injected with human stem cells. A previous study showed that this model successfully reconstituted human immune cells and was able to control pulmonary TB infection by granuloma formation (Calderon et al., 2013). Therefore, this study set out to identify if human immune cells would be recruited and can successfully control CNS-TB infection.

Tuberculosis disease progression is characterised by physical deterioration, neural sequelae and weight loss (Dlodlo RA, 2019). These symptoms were observed in BLT-NSG mice intracerebrally infected with *M. tuberculosis*. Severe weight loss was accompanied by neurological decline presented by head tilting and barrel rolling which is akin to the human symptoms of headaches, loss of consciousness, seizures and stiff necks (Marx and Chan, 2011), all known to present in patients with CNS-TB. Other transgenic mouse models showed that immune incompetent hosts were unable to control bacterial growth and showed signs of significant weight loss by day 15 and ultimately succumbed to infection by day 20 post infection (Francisco *et al*., 2015, Hsu *et al*., 2017). Like these studies, BLT-NSG mice had poor infection control and succumbed to infection within three weeks, suggesting incompetent peripheral immune cell responses.

A previous study of pulmonary tuberculosis in mice reconstituted with human immune cells showed functional leukocyte recruitment to the site of infection. Furthermore, the recruited cells formed lesion comparable to those observed in human disease (Arrey *et al*., 2019). The current study displayed similar results, showing fully functional active human cellular recruitment to the brain post infection. These recruited leukocytes were able to phagocytose *M. tuberculosis* and had the

potential for antigen presentation by expressing HLA-DR. Additionally, there was successful recruitment of adaptive immune $CD3^+$ T cells, however the majority of these cells expressed the naïve $CD45RA^+$ isoform (Courville and Lawrence, 2021) indicating an immature phenotype. Successful recruitment of T cells to the site of infection is imperative for mounting an effective immune response against mycobacterial infection (Xing *et al*., 1998), however the recruitment of immature cells will result in inefficient pathogen control. Thus, we postulate that although BLT-NSG mice were able to recruit T cells to the brain in response to *M. tuberculosis* infection, such cells lacked proper functionality. Moreover, analogous to leukopenia in humans (Lin *et al*., 2015) the low number of recruited human leukocytes to the BLT-NSG mouse brains also contributed to suboptimal infection control.

Conclusion and future studies.

In this study, neurons were for the first time shown to have gene expression changes in response to *M. tuberculosis* infection. The responses revealed that neurons potentially drive proinflammatory immune responses but attempt to maintain homeostasis by generating neuroprotective responses. Furthermore, the findings of cytokine secretion by neurons in response to *M. tuberculosis* infection suggested a potential immune modulatory role for neurons. *In vivo* analysis of neuronal responses to *M. tuberculosis* infection showed increases in MHC class I expression, supporting an immune modulatory function. Understanding how neurons possibly drive CNS immune responses could be valuable for therapeutic intervention which would have one of its major goals to minimise possible neuronal damage and development of neural sequelae.

The importance of cellular crosstalk was highlighted in the current study when neuronal immune responses were shown to activate peripheral immune cells. The current study compared the differences in disease progression and bacterial control in immune competent and incompetent mouse models. The findings showed that adequate recruitment of functional immune cells to the brain is not only a characteristic of inflammation but also critical for protection against CNS-TB infection (Francisco et al., 2015). Furthermore, a novel approach to study human immune responses to CNS-TB was observed. Here the use of BLT-NSG mice demonstrated that functional human immune cells can indeed be recruited to the brain after

intracerebral infection with *M. tuberculosis,* but the functionality and limited number of recruited cells possibly led to failure to control infection. The findings from this study proposes an interesting dilemma for drug discovery because it shows that increased numbers of immune cells recruited to the brain in response to CNS-TB improves disease control but alternatively poses a threat of pathological damage and neural sequelae. Therefore, much consideration needs to be given when formulating strategies to enhance protection from the pathogen while maintaining homeostatic conditions.

With limited literature on neuronal responses during CNS-TB this study showcased a novel neuronal gene expression approach which highlighted the induction of immune modulatory genes in culture. To strengthen these results, it will be important to perform additional gene expression studies on neurons obtained from infected mouse brains. In addition, neurons were shown to produce soluble molecules that stimulate leukocyte activity both *in vitro* and *in vivo*. For future investigations, it would be interesting to explore how these immune responses to *M. tuberculosis* infection influence the electrophysiological activity of neurons. The novel approach of a CNS-TB humanised mouse model for studying the human peripheral immune response was successfully established but the disease outcome was unexpected. Future recommendations would involve performing adoptive transfer experiments with human leukocytes primed against *M. tuberculosis* to observe if more mature lymphocytes would rescue disease progression in BLT-NSG mice.

In conclusion, this study built on previous knowledge and contributed to the field of CNS-TB and neuroimmunology significantly by elucidating novel genetic activity in neurons. Moreover, the novel humanised mouse model approach to studying CNS-TB can contribute to how human immune responses are assessed. Together these results combine to establish a foundation on which to build future translational efforts to limit *M. tuberculosis* infection, reduce neuronal sequelae and possibly reduce mortality and morbidity.

References

AHMED, R. & GRAY, D. 1996. Immunological memory and protective immunity: understanding their relation. *Science,* 272**,** 54-60.

ALI, S., HIRSCHFELD, A., VICTOR, R., FORTUNO, E. S., KOLLMANN, T. R. & TURVEY, S. E. 2010. Functional characterization of human variants of NFKBIA: a key regulator of immune responsiveness implicated in susceptibility to infectious and inflammatory disease. *Allergy, Asthma & Clinical Immunology,* 6**,** P2.

ALLEN, C., THORNTON, P., DENES, A., MCCOLL, B. W., PIEROZYNSKI, A., MONESTIER, M., PINTEAUX, E., ROTHWELL, N. J. & ALLAN, S. M. 2012. Neutrophil cerebrovascular transmigration triggers rapid neurotoxicity through release of proteases associated with decondensed DNA. *J Immunol,* 189**,** 381-92.

ALLIE, N., GRIVENNIKOV, S. I., KEETON, R., HSU, N. J., BOURIGAULT, M. L., COURT, N., FREMOND, C., YEREMEEV, V., SHEBZUKHOV, Y., RYFFEL, B., NEDOSPASOV, S. A., QUESNIAUX, V. F. & JACOBS, M. 2013. Prominent role for T cell-derived tumour necrosis factor for sustained control of Mycobacterium tuberculosis infection. *Sci Rep,* 3**,** 1809.

ALOISI, F., PENNA, G., CERASE, J., MENENDEZ IGLESIAS, B. & ADORINI, L. 1997. IL-12 production by central nervous system microglia is inhibited by astrocytes. *J Immunol,* 159**,** 1604-12.

ALONSO, R., PISA, D., FERNANDEZ-FERNANDEZ, A. M., RABANO, A. & CARRASCO, L. 2017. Fungal infection in neural tissue of patients with amyotrophic lateral sclerosis. *Neurobiol Dis,* 108**,** 249-260.

AMARANTE-MENDES, G. P., ADJEMIAN, S., BRANCO, L. M., ZANETTI, L. C., WEINLICH, R. & BORTOLUCI, K. R. 2018. Pattern Recognition Receptors and the Host Cell Death Molecular Machinery. *Front Immunol,* 9**,** 2379.

ARAUJO, J. M., GOMEZ, A. C., AGUILAR, A., SALGADO, R., BALKO, J. M., BRAVO, L., DOIMI, F., BRETEL, D., MORANTE, Z., FLORES, C., GOMEZ, H. L. & PINTO, J. A. 2018. Effect of CCL5 expression in the recruitment of immune cells in triple negative breast cancer. *Sci Rep,* 8**,** 4899.

ARMSTRONG, J. A. & HART, P. D. 1971. Response of cultured macrophages to Mycobacterium tuberculosis, with observations on fusion of lysosomes with phagosomes. *J Exp Med,* 134**,** 713-40.

ARREY, F., LOWE, D., KUHLMANN, S., KAISER, P., MOURA-ALVES, P., KRISHNAMOORTHY, G., LOZZA, L., MAERTZDORF, J., SKRAHINA, T., SKRAHINA, A., GENGENBACHER, M., NOUAILLES, G. & KAUFMANN, S. H. E. 2019. Humanized Mouse Model Mimicking Pathology of Human Tuberculosis for in vivo Evaluation of Drug Regimens. *Front Immunol,* 10**,** 89.

ASHTON, J. J., BOUKAS, K., STAFFORD, I. S., CHENG, G., HAGGARTY, R., COELHO, T. A. F., BATRA, A., AFZAL, N. A., WILLIAMS, A. P., POLAK, M. E., BEATTIE, R. M. & ENNIS, S. 2022. Deleterious Genetic Variation Across the NOD Signaling Pathway Is Associated With Reduced NFKB Signaling Transcription and Upregulation of Alternative Inflammatory Transcripts in Pediatric Inflammatory Bowel Disease. *Inflammatory Bowel Diseases,* 28**,** 912-922.

AUNG, T., KITAJIMA, S., NOMOTO, M., EN, J., YONEZAWA, S., ARIKAWA, I. & GOTO, M. 2007. Mycobacterium leprae in neurons of the medulla oblongata and spinal cord in leprosy. *J Neuropathol Exp Neurol,* 66**,** 284-94.

BAI, W., LIU, H., JI, Q., ZHOU, Y., LIANG, L., ZHENG, R., CHEN, J., LIU, Z., YANG, H., ZHANG, P., KAUFMANN, S. H. & GE, B. 2014. TLR3 regulates mycobacterial RNA-induced IL-10 production through the PI3K/AKT signaling pathway. *Cell Signal,* 26**,** 942-50.

BAO, M., YI, Z. & FU, Y. 2017. Activation of TLR7 Inhibition of Mycobacterium Tuberculosis Survival by Autophagy in RAW 264.7 Macrophages. *J Cell Biochem,* 118**,** 4222-4229.

BARAL, P., UDIT, S. & CHIU, I. M. 2019. Pain and immunity: implications for host defence. *Nat Rev Immunol,* 19**,** 433-447.

BAYLY-JONES, C., PANG, S. S., SPICER, B. A., WHISSTOCK, J. C. & DUNSTONE, M. A. 2020. Ancient but Not Forgotten: New Insights Into MPEG1, a Macrophage Perforin-Like Immune Effector. *Front Immunol,* 11**,** 581906.

BE, N. A., KLINKENBERG, L. G., BISHAI, W. R., KARAKOUSIS, P. C. & JAIN, S. K. 2011. Strain-dependent CNS dissemination in guinea pigs after Mycobacterium tuberculosis aerosol challenge. *Tuberculosis (Edinb),* 91**,** 386-9.

BEAUDOIN, G. M., 3RD, LEE, S. H., SINGH, D., YUAN, Y., NG, Y. G., REICHARDT, L. F. & ARIKKATH, J. 2012. Culturing pyramidal neurons from the early postnatal mouse hippocampus and cortex. *Nat Protoc,* 7**,** 1741-54.

BHATTACHARYYA, A., HERTA, T., CONRAD, C., FREY, D., GARCIA, P., SUTTORP, N., HIPPENSTIEL, S. & ZAHLTEN, J. 2020. Induction of Kruppel-Like Factor 4 Mediates Polymorphonuclear Neutrophil Activation in Streptococcus pneumoniae Infection. *Front Microbiol,* 11**,** 582070.

BI, F., HUANG, C., TONG, J., QIU, G., HUANG, B., WU, Q., LI, F., XU, Z., BOWSER, R., XIA, X. G. & ZHOU, H. 2013. Reactive astrocytes secrete lcn2 to promote neuron death. *Proc Natl Acad Sci U S A,* 110**,** 4069-74.

BONIZZI, G. & KARIN, M. 2004. The two NF-kappaB activation pathways and their role in innate and adaptive immunity. *Trends Immunol,* 25**,** 280-8.

BOSMA, G. C., CUSTER, R. P. & BOSMA, M. J. 1983. A severe combined immunodeficiency mutation in the mouse. *Nature,* 301**,** 527-30.

BOUCHON, A., HERNANDEZ-MUNAIN, C., CELLA, M. & COLONNA, M. 2001. A DAP12-mediated pathway regulates expression of CC chemokine receptor 7 and maturation of human dendritic cells. *J Exp Med,* 194**,** 1111-22.

BOUDJADI, S., CHATTERJEE, B., SUN, W., VEMU, P. & BARR, F. G. 2018. The expression and function of PAX3 in development and disease. *Gene,* 666**,** 145-157.

BOWEN, S., ATEH, D. D., DEINHARDT, K., BIRD, M. M., PRICE, K. M., BAKER, C. S., ROBSON, J. C., SWASH, M., SHAMSUDDIN, W., KAWAR, S., EL-TAWIL, T., ROOS, J., HOYLE, A., NICKOLS, C. D., KNOWLES, C. H., PULLEN, A. H., LUTHERT, P. J., WELLER, R. O., HAFEZPARAST, M., FRANKLIN, R. J., REVESZ, T., KING, R. H., BERNINGHAUSEN, O., FISHER, E. M., SCHIAVO, G. & MARTIN, J. E. 2007. The phagocytic capacity of neurones. *Eur J Neurosci,* 25**,** 2947-55.

BRISSE, M. & LY, H. 2019. Comparative Structure and Function Analysis of the RIG-I-Like Receptors: RIG-I and MDA5. *Front Immunol,* 10**,** 1586.

BRYK, R., GRIFFIN, P. & NATHAN, C. 2000. Peroxynitrite reductase activity of bacterial peroxiredoxins. *Nature,* 407**,** 211-5.

BURFEIND, K. G., ZHU, X., NORGARD, M. A., LEVASSEUR, P. R., HUISMAN, C., BUENAFE, A. C., OLSON, B., MICHAELIS, K. A., TORRES, E. R., JENG, S., MCWEENEY, S., RABER, J. & MARKS, D. L. 2020. Circulating myeloid cells invade the central nervous system to mediate cachexia during pancreatic cancer. *Elife,* 9.

CABRERO-DE LAS HERAS, S. & MARTINEZ-BALIBREA, E. 2018. CXC family of chemokines as prognostic or predictive biomarkers and possible drug targets in colorectal cancer. *World J Gastroenterol,* 24**,** 4738-4749.

CAI, Z., GREENE, M. I., ZHU, Z. & ZHANG, H. 2020. Structural Features and PF4 Functions that Occur in Heparin-Induced Thrombocytopenia (HIT) Complicated by COVID-19. *Antibodies (Basel),* 9.

CALDERON, V. E., VALBUENA, G., GOEZ, Y., JUDY, B. M., HUANTE, M. B., SUTJITA, P., JOHNSTON, R. K., ESTES, D. M., HUNTER, R. L., ACTOR, J. K., CIRILLO, J. D. & ENDSLEY, J. J. 2013. A humanized mouse model of tuberculosis. *PLoS One,* 8**,** e63331.

CAMPBELL, K. S. & COLONNA, M. 1999. DAP12: a key accessory protein for relaying signals by natural killer cell receptors. *Int J Biochem Cell Biol,* 31**,** 631-6.

CAO, W., LUO, L. L., CHEN, W. W., LIANG, L., ZHANG, R. R., ZHAO, Y. L., CHEN, J. & YUE, J. 2019. Polymorphism in the EREG gene confers susceptibility to tuberculosis. *BMC Med Genet,* 20**,** 7.

CAPPELLI, G., VOLPE, P., SANDUZZI, A., SACCHI, A., COLIZZI, V. & MARIANI, F. 2001. Human macrophage gamma interferon decreases gene expression but not replication of Mycobacterium tuberculosis: analysis of the host-pathogen reciprocal influence on transcription in a comparison of strains H37Rv and CMT97. *Infect Immun,* 69**,** 7262-70.

CARBONELL, W. S., MURASE, S. I., HORWITZ, A. F. & MANDELL, J. W. 2005. Infiltrative microgliosis: activation and long-distance migration of subependymal microglia following periventricular insults. *J Neuroinflammation,* 2**,** 5.

CARPENTER, R. S., KIGERL, K. A., MARBOURG, J. M., GAUDET, A. D., HUEY, D., NIEWIESK, S. & POPOVICH, P. G. 2015. Traumatic spinal cord injury in mice with human immune systems. *Exp Neurol,* 271**,** 432-44.

CEBRIAN, C., ZUCCA, F. A., MAURI, P., STEINBECK, J. A., STUDER, L., SCHERZER, C. R., KANTER, E., BUDHU, S., MANDELBAUM, J., VONSATTEL, J. P., ZECCA, L., LOIKE, J. D. & SULZER, D. 2014. MHC-I expression renders catecholaminergic neurons susceptible to T-cell-mediated degeneration. *Nat Commun,* 5**,** 3633.

CEDILE, O., WLODARCZYK, A. & OWENS, T. 2017. CCL2 recruits T cells into the brain in a CCR2-independent manner. *APMIS,* 125**,** 945-956.

CHAI, Q., SHE, R., HUANG, Y. & FU, Z. F. 2015. Expression of neuronal CXCL10 induced by rabies virus infection initiates infiltration of inflammatory cells,

production of chemokines and cytokines, and enhancement of blood-brain barrier permeability. *J Virol,* 89**,** 870-6.

CHAN, J., TANAKA, K., CARROLL, D., FLYNN, J. & BLOOM, B. R. 1995. Effects of nitric oxide synthase inhibitors on murine infection with Mycobacterium tuberculosis. *Infect Immun,* 63**,** 736-40.

CHEN, B., LIU, H., LIU, Z. & YANG, F. 2023. Benefits and limitations of humanized mouse models for human red blood cell-related disease research. *Frontiers in Hematology,* 1.

CHEN, H. H. & STEWART, A. F. R. 2017. Interferon regulatory factor 2 binding protein 2: a new player of the innate immune response for stroke recovery. *Neural Regen Res,* 12**,** 1762-1764.

CHEN, L., XIE, Q. W. & NATHAN, C. 1998. Alkyl hydroperoxide reductase subunit C (AhpC) protects bacterial and human cells against reactive nitrogen intermediates. *Mol Cell,* 1**,** 795-805.

CHERIAN, A. & THOMAS, S. V. 2011. Central nervous system tuberculosis. *Afr Health Sci,* 11**,** 116-27.

CHEVALIER, G., SUBERBIELLE, E., MONNET, C., DUPLAN, V., MARTIN-BLONDEL, G., FARRUGIA, F., LE MASSON, G., LIBLAU, R. & GONZALEZ-DUNIA, D. 2011. Neurons are MHC class I-dependent targets for CD8 T cells upon neurotropic viral infection. *PLoS Pathog,* 7**,** e1002393.

CHEVALIER, S. A., TURPIN, J., CACHAT, A., AFONSO, P. V., GESSAIN, A., BRADY, J. N., PISE-MASISON, C. A. & MAHIEUX, R. 2014. Gem-induced cytoskeleton remodeling increases cellular migration of HTLV-1-infected cells, formation of infected-to-target T-cell conjugates and viral transmission. *PLoS Pathog,* 10**,** e1003917.

CHO, H., PROLL, S. C., SZRETTER, K. J., KATZE, M. G., GALE, M., JR. & DIAMOND, M. S. 2013. Differential innate immune response programs in neuronal subtypes determine susceptibility to infection in the brain by positive-stranded RNA viruses. *Nat Med,* 19**,** 458-64.

COOPER, A. M. 2014. Mouse model of tuberculosis. *Cold Spring Harb Perspect Med,* 5**,** a018556.

COOPER, A. M., DALTON, D. K., STEWART, T. A., GRIFFIN, J. P., RUSSELL, D. G. & ORME, I. M. 1993. Disseminated tuberculosis in interferon gamma gene-disrupted mice. *J Exp Med,* 178**,** 2243-7.

COOPER, A. M., MAGRAM, J., FERRANTE, J. & ORME, I. M. 1997. Interleukin 12 (IL-12) is crucial to the development of protective immunity in mice intravenously infected with mycobacterium tuberculosis. *J Exp Med,* 186**,** 39-45.

CORN, R. A., HUNTER, C., LIOU, H. C., SIEBENLIST, U. & BOOTHBY, M. R. 2005. Opposing roles for RelB and Bcl-3 in regulation of T-box expressed in T cells, GATA-3, and Th effector differentiation. *J Immunol,* 175**,** 2102-10.

COULTHARD, L. G. & WOODRUFF, T. M. 2015. Is the complement activation product C3a a proinflammatory molecule? Re-evaluating the evidence and the myth. *J Immunol,* 194**,** 3542-8.

COURVILLE, E. L. & LAWRENCE, M. G. 2021. Characteristic CD45RA/CD45RO maturation pattern by flow cytometry associated with the CD45 C77G polymorphism. *Cytometry B Clin Cytom,* 100**,** 602-605.

CRESPO, J., KOH, Y. T., HU, N., MOORE, P. A., BONVINI, E., GLASEBROOK, A. L., MARTIN, A. P. & BENSCHOP, R. J. 2021. A humanized CD3epsilon-knock-in mouse model for pre-clinical testing of anti-human CD3 therapy. *PLoS One,* 16**,** e0245917.

CUI, H., GUO, M., XU, D., DING, Z. C., ZHOU, G., DING, H. F., ZHANG, J., TANG, Y. & YAN, C. 2015. The stress-responsive gene ATF3 regulates the histone acetyltransferase Tip60. *Nat Commun,* 6**,** 6752.

CURTO, M., REALI, C., PALMIERI, G., SCINTU, F., SCHIVO, M. L., SOGOS, V., MARCIALIS, M. A., ENNAS, M. G., SCHWARZ, H., POZZI, G. & GREMO, F. 2004. Inhibition of cytokines expression in human microglia infected by virulent and non-virulent mycobacteria. *Neurochem Int,* 44**,** 381-92.

D'AGOSTINO, P. M., GOTTFRIED-BLACKMORE, A., ANANDASABAPATHY, N. & BULLOCH, K. 2012. Brain dendritic cells: biology and pathology. *Acta Neuropathol,* 124**,** 599-614.

DE HAAS, A. H., VAN WEERING, H. R., DE JONG, E. K., BODDEKE, H. W. & BIBER, K. P. 2007. Neuronal chemokines: versatile messengers in central nervous system cell interaction. *Mol Neurobiol,* 36**,** 137-51.

DE KLERK, N., SAROJ, S. D., WASSING, G. M., MAUDSDOTTER, L. & JONSSON, A. B. 2017. The Host Cell Transcription Factor EGR1 Is Induced by Bacteria through the EGFR-ERK1/2 Pathway. *Front Cell Infect Microbiol,* 7**,** 16.

DE MASI, R. & ORLANDO, S. 2020. IFI35 as a biomolecular marker of neuroinflammation and treatment response in multiple sclerosis. *Life Sci,* 259**,** 118233.

DENISENKO, E., GULER, R., MHLANGA, M., SUZUKI, H., BROMBACHER, F. & SCHMEIER, S. 2019. Transcriptionally induced enhancers in the macrophage immune response to Mycobacterium tuberculosis infection. *BMC Genomics,* 20**,** 71.

DIAZ, M. F., HORTON, P. D., KUMAR, A., LIVINGSTON, M., MOHAMMADALIPOUR, A., XUE, H., SKIBBER, M. A., EWERE, A., TOLEDANO FURMAN, N. E., AROOM, K. R., ZHANG, S., GILL, B. S., COX, C. S., JR. & WENZEL, P. L. 2020. Injury intensifies T cell mediated graft-versus-host disease in a humanized model of traumatic brain injury. *Sci Rep,* 10**,** 10729.

DISTELDORF, E. M., KREBS, C. F., PAUST, H. J., TURNER, J. E., NOUAILLES, G., TITTEL, A., MEYER-SCHWESINGER, C., STEGE, G., BRIX, S., VELDEN, J., WIECH, T., HELMCHEN, U., STEINMETZ, O. M., PETERS, A., BENNSTEIN, S. B., KAFFKE, A., LLANTO, C., LIRA, S. A., MITTRUCKER, H. W., STAHL, R. A., KURTS, C., KAUFMANN, S. H. & PANZER, U. 2015. CXCL5 drives neutrophil recruitment in TH17-mediated GN. *J Am Soc Nephrol,* 26**,** 55-66.

DJUKIC, M., MILDNER, A., SCHMIDT, H., CZESNIK, D., BRUCK, W., PRILLER, J., NAU, R. & PRINZ, M. 2006. Circulating monocytes engraft in the brain, differentiate into microglia and contribute to the pathology following meningitis in mice. *Brain,* 129**,** 2394-403.

DLODLO RA, B. G., HELDAL E, ALLWOOD B, CHIANG C-Y, FUJIWARA PI, GRAHAM SM, GUILLERM N, HARRIES AD, KOURA KG, KUMAR AMV, LIN

Y, MEGHJI J, MORTIMER K, PIUBELLO A, ROTH B, SATYANARAYANA S, SEKADDE M, SOLOVIČ I, TONSING J, VAN DEUN A 2019. *Management of Tuberculosis: a Guide to Essential Practice.*, Paris, France: International Union Against Tuberculosis and Lung Disease.

DONALD, P. R., SCHAAF, H. S. & SCHOEMAN, J. F. 2005. Tuberculous meningitis and miliary tuberculosis: the Rich focus revisited. *J Infect,* 50**,** 193-5.

DRAMSI, S., LEVI, S., TRILLER, A. & COSSART, P. 1998. Entry of Listeria monocytogenes into neurons occurs by cell-to-cell spread: an in vitro study. *Infect Immun,* 66**,** 4461-8.

DRENNAN, M. B., NICOLLE, D., QUESNIAUX, V. J., JACOBS, M., ALLIE, N., MPAGI, J., FREMOND, C., WAGNER, H., KIRSCHNING, C. & RYFFEL, B. 2004. Toll-like receptor 2-deficient mice succumb to Mycobacterium tuberculosis infection. *Am J Pathol,* 164**,** 49-57.

EDILOVA, M. I., ABDUL-SATER, A. A. & WATTS, T. H. 2018. TRAF1 Signaling in Human Health and Disease. *Front Immunol,* 9**,** 2969.

EGANA-GORRONO, L., CHINNASAMY, P., CASIMIRO, I., ALMONTE, V. M., PARIKH, D., OLIVEIRA-PAULA, G. H., JAYAKUMAR, S., LAW, C., RIASCOS-BERNAL, D. F. & SIBINGA, N. E. S. 2019. Allograft inflammatory factor-1 supports macrophage survival and efferocytosis and limits necrosis in atherosclerotic plaques. *Atherosclerosis,* 289**,** 184-194.

ELLIS, P. K., MARTIN, W. J. & DODD, P. J. 2017. CD4 count and tuberculosis risk in HIV-positive adults not on ART: a systematic review and meta-analysis. *PeerJ,* 5**,** e4165.

ENGELAND, K. 2022. Cell cycle regulation: p53-p21-RB signaling. *Cell Death Differ,* 29**,** 946-960.

ENGELHARDT, B. & RANSOHOFF, R. M. 2005. The ins and outs of T-lymphocyte trafficking to the CNS: anatomical sites and molecular mechanisms. *Trends Immunol,* 26**,** 485-95.

ENGELMANN, C., RIEMANN, M., CARLSTEDT, S., GRIMLOWSKI, R., ANDREAS, N., KOLIESNIK, I., MEIER, E., AUSTERFIELD, P. & HAENOLD, R. 2020. Identification of undescribed Relb expression domains in the murine brain by new Relb:cre-katushka reporter mice. *Dev Dyn,* 249**,** 983-997.

EUM, S. Y., KONG, J. H., HONG, M. S., LEE, Y. J., KIM, J. H., HWANG, S. H., CHO, S. N., VIA, L. E. & BARRY, C. E., 3RD 2010. Neutrophils are the predominant infected phagocytic cells in the airways of patients with active pulmonary TB. *Chest,* 137**,** 122-8.

EVERING, T. H. & TSUJI, M. 2018. Human Immune System Mice for the Study of Human Immunodeficiency Virus-Type 1 Infection of the Central Nervous System. *Front Immunol,* 9**,** 649.

FAN, H., LONGACRE, A., MENG, F., PATEL, V., HSIAO, K., KOH, J. S. & LEVINE, J. S. 2004. Cytokine dysregulation induced by apoptotic cells is a shared characteristic of macrophages from nonobese diabetic and systemic lupus erythematosus-prone mice. *J Immunol,* 172**,** 4834-43.

FARIDGOHAR, M. & NIKOUEINEJAD, H. 2017. New findings of Toll-like receptors involved in Mycobacterium tuberculosis infection. *Pathog Glob Health,* 111**,** 256-264.

FARKAS, I., BARANYI, L., LIPOSITS, Z. S., YAMAMOTO, T. & OKADA, H. 1998. Complement C5a anaphylatoxin fragment causes apoptosis in TGW neuroblastoma cells. *Neuroscience,* 86**,** 903-11.

FAROOQ, M., BATOOL, M., KIM, M. S. & CHOI, S. 2021. Toll-Like Receptors as a Therapeutic Target in the Era of Immunotherapies. *Front Cell Dev Biol,* 9**,** 756315.

FENG, Y., DUAN, T., DU, Y., JIN, S., WANG, M., CUI, J. & WANG, R. F. 2017. LRRC25 Functions as an Inhibitor of NF-kappaB Signaling Pathway by Promoting p65/RelA for Autophagic Degradation. *Sci Rep,* 7**,** 13448.

FERREIRA, C., PALMER, D., BLAKE, K., GARDEN, O. A. & DYSON, J. 2014. Reduced regulatory T cell diversity in NOD mice is linked to early events in the thymus. *J Immunol,* 192**,** 4145-52.

FLYNN, J. L., CHAN, J. & LIN, P. L. 2011. Macrophages and control of granulomatous inflammation in tuberculosis. *Mucosal Immunol,* 4**,** 271-8.

FLYNN, J. L., CHAN, J., TRIEBOLD, K. J., DALTON, D. K., STEWART, T. A. & BLOOM, B. R. 1993. An essential role for interferon gamma in resistance to Mycobacterium tuberculosis infection. *J Exp Med,* 178**,** 2249-54.

FLYNN, J. L., SCANGA, C. A., TANAKA, K. E. & CHAN, J. 1998. Effects of aminoguanidine on latent murine tuberculosis. *J Immunol,* 160**,** 1796-803.

FONG, A. M., ROBINSON, L. A., STEEBER, D. A., TEDDER, T. F., YOSHIE, O., IMAI, T. & PATEL, D. D. 1998. Fractalkine and CX3CR1 mediate a novel mechanism of leukocyte capture, firm adhesion, and activation under physiologic flow. *J Exp Med,* 188**,** 1413-9.

FOSTER, J. A., QUAN, N., STERN, E. L., KRISTENSSON, K. & HERKENHAM, M. 2002. Induced neuronal expression of class I major histocompatibility complex mRNA in acute and chronic inflammation models. *J Neuroimmunol,* 131**,** 83-91.

FRANCISCO, N. M., HSU, N. J., KEETON, R., RANDALL, P., SEBESHO, B., ALLIE, N., GOVENDER, D., QUESNIAUX, V., RYFFEL, B., KELLAWAY, L. & JACOBS, M. 2015. TNF-dependent regulation and activation of innate immune cells are essential for host protection against cerebral tuberculosis. *J Neuroinflammation,* 12**,** 125.

FREMOND, C. M., YEREMEEV, V., NICOLLE, D. M., JACOBS, M., QUESNIAUX, V. F. & RYFFEL, B. 2004. Fatal Mycobacterium tuberculosis infection despite adaptive immune response in the absence of MyD88. *J Clin Invest,* 114**,** 1790-9.

GIORDANA, M. T., ATTANASIO, A., CAVALLA, P., MIGHELI, A., VIGLIANI, M. C. & SCHIFFER, D. 1994. Reactive cell proliferation and microglia following injury to the rat brain. *Neuropathol Appl Neurobiol,* 20**,** 163-74.

GIORDANO, M., RONCAGALLI, R., BOURDELY, P., CHASSON, L., BUFERNE, M., YAMASAKI, S., BEYAERT, R., VAN LOO, G., AUPHAN-ANEZIN, N., SCHMITT-VERHULST, A. M. & VERDEIL, G. 2014. The tumor necrosis factor alpha-induced protein 3 (TNFAIP3, A20) imposes a brake on antitumor activity of CD8 T cells. *Proc Natl Acad Sci U S A,* 111**,** 11115-20.

GOPALAKRISHNAN, A. & SALGAME, P. 2016. Toll-like receptor 2 in host defense against Mycobacterium tuberculosis: to be or not to be-that is the question. *Curr Opin Immunol,* 42**,** 76-82.

GORELIK, A., SAPIR, T., WOODRUFF, T. M. & REINER, O. 2017. Serping1/C1 Inhibitor Affects Cortical Development in a Cell Autonomous and Non-cell Autonomous Manner. *Front Cell Neurosci,* 11**,** 169.

GROTZKE, J. E., HARRIFF, M. J., SILER, A. C., NOLT, D., DELEPINE, J., LEWINSOHN, D. A. & LEWINSOHN, D. M. 2009. The Mycobacterium tuberculosis Phagosome Is a HLA-I Processing Competent Organelle. *PLOS Pathogens,* 5**,** e1000374.

GUAN, D. & KAO, H. Y. 2015. The function, regulation and therapeutic implications of the tumor suppressor protein, PML. *Cell Biosci,* 5**,** 60.

GUTTI, T. L., KNIBBE, J. S., MAKAROV, E., ZHANG, J., YANNAM, G. R., GORANTLA, S., SUN, Y., MERCER, D. F., SUEMIZU, H., WISECARVER, J. L., OSNA, N. A., BRONICH, T. K. & POLUEKTOVA, L. Y. 2014. Human hepatocytes and hematolymphoid dual reconstitution in treosulfan-conditioned uPA-NOG mice. *Am J Pathol,* 184**,** 101-9.

HALL, B., LIMAYE, A. & KULKARNI, A. B. 2009. Overview: generation of gene knockout mice. *Curr Protoc Cell Biol,* Chapter 19**,** Unit 19 12 19 12 1-17.

HAMMER, M., ECHTENACHTER, B., WEIGHARDT, H., JOZEFOWSKI, K., ROSE-JOHN, S., MANNEL, D. N., HOLZMANN, B. & LANG, R. 2010. Increased inflammation and lethality of Dusp1-/- mice in polymicrobial peritonitis models. *Immunology,* 131**,** 395-404.

HART, P. D., ARMSTRONG, J. A., BROWN, C. A. & DRAPER, P. 1972. Ultrastructural study of the behavior of macrophages toward parasitic mycobacteria. *Infect Immun,* 5**,** 803-7.

HATTERMANN, K., KNERLICH-LUKOSCHUS, F., LUCIUS, R., MEHDORN, M. & HELD-FEINDT, J. 2015. Erythropoietin and CCL3 antagonise their functional properties during neuroinflammation. *Neurological Research,* 37**,** 1025-1028.

HECKMANN, B. L., ZHANG, X., XIE, X. & LIU, J. 2013. The G0/G1 switch gene 2 (G0S2): regulating metabolism and beyond. *Biochim Biophys Acta,* 1831**,** 276-81.

HENNECKE, J. & WILEY, D. C. 2001. T cell receptor-MHC interactions up close. *Cell,* 104**,** 1-4.

HERNANDEZ PANDO, R., AGUILAR, D., COHEN, I., GUERRERO, M., RIBON, W., ACOSTA, P., OROZCO, H., MARQUINA, B., SALINAS, C., REMBAO, D. & ESPITIA, C. 2010. Specific bacterial genotypes of Mycobacterium tuberculosis cause extensive dissemination and brain infection in an experimental model. *Tuberculosis (Edinb),* 90**,** 268-77.

HERRERA-RINCON, C., PARÉ, J.-F., MARTYNIUK, C. J., JANNETTY, S. K., HARRISON, C., FISCHER, A., DINIS, A., KESHARI, V., NOVAK, R. & LEVIN, M. 2020. An in vivo brain–bacteria interface: the developing brain as a key regulator of innate immunity. *npj Regenerative Medicine,* 5**,** 2.

HEWITT, E. W. 2003. The MHC class I antigen presentation pathway: strategies for viral immune evasion. *Immunology,* 110**,** 163-9.

HIKICHI, H., SETO, S., WAKABAYASHI, K., HIJIKATA, M. & KEICHO, N. 2022. Transcription factor MAFB controls type I and II interferon response-mediated host immunity in Mycobacterium tuberculosis-infected macrophages. *Front Microbiol,* 13**,** 962306.

HOFFMANN, O., BRAUN, J. S., BECKER, D., HALLE, A., FREYER, D., DAGAND, E., LEHNARDT, S. & WEBER, J. R. 2007. TLR2 mediates neuroinflammation and neuronal damage. *J Immunol,* 178**,** 6476-81.

HOFFMANN, O., RUNG, O., HELD, J., BOETTCHER, C., PROKOP, S., STENZEL, W. & PRILLER, J. 2015. Lymphocytes modulate innate immune responses and neuronal damage in experimental meningitis. *Infect Immun,* 83**,** 259-67.

HOLDEN, S. S., GRANDI, F. C., ABOUBAKR, O., HIGASHIKUBO, B., CHO, F. S., CHANG, A. H., FORERO, A. O., MORNINGSTAR, A. R., MATHUR, V., KUHN, L. J., SURI, P., SANKARANARAYANAN, S., ANDREWS-ZWILLING, Y., TENNER, A. J., LUTHI, A., ARONICA, E., CORCES, M. R., YEDNOCK, T. & PAZ, J. T. 2021. Complement factor C1q mediates sleep spindle loss and epileptic spikes after mild brain injury. *Science,* 373**,** eabj2685.

HOLERS, V. M. 2014. Complement and its receptors: new insights into human disease. *Annu Rev Immunol,* 32**,** 433-59.

HOUBEN, R. M. & DODD, P. J. 2016. The Global Burden of Latent Tuberculosis Infection: A Re-estimation Using Mathematical Modelling. *PLoS Med,* 13**,** e1002152.

HOWE, C. L., LAFRANCE-COREY, R. G., GODDERY, E. N., JOHNSON, R. K. & MIRCHIA, K. 2017. Neuronal CCL2 expression drives inflammatory monocyte infiltration into the brain during acute virus infection. *J Neuroinflammation,* 14**,** 238.

HSU, N. J., FRANCISCO, N. M., KEETON, R., ALLIE, N., QUESNIAUX, V. F., RYFFEL, B. & JACOBS, M. 2017. Myeloid and T Cell-Derived TNF Protects against Central Nervous System Tuberculosis. *Front Immunol,* 8**,** 180.

HUANG, F., WANG, K. & SHEN, J. 2020. Lipoprotein-associated phospholipase A2: The story continues. *Medicinal Research Reviews,* 40**,** 79-134.

HUET, S., GROUX, H., CAILLOU, B., VALENTIN, H., PRIEUR, A. M. & BERNARD, A. 1989. CD44 contributes to T cell activation. *J Immunol,* 143**,** 798-801.

HUO, B., YANG, Y., LI, M., WAN, J., ZHANG, W., YU, B. & CHEN, X. 2021. Pax3 inhibits Neuro-2a cells proliferation and neurite outgrowth. *J Cell Mol Med,* 25**,** 1252-1262.

IBRAHIM, M. K., ABDELHAFEZ, T. H., TAKEUCHI, J. S., WAKAE, K., SUGIYAMA, M., TSUGE, M., ITO, M., WATASHI, K., EL KASSAS, M., KATO, T., MURAYAMA, A., SUZUKI, T., CHAYAMA, K., SHIMOTOHNO, K., MURAMATSU, M., ALY, H. H. & WAKITA, T. 2021. MafF Is an Antiviral Host Factor That Suppresses Transcription from Hepatitis B Virus Core Promoter. *J Virol,* 95**,** e0076721.

IGARASHI, A., OKOCHI, H., BRADHAM, D. M. & GROTENDORST, G. R. 1993. Regulation of connective tissue growth factor gene expression in human skin fibroblasts and during wound repair. *Mol Biol Cell,* 4**,** 637-45.

ILIEVSKA-POPOSKA, B., METODIEVA, M., ZAKOSKA, M., VRAGOTEROVA, C. & TRAJKOV, D. 2018. Latent Tuberculosis Infection - Diagnosis and Treatment. *Open Access Maced J Med Sci,* 6**,** 651-655.

IP, P.-P. & LIAO, F. 2010. Resistance to Dengue Virus Infection in Mice Is Potentiated by CXCL10 and Is Independent of CXCL10-Mediated Leukocyte Recruitment. *The Journal of Immunology,* 184**,** 5705-5714.

ISHIKAWA, E., ISHIKAWA, T., MORITA, Y. S., TOYONAGA, K., YAMADA, H., TAKEUCHI, O., KINOSHITA, T., AKIRA, S., YOSHIKAI, Y. & YAMASAKI, S. 2009. Direct recognition of the mycobacterial glycolipid, trehalose dimycolate, by C-type lectin Mincle. *J Exp Med,* 206**,** 2879-88.

ISHIMARU, M., YUSUKE, N., TSUKIMOTO, M., HARADA, H., TAKENOUCHI, T., KITANI, H. & KOJIMA, S. 2014. Purinergic signaling via P2Y receptors up-mediates IL-6 production by liver macrophages/Kupffer cells. *J Toxicol Sci,* 39**,** 413-23.

ISLES, H. M., HERMAN, K. D., ROBERTSON, A. L., LOYNES, C. A., PRINCE, L. R., ELKS, P. M. & RENSHAW, S. A. 2019. The CXCL12/CXCR4 Signaling Axis Retains Neutrophils at Inflammatory Sites in Zebrafish. *Front Immunol,* 10**,** 1784.

JAEGER, M., VAN DER LEE, R., CHENG, S. C., JOHNSON, M. D., KUMAR, V., NG, A., PLANTINGA, T. S., SMEEKENS, S. P., OOSTING, M., WANG, X., BARCHET, W., FITZGERALD, K., JOOSTEN, L. A. B., PERFECT, J. R., WIJMENGA, C., VAN DE VEERDONK, F. L., HUYNEN, M. A., XAVIER, R. J., KULLBERG, B. J. & NETEA, M. G. 2015. The RIG-I-like helicase receptor MDA5 (IFIH1) is involved in the host defense against Candida infections. *Eur J Clin Microbiol Infect Dis,* 34**,** 963-974.

JASENOSKY, L. D., SCRIBA, T. J., HANEKOM, W. A. & GOLDFELD, A. E. 2015. T cells and adaptive immunity to Mycobacterium tuberculosis in humans. *Immunol Rev,* 264**,** 74-87.

JOCHUM, W., PASSEGUE, E. & WAGNER, E. F. 2001. AP-1 in mouse development and tumorigenesis. *Oncogene,* 20**,** 2401-12.

JOHANSSON, S. E., HALL, H., BJORKLUND, J. & HOGLUND, P. 2004. Broadly impaired NK cell function in non-obese diabetic mice is partially restored by NK cell activation in vivo and by IL-12/IL-18 in vitro. *Int Immunol,* 16**,** 1-11.

JOSHI, Y. B., GIANNOPOULOS, P. F., CHU, J. & PRATICO, D. 2014. Modulation of lipopolysaccharide-induced memory insult, gamma-secretase, and neuroinflammation in triple transgenic mice by 5-lipoxygenase. *Neurobiol Aging,* 35**,** 1024-31.

KALSCHEUER, R., PALACIOS, A., ANSO, I., CIFUENTE, J., ANGUITA, J., JACOBS, W. R., JR., GUERIN, M. E. & PRADOS-ROSALES, R. 2019. The Mycobacterium tuberculosis capsule: a cell structure with key implications in pathogenesis. *Biochem J,* 476**,** 1995-2016.

KANEHISA, M. 2019. Toward understanding the origin and evolution of cellular organisms. *Protein Sci,* 28**,** 1947-1951.

KANEHISA, M., FURUMICHI, M., SATO, Y., ISHIGURO-WATANABE, M. & TANABE, M. 2021. KEGG: integrating viruses and cellular organisms. *Nucleic Acids Res,* 49**,** D545-D551.

KANEHISA, M. & GOTO, S. 2000. KEGG: kyoto encyclopedia of genes and genomes. *Nucleic Acids Res,* 28**,** 27-30.

KARMAN, J., CHU, H. H., CO, D. O., SEROOGY, C. M., SANDOR, M. & FABRY, Z. 2006. Dendritic cells amplify T cell-mediated immune responses in the central nervous system. *J Immunol,* 177**,** 7750-60.

KARPEL, M. E., BOUTWELL, C. L. & ALLEN, T. M. 2015. BLT humanized mice as a small animal model of HIV infection. *Curr Opin Virol,* 13**,** 75-80.

KASAHARA, K., SATO, I., OGURA, K., TAKEUCHI, H., KOBAYASHI, K. & ADACHI, M. 1998. Expression of chemokines and induction of rapid cell death in human blood neutrophils by Mycobacterium tuberculosis. *J Infect Dis,* 178**,** 127-37.

KAUL, D., HABBEL, P., DERKOW, K., KRUGER, C., FRANZONI, E., WULCZYN, F. G., BERESWILL, S., NITSCH, R., SCHOTT, E., VEH, R., NAUMANN, T. & LEHNARDT, S. 2012. Expression of Toll-like receptors in the developing brain. *PLoS One,* 7**,** e37767.

KAUSHAL, V., DYE, R., PAKAVATHKUMAR, P., FOVEAU, B., FLORES, J., HYMAN, B., GHETTI, B., KOLLER, B. H. & LEBLANC, A. C. 2015. Neuronal NLRP1 inflammasome activation of Caspase-1 coordinately regulates inflammatory interleukin-1-beta production and axonal degeneration-associated Caspase-6 activation. *Cell Death Differ,* 22**,** 1676-86.

KEETON, R., ALLIE, N., DAMBUZA, I., ABEL, B., HSU, N. J., SEBESHO, B., RANDALL, P., BURGER, P., FICK, E., QUESNIAUX, V. F., RYFFEL, B. & JACOBS, M. 2014. Soluble TNFRp75 regulates host protective immunity against Mycobacterium tuberculosis. *J Clin Invest,* 124**,** 1537-51.

KIRBY, E. D., JENSEN, K., GOOSENS, K. A. & KAUFER, D. 2012. Stereotaxic surgery for excitotoxic lesion of specific brain areas in the adult rat. *J Vis Exp***,** e4079.

KITAMURA, A., MAEKAWA, Y., UEHARA, H., IZUMI, K., KAWACHI, I., NISHIZAWA, M., TOYOSHIMA, Y., TAKAHASHI, H., STANDLEY, D. M., TANAKA, K., HAMAZAKI, J., MURATA, S., OBARA, K., TOYOSHIMA, I. & YASUTOMO, K. 2011. A mutation in the immunoproteasome subunit PSMB8 causes autoinflammation and lipodystrophy in humans. *J Clin Invest,* 121**,** 4150-60.

KLEIN, R. S., LIN, E., ZHANG, B., LUSTER, A. D., TOLLETT, J., SAMUEL, M. A., ENGLE, M. & DIAMOND, M. S. 2005. Neuronal CXCL10 directs CD8+ T-cell recruitment and control of West Nile virus encephalitis. *J Virol,* 79**,** 11457-66.

KO, C. Y., CHANG, L. H., LEE, Y. C., STERNECK, E., CHENG, C. P., CHEN, S. H., HUANG, A. M., TSENG, J. T. & WANG, J. M. 2012. CCAAT/enhancer binding protein delta (CEBPD) elevating PTX3 expression inhibits macrophage-mediated phagocytosis of dying neuron cells. *Neurobiol Aging,* 33**,** 422 e11-25.

KOMATSU, K., LEE, J. Y., MIYATA, M., HYANG LIM, J., JONO, H., KOGA, T., XU, H., YAN, C., KAI, H. & LI, J. D. 2013. Inhibition of PDE4B suppresses inflammation by increasing expression of the deubiquitinase CYLD. *Nat Commun,* 4**,** 1684.

KONI, P. A., JOSHI, S. K., TEMANN, U. A., OLSON, D., BURKLY, L. & FLAVELL, R. A. 2001. Conditional vascular cell adhesion molecule 1 deletion in mice: impaired lymphocyte migration to bone marrow. *J Exp Med,* 193**,** 741-54.

KORBECKI, J., GROCHANS, S., GUTOWSKA, I., BARCZAK, K. & BARANOWSKA-BOSIACKA, I. 2020a. CC Chemokines in a Tumor: A Review of Pro-Cancer and Anti-Cancer Properties of Receptors CCR5, CCR6, CCR7, CCR8, CCR9, and CCR10 Ligands. *Int J Mol Sci,* 21.

KORBECKI, J., KOJDER, K., SIMINSKA, D., BOHATYREWICZ, R., GUTOWSKA, I., CHLUBEK, D. & BARANOWSKA-BOSIACKA, I. 2020b. CC Chemokines in a Tumor: A Review of Pro-Cancer and Anti-Cancer Properties of the Ligands of Receptors CCR1, CCR2, CCR3, and CCR4. *Int J Mol Sci,* 21.

KRISHNAN, N., ROBERTSON, B. D. & THWAITES, G. 2013. Pathways of IL-1beta secretion by macrophages infected with clinical Mycobacterium tuberculosis strains. *Tuberculosis (Edinb),* 93**,** 538-47.

KUCHTA, K., KNIZEWSKI, L., WYRWICZ, L. S., RYCHLEWSKI, L. & GINALSKI, K. 2009. Comprehensive classification of nucleotidyltransferase fold proteins: identification of novel families and their representatives in human. *Nucleic Acids Res,* 37**,** 7701-14.

KURIAKOSE, T. & KANNEGANTI, T. D. 2018. ZBP1: Innate Sensor Regulating Cell Death and Inflammation. *Trends Immunol,* 39**,** 123-134.

KUROKAWA, C., IANKOV, I. D. & GALANIS, E. 2019. A key anti-viral protein, RSAD2/VIPERIN, restricts the release of measles virus from infected cells. *Virus Res,* 263**,** 145-150.

LAI, Y. F., LIN, T. M., WANG, C. H., SU, P. Y., WU, J. T., LIN, M. C. & ENG, H. L. 2016. Functional polymorphisms of the TLR7 and TLR8 genes contribute to Mycobacterium tuberculosis infection. *Tuberculosis (Edinb),* 98**,** 125-31.

LANDES, M. B., RAJARAM, M. V., NGUYEN, H. & SCHLESINGER, L. S. 2015. Role for NOD2 in Mycobacterium tuberculosis-induced iNOS expression and NO production in human macrophages. *J Leukoc Biol,* 97**,** 1111-9.

LANFRANCO, M. F., MOCCHETTI, I., BURNS, M. P. & VILLAPOL, S. 2017. Glial- and Neuronal-Specific Expression of CCL5 mRNA in the Rat Brain. *Front Neuroanat,* 11**,** 137.

LI, C., MENORET, A., FARRAGHER, C., OUYANG, Z., BONIN, C., HOLVOET, P., VELLA, A. T. & ZHOU, B. 2019. Single cell transcriptomics based-MacSpectrum reveals novel macrophage activation signatures in diseases. *JCI Insight,* 5.

LI, Q., CANOSA, S., FLYNN, K., MICHAUD, M., KRAUTHAMMER, M. & MADRI, J. A. 2013. Modeling the neurovascular niche: unbiased transcriptome analysis of the murine subventricular zone in response to hypoxic insult. *PLoS One,* 8**,** e76265.

LIAO, W., LIN, J. X. & LEONARD, W. J. 2013. Interleukin-2 at the crossroads of effector responses, tolerance, and immunotherapy. *Immunity,* 38**,** 13-25.

LIBLAU, R. S., GONZALEZ-DUNIA, D., WIENDL, H. & ZIPP, F. 2013. Neurons as targets for T cells in the nervous system. *Trends Neurosci,* 36**,** 315-24.

LIDDELOW, S. A., GUTTENPLAN, K. A., CLARKE, L. E., BENNETT, F. C., BOHLEN, C. J., SCHIRMER, L., BENNETT, M. L., MUNCH, A. E., CHUNG, W. S., PETERSON, T. C., WILTON, D. K., FROUIN, A., NAPIER, B. A., PANICKER, N., KUMAR, M., BUCKWALTER, M. S., ROWITCH, D. H., DAWSON, V. L.,

DAWSON, T. M., STEVENS, B. & BARRES, B. A. 2017. Neurotoxic reactive astrocytes are induced by activated microglia. *Nature,* 541**,** 481-487.

LIM, J. C., LU, W., BECKEL, J. M. & MITCHELL, C. H. 2016. Neuronal Release of Cytokine IL-3 Triggered by Mechanosensitive Autostimulation of the P2X7 Receptor Is Neuroprotective. *Front Cell Neurosci,* 10**,** 270.

LIN, F. S., WU, M. Y., TU, W. J., PAN, H. Q., ZHENG, J., SHI, J. W., FEI, Z. T., ZHANG, R. M., YAN, W. G., SHANG, M. Q., ZHENG, Q., WANG, M. J. & ZHANG, X. 2015. A cross-sectional and follow-up study of leukopenia in tuberculosis patients: prevalence, risk factors and impact of anti-tuberculosis treatment. *J Thorac Dis,* 7**,** 2234-42.

LIN, P. L. & FLYNN, J. L. 2015. CD8 T cells and Mycobacterium tuberculosis infection. *Semin Immunopathol,* 37**,** 239-49.

LIN, P. L., RUTLEDGE, T., GREEN, A. M., BIGBEE, M., FUHRMAN, C., KLEIN, E. & FLYNN, J. L. 2012. CD4 T cell depletion exacerbates acute Mycobacterium tuberculosis while reactivation of latent infection is dependent on severity of tissue depletion in cynomolgus macaques. *AIDS Res Hum Retroviruses,* 28**,** 1693-702.

LING, C., SANDOR, M., SURESH, M. & FABRY, Z. 2006. Traumatic injury and the presence of antigen differentially contribute to T-cell recruitment in the CNS. *J Neurosci,* 26**,** 731-41.

LIOU, J. T., YUAN, H. B., MAO, C. C., LAI, Y. S. & DAY, Y. J. 2012. Absence of C-C motif chemokine ligand 5 in mice leads to decreased local macrophage recruitment and behavioral hypersensitivity in a murine neuropathic pain model. *Pain,* 153**,** 1283-1291.

LITUMA, P. J., WOO, E., O'HARA, B. F., CASTILLO, P. E., SIBINGA, N. E. S. & NANDI, S. 2021. Altered synaptic connectivity and brain function in mice lacking microglial adapter protein Iba1. *Proc Natl Acad Sci U S A,* 118.

LIU, C., LI, Z., XU, L., SHI, Y., ZHANG, X., SHI, S., HOU, K., FAN, Y., LI, C., WANG, X., ZHOU, L., LIU, Y., QU, X. & CHE, X. 2020a. GALNT6 promotes breast cancer metastasis by increasing mucin-type O-glycosylation of alpha2M. *Aging (Albany NY),* 12**,** 11794-11811.

LIU, F., WANG, Z., QIU, Y., WEI, M., LI, C., XIE, Y., SHEN, L., HUANG, Y. & MA, C. 2017. Suppression of MyD88-dependent signaling alleviates neuropathic pain induced by peripheral nerve injury in the rat. *J Neuroinflammation,* 14**,** 70.

LIU, L., ZHANG, Z., ZHANG, G., WANG, T., MA, Y. & GUO, W. 2020b. Down-regulation of PADI2 prevents proliferation and epithelial-mesenchymal transition in ovarian cancer through inhibiting JAK2/STAT3 pathway in vitro and in vivo, alone or in combination with Olaparib. *J Transl Med,* 18**,** 357.

LIU, X., LI, F., NIU, H., MA, L., CHEN, J., ZHANG, Y., PENG, L., GAN, C., MA, X. & ZHU, B. 2020c. Corrigendum: IL-2 Restores T-Cell Dysfunction Induced by Persistent Mycobacterium tuberculosis Antigen Stimulation. *Front Immunol,* 11**,** 1671.

LIU, X., NEMETH, D. P., MCKIM, D. B., ZHU, L., DISABATO, D. J., BERDYSZ, O., GORANTLA, G., OLIVER, B., WITCHER, K. G., WANG, Y., NEGRAY, C. E., VEGESNA, R. S., SHERIDAN, J. F., GODBOUT, J. P., ROBSON, M. J., BLAKELY, R. D., POPOVICH, P. G., BILBO, S. D. & QUAN, N. 2019. Cell-Type-

Specific Interleukin 1 Receptor 1 Signaling in the Brain Regulates Distinct Neuroimmune Activities. *Immunity,* 50**,** 764-766.

LIU, Y., LIU, K., HUANG, Y., SUN, M., TIAN, Q., ZHANG, S. & QIN, Y. 2020d. TRIM25 Promotes TNF-α–Induced NF-κB Activation through Potentiating the K63-Linked Ubiquitination of TRAF2. *The Journal of Immunology,* 204**,** 1499-1507.

LIU, Y., TEIGE, I., BIRNIR, B. & ISSAZADEH-NAVIKAS, S. 2006. Neuron-mediated generation of regulatory T cells from encephalitogenic T cells suppresses EAE. *Nat Med,* 12**,** 518-25.

LOPEZ-GRANADOS, E., KEENAN, J. E., KINNEY, M. C., LEO, H., JAIN, N., MA, C. A., QUINONES, R., GELFAND, E. W. & JAIN, A. 2008. A novel mutation in NFKBIA/IKBA results in a degradation-resistant N-truncated protein and is associated with ectodermal dysplasia with immunodeficiency. *Hum Mutat,* 29**,** 861-8.

LOUVEAU, A., HERZ, J., ALME, M. N., SALVADOR, A. F., DONG, M. Q., VIAR, K. E., HEROD, S. G., KNOPP, J., SETLIFF, J. C., LUPI, A. L., DA MESQUITA, S., FROST, E. L., GAULTIER, A., HARRIS, T. H., CAO, R., HU, S., LUKENS, J. R., SMIRNOV, I., OVERALL, C. C., OLIVER, G. & KIPNIS, J. 2018. CNS lymphatic drainage and neuroinflammation are regulated by meningeal lymphatic vasculature. *Nat Neurosci,* 21**,** 1380-1391.

LOUVEAU, A., SMIRNOV, I., KEYES, T. J., ECCLES, J. D., ROUHANI, S. J., PESKE, J. D., DERECKI, N. C., CASTLE, D., MANDELL, J. W., LEE, K. S., HARRIS, T. H. & KIPNIS, J. 2015. Structural and functional features of central nervous system lymphatic vessels. *Nature,* 523**,** 337-41.

LUCKHEERAM, R. V., ZHOU, R., VERMA, A. D. & XIA, B. 2012. CD4(+)T cells: differentiation and functions. *Clin Dev Immunol,* 2012**,** 925135.

LUND, H., PIEBER, M., PARSA, R., HAN, J., GROMMISCH, D., EWING, E., KULAR, L., NEEDHAMSEN, M., ESPINOSA, A., NILSSON, E., OVERBY, A. K., BUTOVSKY, O., JAGODIC, M., ZHANG, X. M. & HARRIS, R. A. 2018. Competitive repopulation of an empty microglial niche yields functionally distinct subsets of microglia-like cells. *Nat Commun,* 9**,** 4845.

MACHUCA, I., VIDAL, E., DE LA TORRE-CISNEROS, J. & RIVERO-ROMAN, A. 2018. Tuberculosis in immunosuppressed patients. *Enferm Infecc Microbiol Clin (Engl Ed),* 36**,** 366-374.

MACMICKING, J. D., NORTH, R. J., LACOURSE, R., MUDGETT, J. S., SHAH, S. K. & NATHAN, C. F. 1997. Identification of nitric oxide synthase as a protective locus against tuberculosis. *Proc Natl Acad Sci U S A,* 94**,** 5243-8.

MAGRINI, E., MANTOVANI, A. & GARLANDA, C. 2016. The Dual Complexity of PTX3 in Health and Disease: A Balancing Act? *Trends Mol Med,* 22**,** 497-510.

MALIN, S. A. & MOLLIVER, D. C. 2010. Gi- and Gq-coupled ADP (P2Y) receptors act in opposition to modulate nociceptive signaling and inflammatory pain behavior. *Mol Pain,* 6**,** 21.

MANJALLY, A. V. & TAY, T. L. 2022. Attack of the Clones: Microglia in Health and Disease. *Front Cell Neurosci,* 16**,** 831747.

MARIANI, M. M. & KIELIAN, T. 2009. Microglia in infectious diseases of the central nervous system. *J Neuroimmune Pharmacol,* 4**,** 448-61.

MARQUES, C. P., CHEERAN, M. C., PALMQUIST, J. M., HU, S. & LOKENSGARD, J. R. 2008. Microglia are the major cellular source of inducible nitric oxide synthase during experimental herpes encephalitis. *J Neurovirol,* 14**,** 229-38.

MARSHALL, J. S., WARRINGTON, R., WATSON, W. & KIM, H. L. 2018. An introduction to immunology and immunopathology. *Allergy Asthma Clin Immunol,* 14**,** 49.

MARX, G. E. & CHAN, E. D. 2011. Tuberculous meningitis: diagnosis and treatment overview. *Tuberc Res Treat,* 2011**,** 798764.

MAYER-BARBER, K. D. & BARBER, D. L. 2015. Innate and Adaptive Cellular Immune Responses to Mycobacterium tuberculosis Infection. *Cold Spring Harb Perspect Med,* 5.

MAZZOLLA, R., PULITI, M., BARLUZZI, R., NEGLIA, R., BISTONI, F., BARBOLINI, G. & BLASI, E. 2002. Differential microbial clearance and immunoresponse of Balb/c (Nramp1 susceptible) and DBA2 (Nramp1 resistant) mice intracerebrally infected with Mycobacterium bovis BCG (BCG). *FEMS Immunol Med Microbiol,* 32**,** 149-58.

MCNAB, F. W., EWBANK, J., RAJSBAUM, R., STAVROPOULOS, E., MARTIROSYAN, A., REDFORD, P. S., WU, X., GRAHAM, C. M., SARAIVA, M., TSICHLIS, P., CHAUSSABEL, D., LEY, S. C. & O'GARRA, A. 2013. TPL-2-ERK1/2 signaling promotes host resistance against intracellular bacterial infection by negative regulation of type I IFN production. *J Immunol,* 191**,** 1732-43.

MCNEILL, E., STYLIANOU, E., CRABTREE, M. J., HARRINGTON-KANDT, R., KOLB, A. L., DIOTALLEVI, M., HALE, A. B., BETTENCOURT, P., TANNER, R., O'SHEA, M. K., MATSUMIYA, M., LOCKSTONE, H., MULLER, J., FLETCHER, H. A., GREAVES, D. R., MCSHANE, H. & CHANNON, K. M. 2018. Regulation of mycobacterial infection by macrophage Gch1 and tetrahydrobiopterin. *Nat Commun,* 9**,** 5409.

MESQUITA, L. P., COSTA, R. C., ZANATTO, D. A., BRUHN, F. R. P., MESQUITA, L. L. R., LARA, M., VILLALOBOS, E. M. C., MASSOCO, C. O., MORI, C. M. C., MORI, E. & MAIORKA, P. C. 2021. Equine herpesvirus 1 elicits a strong pro-inflammatory response in the brain of mice. *J Gen Virol,* 102.

MICHAEL, B. D., BRICIO-MORENO, L., SORENSEN, E. W., MIYABE, Y., LIAN, J., SOLOMON, T., KURT-JONES, E. A. & LUSTER, A. D. 2020. Astrocyte- and Neuron-Derived CXCL1 Drives Neutrophil Transmigration and Blood-Brain Barrier Permeability in Viral Encephalitis. *Cell Rep,* 32**,** 108150.

MO, J., KIM, C. H., LEE, D., SUN, W., LEE, H. W. & KIM, H. 2015. Early growth response 1 (Egr-1) directly regulates GABAA receptor alpha2, alpha4, and theta subunits in the hippocampus. *J Neurochem,* 133**,** 489-500.

MOCKENHAUPT, K., GONSIEWSKI, A. & KORDULA, T. 2021. RelB and Neuroinflammation. *Cells,* 10.

MOHAMMAD, M. G., TSAI, V. W., RUITENBERG, M. J., HASSANPOUR, M., LI, H., HART, P. H., BREIT, S. N., SAWCHENKO, P. E. & BROWN, D. A. 2014. Immune cell trafficking from the brain maintains CNS immune tolerance. *J Clin Invest,* 124**,** 1228-41.

MOHANTY, T., FISHER, J., BAKOCHI, A., NEUMANN, A., CARDOSO, J. F. P., KARLSSON, C. A. Q., PAVAN, C., LUNDGAARD, I., NILSON, B., REINSTRUP, P., BONNEVIER, J., CEDERBERG, D., MALMSTROM, J., BENTZER, P. & LINDER, A. 2019. Neutrophil extracellular traps in the central nervous system hinder bacterial clearance during pneumococcal meningitis. *Nat Commun,* 10**,** 1667.

MONTEITH, A. J., MILLER, J. M., MAXWELL, C. N., CHAZIN, W. J. & SKAAR, E. P. 2021. Neutrophil extracellular traps enhance macrophage killing of bacterial pathogens. *Sci Adv,* 7**,** eabj2101.

MOULE, M. G. & CIRILLO, J. D. 2020. Mycobacterium tuberculosis Dissemination Plays a Critical Role in Pathogenesis. *Front Cell Infect Microbiol,* 10**,** 65.

MULLER, M. L., CHIANG, S. C., MEETHS, M., TESI, B., ENTESARIAN, M., NILSSON, D., WOOD, S. M., NORDENSKJOLD, M., HENTER, J. I., NAQVI, A. & BRYCESON, Y. T. 2014. An N-Terminal Missense Mutation in STX11 Causative of FHL4 Abrogates Syntaxin-11 Binding to Munc18-2. *Front Immunol,* 4**,** 515.

NAVARRO-FLORES, A., FERNANDEZ-CHINGUEL, J. E., PACHECO-BARRIOS, N., SORIANO-MORENO, D. R. & PACHECO-BARRIOS, K. 2022. Global morbidity and mortality of central nervous system tuberculosis: a systematic review and meta-analysis. *J Neurol,* 269**,** 3482-3494.

NAYAK, D., ZINSELMEYER, B. H., CORPS, K. N. & MCGAVERN, D. B. 2012. In vivo dynamics of innate immune sentinels in the CNS. *Intravital,* 1**,** 95-106.

NELSON, K. L., ROGERS, J. A., BOWMAN, T. L., JOVE, R. & SMITHGALL, T. E. 1998. Activation of STAT3 by the c-Fes protein-tyrosine kinase. *J Biol Chem,* 273**,** 7072-7.

NEUMANN, H., CAVALIE, A., JENNE, D. E. & WEKERLE, H. 1995. Induction of MHC class I genes in neurons. *Science,* 269**,** 549-52.

NISHITANI, H. & LYGEROU, Z. 2004. DNA replication licensing. *Front Biosci,* 9**,** 2115-32.

NOLL, J. E., HEWETT, D. R., WILLIAMS, S. A., VANDYKE, K., KOK, C., TO, L. B. & ZANNETTINO, A. C. 2014. SAMSN1 is a tumor suppressor gene in multiple myeloma. *Neoplasia,* 16**,** 572-85.

OECKINGHAUS, A. & GHOSH, S. 2009. The NF-kappaB family of transcription factors and its regulation. *Cold Spring Harb Perspect Biol,* 1**,** a000034.

OKABE, M., TAKARADA, S., MIYAO, N., NAKAOKA, H., IBUKI, K., OZAWA, S., WATANABE, K., TSUJI, H., HASHIMOTO, I., HATASAKI, K., HAYAKAWA, S., HAMAGUCHI, Y., HAMADA, M., ICHIDA, F. & HIRONO, K. 2022. G0S2 regulates innate immunity in Kawasaki disease via lncRNA HSD11B1-AS1. *Pediatr Res,* 92**,** 378-387.

OKADA, S., SHIKATA, K., MATSUDA, M., OGAWA, D., USUI, H., KIDO, Y., NAGASE, R., WADA, J., SHIKATA, Y. & MAKINO, H. 2003. Intercellular adhesion molecule-1-deficient mice are resistant against renal injury after induction of diabetes. *Diabetes,* 52**,** 2586-93.

OLIN, M. R., ARMIEN, A. G., CHEERAN, M. C., ROCK, R. B., MOLITOR, T. W. & PETERSON, P. K. 2008. Role of nitric oxide in defense of the central nervous system against Mycobacterium tuberculosis. *J Infect Dis,* 198**,** 886-9.

OTHMAN, F. N., MUTHURAJU, S., NOOR, S. S. M., ABDULLAH, S., MOHD YUSOFF, A. A., THARAKAN, J., BHASKAR, S., MAHMOOD, M. S., KASSIM, F., RAFIA, H., MOHD HASPANI, M. S., ALIAS, A., PANDO, R. H., ABDULLAH, J. M. & JAAFAR, H. 2018. Human tuberculosis brain promotes neuronal apoptosis but not in astrocytes with high expression of vascular endothelial growth factor. *Tuberculosis (Edinb),* 112**,** 45-51.

OYAGI, A. & HARA, H. 2012. Essential roles of heparin-binding epidermal growth factor-like growth factor in the brain. *CNS Neurosci Ther,* 18**,** 803-10.

PAI, M., BEHR, M. A., DOWDY, D., DHEDA, K., DIVANGAHI, M., BOEHME, C. C., GINSBERG, A., SWAMINATHAN, S., SPIGELMAN, M., GETAHUN, H., MENZIES, D. & RAVIGLIONE, M. 2016. Tuberculosis. *Nature Reviews Disease Primers,* 2**,** 16076.

PANG, Z., RAUDONIS, R., MCCORMICK, C. & CHENG, Z. 2019. Early Growth Response 1 Deficiency Protects the Host against Pseudomonas aeruginosa Lung Infection. *Infect Immun,* 88.

PARK, J. G., RYU, S. Y., JUNG, I. H., LEE, Y. H., KANG, K. J., LEE, M. R., LEE, M. N., SONN, S. K., LEE, J. H., LEE, H., OH, G. T., MOON, K. & SHIM, H. 2013. Evaluation of VCAM-1 antibodies as therapeutic agent for atherosclerosis in apolipoprotein E-deficient mice. *Atherosclerosis,* 226**,** 356-63.

PARK, W. Y., AHN, J. H., FELDMAN, R. A. & SEO, J. S. 1998. c-Fes tyrosine kinase binds to and activates STAT3 after granulocyte-macrophage colony-stimulating factor stimulation. *Cancer Lett,* 129**,** 29-37.

PEI, L., CASTRILLO, A. & TONTONOZ, P. 2006. Regulation of macrophage inflammatory gene expression by the orphan nuclear receptor Nur77. *Mol Endocrinol,* 20**,** 786-94.

PERNG, Y. C. & LENSCHOW, D. J. 2018. ISG15 in antiviral immunity and beyond. *Nat Rev Microbiol,* 16**,** 423-439.

PERSIDSKY, Y., RAMIREZ, S. H., HAORAH, J. & KANMOGNE, G. D. 2006. Blood-brain barrier: structural components and function under physiologic and pathologic conditions. *J Neuroimmune Pharmacol,* 1**,** 223-36.

PETERSON, P. K., GEKKER, G., HU, S., SHENG, W. S., ANDERSON, W. R., ULEVITCH, R. J., TOBIAS, P. S., GUSTAFSON, K. V., MOLITOR, T. W. & CHAO, C. C. 1995. CD14 receptor-mediated uptake of nonopsonized Mycobacterium tuberculosis by human microglia. *Infect Immun,* 63**,** 1598-602.

PICHLMAIR, A., LASSNIG, C., EBERLE, C. A., GORNA, M. W., BAUMANN, C. L., BURKARD, T. R., BURCKSTUMMER, T., STEFANOVIC, A., KRIEGER, S., BENNETT, K. L., RULICKE, T., WEBER, F., COLINGE, J., MULLER, M. & SUPERTI-FURGA, G. 2011. IFIT1 is an antiviral protein that recognizes 5'-triphosphate RNA. *Nat Immunol,* 12**,** 624-30.

PIGANELLI, J. D., MARTIN, T. & HASKINS, K. 1998. Splenic macrophages from the NOD mouse are defective in the ability to present antigen. *Diabetes,* 47**,** 1212-8.

PISHESHA, N., HARMAND, T. J. & PLOEGH, H. L. 2022. A guide to antigen processing and presentation. *Nat Rev Immunol,* 22**,** 751-764.

POMBINHO, R., PINHEIRO, J., RESENDE, M., MEIRELES, D., JALKANEN, S., SOUSA, S. & CABANES, D. 2021. Stabilin-1 plays a protective role against Listeria

monocytogenes infection through the regulation of cytokine and chemokine production and immune cell recruitment. *Virulence,* 12**,** 2088-2103.

QIAN, Z., QIN, J., LAI, Y., ZHANG, C. & ZHANG, X. 2023. Large-Scale Integration of Single-Cell RNA-Seq Data Reveals Astrocyte Diversity and Transcriptomic Modules across Six Central Nervous System Disorders. *Biomolecules,* 13.

QIAO, W., FAN, J., SHANG, X., WANG, L., TUOHETAERBAIKE, B., LI, Y., ZHANG, L., HUO, Y., WANG, J. & MA, X. 2022. Bioinformation Analysis Reveals IFIT1 as Potential Biomarkers in Central Nervous System Tuberculosis. *Infect Drug Resist,* 15**,** 35-45.

QUINTANA, F. J., YESTE, A. & MASCANFRONI, I. D. 2015. Role and therapeutic value of dendritic cells in central nervous system autoimmunity. *Cell Death Differ,* 22**,** 215-24.

RAMOS-KICHIK, V., MONDRAGON-FLORES, R., MONDRAGON-CASTELAN, M., GONZALEZ-POZOS, S., MUNIZ-HERNANDEZ, S., ROJAS-ESPINOSA, O., CHACON-SALINAS, R., ESTRADA-PARRA, S. & ESTRADA-GARCIA, I. 2009. Neutrophil extracellular traps are induced by Mycobacterium tuberculosis. *Tuberculosis (Edinb),* 89**,** 29-37.

RANDALL, P. J., HSU, N. J., LANG, D., COOPER, S., SEBESHO, B., ALLIE, N., KEETON, R., FRANCISCO, N. M., SALIE, S., LABUSCHAGNE, A., QUESNIAUX, V., RYFFEL, B., KELLAWAY, L. & JACOBS, M. 2014. Neurons are host cells for Mycobacterium tuberculosis. *Infect Immun,* 82**,** 1880-90.

RANDALL, P. J., HSU, N. J., QUESNIAUX, V., RYFFEL, B. & JACOBS, M. 2015. Mycobacterium tuberculosis infection of the 'non-classical immune cell'. *Immunol Cell Biol,* 93**,** 789-95.

REYNOLDS, J. J., BICKNELL, L. S., CARROLL, P., HIGGS, M. R., SHAHEEN, R., MURRAY, J. E., PAPADOPOULOS, D. K., LEITCH, A., MURINA, O., TARNAUSKAITE, Z., WESSEL, S. R., ZLATANOU, A., VERNET, A., VON KRIEGSHEIM, A., MOTTRAM, R. M., LOGAN, C. V., BYE, H., LI, Y., BREAN, A., MADDIREVULA, S., CHALLIS, R. C., SKOULOUDAKI, K., ALMOISHEER, A., ALSAIF, H. S., AMAR, A., PRESCOTT, N. J., BOBER, M. B., DUKER, A., FAQEIH, E., SEIDAHMED, M. Z., AL TALA, S., ALSWAID, A., AHMED, S., AL-AAMA, J. Y., ALTMULLER, J., AL BALWI, M., BRADY, A. F., CHESSA, L., COX, H., FISCHETTO, R., HELLER, R., HENDERSON, B. D., HOBSON, E., NURNBERG, P., PERCIN, E. F., PERON, A., SPACCINI, L., QUIGLEY, A. J., THAKUR, S., WISE, C. A., YOON, G., ALNEMER, M., TOMANCAK, P., YIGIT, G., TAYLOR, A. M., REIJNS, M. A., SIMPSON, M. A., CORTEZ, D., ALKURAYA, F. S., MATHEW, C. G., JACKSON, A. P. & STEWART, G. S. 2017. Mutations in DONSON disrupt replication fork stability and cause microcephalic dwarfism. *Nat Genet,* 49**,** 537-549.

RIBES, S., NESSLER, S., HEIDE, E. C., MALZAHN, D., PERSKE, C., BRUCK, W. & NAU, R. 2017. The Early Adaptive Immune Response in the Pathophysiological Process of Pneumococcal Meningitis. *J Infect Dis,* 215**,** 150-158.

RIEDEL, D. D. & KAUFMANN, S. H. 1997. Chemokine secretion by human polymorphonuclear granulocytes after stimulation with Mycobacterium tuberculosis and lipoarabinomannan. *Infect Immun,* 65**,** 4620-3.

RITCHIE, M. E., PHIPSON, B., WU, D., HU, Y., LAW, C. W., SHI, W. & SMYTH, G. K. 2015. limma powers differential expression analyses for RNA-sequencing and microarray studies. *Nucleic Acids Res,* 43**,** e47.

ROCK, R. B., GEKKER, G., HU, S., SHENG, W. S., CHEERAN, M., LOKENSGARD, J. R. & PETERSON, P. K. 2004. Role of microglia in central nervous system infections. *Clin Microbiol Rev,* 17**,** 942-64, table of contents.

ROCK, R. B., HU, S., GEKKER, G., SHENG, W. S., MAY, B., KAPUR, V. & PETERSON, P. K. 2005. Mycobacterium tuberculosis-induced cytokine and chemokine expression by human microglia and astrocytes: effects of dexamethasone. *J Infect Dis,* 192**,** 2054-8.

ROCK, R. B., OLIN, M., BAKER, C. A., MOLITOR, T. W. & PETERSON, P. K. 2008. Central nervous system tuberculosis: pathogenesis and clinical aspects. *Clin Microbiol Rev,* 21**,** 243-61, table of contents.

RODRIGUEZ-TAKEUCHI, S. Y., RENJIFO, M. E. & MEDINA, F. J. 2019. Extrapulmonary Tuberculosis: Pathophysiology and Imaging Findings. *Radiographics,* 39**,** 2023-2037.

RONCA, S. E., DINELEY, K. T. & PAESSLER, S. 2016. Neurological Sequelae Resulting from Encephalitic Alphavirus Infection. *Front Microbiol,* 7**,** 959.

ROTHENFLUH, A., YOUNG, M. W. & SAEZ, L. 2000. A TIMELESS-independent function for PERIOD proteins in the Drosophila clock. *Neuron,* 26**,** 505-14.

ROTOLI, B. M., BARILLI, A., VISIGALLI, R., INGOGLIA, F., MILIOLI, M., DI LASCIA, M., RICCARDI, B., PUCCINI, P. & DALL'ASTA, V. 2018. Downregulation of SLC7A7 Triggers an Inflammatory Phenotype in Human Macrophages and Airway Epithelial Cells. *Front Immunol,* 9**,** 508.

RUMZHUM, N. N. & AMMIT, A. J. 2016. Cyclooxygenase 2: its regulation, role and impact in airway inflammation. *Clin Exp Allergy,* 46**,** 397-410.

RUSSO, M. V. & MCGAVERN, D. B. 2015. Immune Surveillance of the CNS following Infection and Injury. *Trends Immunol,* 36**,** 637-650.

SACCHETTI, P., CARPENTIER, R., SEGARD, P., OLIVE-CREN, C. & LEFEBVRE, P. 2006. Multiple signaling pathways regulate the transcriptional activity of the orphan nuclear receptor NURR1. *Nucleic Acids Res,* 34**,** 5515-27.

SAENZ, B., HERNANDEZ-PANDO, R., FRAGOSO, G., BOTTASSO, O. & CARDENAS, G. 2013. The dual face of central nervous system tuberculosis: a new Janus Bifrons? *Tuberculosis (Edinb),* 93**,** 130-5.

SAGHAZADEH, A. & REZAEI, N. 2022. Central Inflammatory Cytokines in Tuberculous Meningitis: A Systematic Review and Meta-analysis. *Journal of Interferon & Cytokine Research,* 42**,** 95-107.

SANTIN, I., MOORE, F., GRIECO, F. A., MARCHETTI, P., BRANCOLINI, C. & EIZIRIK, D. L. 2012. USP18 is a key regulator of the interferon-driven gene network modulating pancreatic beta cell inflammation and apoptosis. *Cell Death Dis,* 3**,** e419.

SAREILA, O., JAAKKOLA, N., OLOFSSON, P., KELKKA, T. & HOLMDAHL, R. 2013. Identification of a region in p47phox/NCF1 crucial for phagocytic NADPH oxidase (NOX2) activation. *J Leukoc Biol,* 93**,** 427-35.

SAWANT, K. V., POLURI, K. M., DUTTA, A. K., SEPURU, K. M., TROSHKINA, A., GAROFALO, R. P. & RAJARATHNAM, K. 2016. Chemokine CXCL1 mediated neutrophil recruitment: Role of glycosaminoglycan interactions. *Sci Rep,* 6**,** 33123.

SAWANT, K. V., SEPURU, K. M., LOWRY, E., PENARANDA, B., FREVERT, C. W., GAROFALO, R. P. & RAJARATHNAM, K. 2021. Neutrophil recruitment by chemokines Cxcl1/KC and Cxcl2/MIP2: Role of Cxcr2 activation and glycosaminoglycan interactions. *J Leukoc Biol,* 109**,** 777-791.

SCANGA, C. A., MOHAN, V. P., TANAKA, K., ALLAND, D., FLYNN, J. L. & CHAN, J. 2001. The inducible nitric oxide synthase locus confers protection against aerogenic challenge of both clinical and laboratory strains of Mycobacterium tuberculosis in mice. *Infect Immun,* 69**,** 7711-7.

SCARL, R. T., LAWRENCE, C. M., GORDON, H. M. & NUNEMAKER, C. S. 2017. STEAP4: its emerging role in metabolism and homeostasis of cellular iron and copper. *J Endocrinol,* 234**,** R123-R134.

SCHIFFER, R., BARON, J., DAGTEKIN, G., JAHNEN-DECHENT, W. & ZWADLO-KLARWASSER, G. 2002. Differential regulation of the expression of transporters associated with antigen processing, TAP1 and TAP2, by cytokines and lipopolysaccharide in primary human macrophages. *Inflamm Res,* 51**,** 403-8.

SEDER, R. A., DARRAH, P. A. & ROEDERER, M. 2008. T-cell quality in memory and protection: implications for vaccine design. *Nat Rev Immunol,* 8**,** 247-58.

SHAFIANI, S., TUCKER-HEARD, G., KARIYONE, A., TAKATSU, K. & URDAHL, K. B. 2010. Pathogen-specific regulatory T cells delay the arrival of effector T cells in the lung during early tuberculosis. *J Exp Med,* 207**,** 1409-20.

SHARMA, P. K., SAHA, P. K., SINGH, A., SHARMA, S. K., GHOSH, B. & MITRA, D. K. 2009. FoxP3+ regulatory T cells suppress effector T-cell function at pathologic site in miliary tuberculosis. *Am J Respir Crit Care Med,* 179**,** 1061-70.

SHATZ, C. J. 2009. MHC class I: an unexpected role in neuronal plasticity. *Neuron,* 64**,** 40-5.

SHRESTHA, B., GOTTLIEB, D. & DIAMOND, M. S. 2003. Infection and injury of neurons by West Nile encephalitis virus. *J Virol,* 77**,** 13203-13.

SIMHADRI, V. R., MARIANO, J. L., GIL-KRZEWSKA, A., ZHOU, Q. & BORREGO, F. 2013. CD300c is an activating receptor expressed on human monocytes. *J Innate Immun,* 5**,** 389-400.

SJOO, F., HASSAN, Z., ABEDI-VALUGERDI, M., GRISKEVICIUS, L., NILSSON, C., REMBERGER, M., ASCHAN, J., CONCHA, H., GAUGHAN, U. & HASSAN, M. 2006. Myeloablative and immunosuppressive properties of treosulfan in mice. *Exp Hematol,* 34**,** 115-21.

SLAUCH, J. M. 2011. How does the oxidative burst of macrophages kill bacteria? Still an open question. *Mol Microbiol,* 80**,** 580-3.

SMOLDERS, J., REMMERSWAAL, E. B., SCHUURMAN, K. G., MELIEF, J., VAN EDEN, C. G., VAN LIER, R. A., HUITINGA, I. & HAMANN, J. 2013. Characteristics of differentiated CD8(+) and CD4 (+) T cells present in the human brain. *Acta Neuropathol,* 126**,** 525-35.

SMYTH, G. K. 2004. Linear models and empirical bayes methods for assessing differential expression in microarray experiments. *Stat Appl Genet Mol Biol,* 3**,** Article3.

SMYTH, P., SASIWACHIRANGKUL, J., WILLIAMS, R. & SCOTT, C. J. 2022. Cathepsin S (CTSS) activity in health and disease - A treasure trove of untapped clinical potential. *Mol Aspects Med,* 88**,** 101106.

SOFRONIEW, M. V. & VINTERS, H. V. 2010. Astrocytes: biology and pathology. *Acta Neuropathol,* 119**,** 7-35.

SOLDEVILLA, P., VILAPLANA, C. & CARDONA, P. J. 2022. Mouse Models for Mycobacterium tuberculosis Pathogenesis: Show and Do Not Tell. *Pathogens,* 12.

SPANDAU, U., BROCKER, E. B., KAMPGEN, E. & GILLITZER, R. 2002. CC and CXC chemokines are differentially expressed in erythema multiforme in vivo. *Arch Dermatol,* 138**,** 1027-33.

SPANOS, J. P., HSU, N. J. & JACOBS, M. 2015. Microglia are crucial regulators of neuro-immunity during central nervous system tuberculosis. *Front Cell Neurosci,* 9**,** 182.

STATSSA 2020. Mortality and causes of death in South Africa: Findings from death notification. Department: Statistics South Africa.

STOOLMAN, J. S., DUNCKER, P. C., HUBER, A. K., GILES, D. A., WASHNOCK-SCHMID, J. M., SOULIKA, A. M. & SEGAL, B. M. 2018. An IFNgamma/CXCL2 regulatory pathway determines lesion localization during EAE. *J Neuroinflammation,* 15**,** 208.

STRACHAN, L., MURISON, J. G., PRESTIDGE, R. L., SLEEMAN, M. A., WATSON, J. D. & KUMBLE, K. D. 2001. Cloning and biological activity of epigen, a novel member of the epidermal growth factor superfamily. *J Biol Chem,* 276**,** 18265-71.

STRATOULIAS, V., VENERO, J. L., TREMBLAY, M. E. & JOSEPH, B. 2019. Microglial subtypes: diversity within the microglial community. *EMBO J,* 38**,** e101997.

STRIETER, R. M., GOMPERTS, B. N. & KEANE, M. P. 2007. The role of CXC chemokines in pulmonary fibrosis. *J Clin Invest,* 117**,** 549-56.

SU, S., ZHU, H., XU, X., WANG, X., DONG, Y., KAPUKU, G., TREIBER, F., GUTIN, B., HARSHFIELD, G., SNIEDER, H. & WANG, X. 2014. DNA methylation of the LY86 gene is associated with obesity, insulin resistance, and inflammation. *Twin Res Hum Genet,* 17**,** 183-91.

SULLIVAN, B. M., JOBE, O., LAZAREVIC, V., VASQUEZ, K., BRONSON, R., GLIMCHER, L. H. & KRAMNIK, I. 2005. Increased susceptibility of mice lacking T-bet to infection with Mycobacterium tuberculosis correlates with increased IL-10 and decreased IFN-gamma production. *J Immunol,* 175**,** 4593-602.

SUN, Y., MA, J., LI, D., LI, P., ZHOU, X., LI, Y., HE, Z., QIN, L., LIANG, L. & LUO, X. 2019. Interleukin-10 inhibits interleukin-1beta production and inflammasome activation of microglia in epileptic seizures. *J Neuroinflammation,* 16**,** 66.

SWEENEY, M. D., ZHAO, Z., MONTAGNE, A., NELSON, A. R. & ZLOKOVIC, B. V. 2019. Blood-Brain Barrier: From Physiology to Disease and Back. *Physiol Rev,* 99**,** 21-78.

SWEET, R. A., NICKERSON, K. M., CULLEN, J. L., WANG, Y. & SHLOMCHIK, M. J. 2017. B Cell-Extrinsic Myd88 and Fcer1g Negatively Regulate Autoreactive and Normal B Cell Immune Responses. *J Immunol,* 199**,** 885-893.

SZEPESI, Z., MANOUCHEHRIAN, O., BACHILLER, S. & DEIERBORG, T. 2018. Bidirectional Microglia-Neuron Communication in Health and Disease. *Front Cell Neurosci,* 12**,** 323.

TAKEUCHI, O., KAWAI, T., MUHLRADT, P. F., MORR, M., RADOLF, J. D., ZYCHLINSKY, A., TAKEDA, K. & AKIRA, S. 2001. Discrimination of bacterial lipoproteins by Toll-like receptor 6. *Int Immunol,* 13**,** 933-40.

TAN, B. H., MEINKEN, C., BASTIAN, M., BRUNS, H., LEGASPI, A., OCHOA, M. T., KRUTZIK, S. R., BLOOM, B. R., GANZ, T., MODLIN, R. L. & STENGER, S. 2006. Macrophages acquire neutrophil granules for antimicrobial activity against intracellular pathogens. *J Immunol,* 177**,** 1864-71.

TAN, E. E., HOPKINS, R. A., LIM, C. K., JAMUAR, S. S., ONG, C., THOON, K. C., KOH, M. J., SHIN, E. M., LIAN, D. W., WEERASOORIYA, M., LEE, C. Z., SOETEDJO, A. A. P., LIM, C. S., AU, V. B., CHUA, E., LEE, H. Y., JONES, L. A., JAMES, S. S., KALIAPERUMAL, N., KWOK, J., TAN, E. S., THOMAS, B., WU, L. X., HO, L., FAIRHURST, A. M., GINHOUX, F., TEO, A. K., ZHANG, Y. L., ONG, K. H., YU, W., VENKATESH, B., TERGAONKAR, V., REVERSADE, B., CHIN, K. C., TAN, A. M., LIEW, W. K. & CONNOLLY, J. E. 2020. Dominant-negative NFKBIA mutation promotes IL-1beta production causing hepatic disease with severe immunodeficiency. *J Clin Invest,* 130**,** 5817-5832.

TARASSISHIN, L., SUH, H. S. & LEE, S. C. 2014. LPS and IL-1 differentially activate mouse and human astrocytes: role of CD14. *Glia,* 62**,** 999-1013.

TARCA, A. L., DRAGHICI, S., KHATRI, P., HASSAN, S. S., MITTAL, P., KIM, J. S., KIM, C. J., KUSANOVIC, J. P. & ROMERO, R. 2009. A novel signaling pathway impact analysis. *Bioinformatics,* 25**,** 75-82.

TERRY, R. L., GETTS, D. R., DEFFRASNES, C., VAN VREDEN, C., CAMPBELL, I. L. & KING, N. J. 2012. Inflammatory monocytes and the pathogenesis of viral encephalitis. *J Neuroinflammation,* 9**,** 270.

THAIR, S. A., TOPCHIY, E., BOYD, J. H., CIRSTEA, M., WANG, C., NAKADA, T. A., FJELL, C. D., WURFEL, M., RUSSELL, J. A. & WALLEY, K. R. 2016. TNFAIP2 Inhibits Early TNFalpha-Induced NF-x03BA;B Signaling and Decreases Survival in Septic Shock Patients. *J Innate Immun,* 8**,** 57-66.

TIAN, L., MA, L., KAARELA, T. & LI, Z. 2012. Neuroimmune crosstalk in the central nervous system and its significance for neurological diseases. *J Neuroinflammation,* 9**,** 155.

TIAN, T., WOODWORTH, J., SKOLD, M. & BEHAR, S. M. 2005. In vivo depletion of CD11c+ cells delays the CD4+ T cell response to Mycobacterium tuberculosis and exacerbates the outcome of infection. *J Immunol,* 175**,** 3268-72.

TOKAREV, A., SKASKO, M., FITZPATRICK, K. & GUATELLI, J. 2009. Antiviral activity of the interferon-induced cellular protein BST-2/tetherin. *AIDS Res Hum Retroviruses,* 25**,** 1197-210.

TRIANTAFILOU, M., GAMPER, F. G., HASTON, R. M., MOURATIS, M. A., MORATH, S., HARTUNG, T. & TRIANTAFILOU, K. 2006. Membrane sorting of toll-like

receptor (TLR)-2/6 and TLR2/1 heterodimers at the cell surface determines heterotypic associations with CD36 and intracellular targeting. *J Biol Chem,* 281**,** 31002-11.

TSENOVA, L., BERGTOLD, A., FREEDMAN, V. H., YOUNG, R. A. & KAPLAN, G. 1999. Tumor necrosis factor alpha is a determinant of pathogenesis and disease progression in mycobacterial infection in the central nervous system. *Proc Natl Acad Sci U S A,* 96**,** 5657-62.

TSENOVA, L., ELLISON, E., HARBACHEUSKI, R., MOREIRA, A. L., KUREPINA, N., REED, M. B., MATHEMA, B., BARRY, C. E., 3RD & KAPLAN, G. 2005. Virulence of selected Mycobacterium tuberculosis clinical isolates in the rabbit model of meningitis is dependent on phenolic glycolipid produced by the bacilli. *J Infect Dis,* 192**,** 98-106.

TSENOVA, L., SOKOL, K., FREEDMAN, V. H. & KAPLAN, G. 1998. A combination of thalidomide plus antibiotics protects rabbits from mycobacterial meningitis-associated death. *J Infect Dis,* 177**,** 1563-72.

TUFARIELLO, J. M., CHAN, J. & FLYNN, J. L. 2003. Latent tuberculosis: mechanisms of host and bacillus that contribute to persistent infection. *The Lancet Infectious Diseases,* 3**,** 578-590.

TURNER, J., GONZALEZ-JUARRERO, M., SAUNDERS, B. M., BROOKS, J. V., MARIETTA, P., ELLIS, D. L., FRANK, A. A., COOPER, A. M. & ORME, I. M. 2001. Immunological basis for reactivation of tuberculosis in mice. *Infect Immun,* 69**,** 3264-70.

URIBE-QUEROL, E. & ROSALES, C. 2017. Control of Phagocytosis by Microbial Pathogens. *Front Immunol,* 8**,** 1368.

VAGASKA, B., NEW, S. E., ALVAREZ-GONZALEZ, C., D'ACQUISTO, F., GOMEZ, S. G., BULSTRODE, N. W., MADRIGAL, A. & FERRETTI, P. 2016. MHC-class-II are expressed in a subpopulation of human neural stem cells in vitro in an IFNgamma-independent fashion and during development. *Sci Rep,* 6**,** 24251.

VAN SCHAARENBURG, R. A., DAHA, N. A., SCHONKEREN, J. J., NIVINE LEVARHT, E. W., VAN GIJLSWIJK-JANSSEN, D. J., KURREEMAN, F. A., ROOS, A., VAN KOOTEN, C., KOELMAN, C. A., ERNST-KRUIS, M. R., TOES, R. E., HUIZINGA, T. W., LANKESTER, A. C. & TROUW, L. A. 2015. Identification of a novel non-coding mutation in C1qB in a Dutch child with C1q deficiency associated with recurrent infections. *Immunobiology,* 220**,** 422-7.

VAN WELL, G. T., WIELAND, C. W., FLORQUIN, S., ROORD, J. J., VAN DER POLL, T. & VAN FURTH, A. M. 2007. A new murine model to study the pathogenesis of tuberculous meningitis. *J Infect Dis,* 195**,** 694-7.

VEREMEYKO, T., YUNG, A. W. Y., ANTHONY, D. C., STREKALOVA, T. & PONOMAREV, E. D. 2018. Early Growth Response Gene-2 Is Essential for M1 and M2 Macrophage Activation and Plasticity by Modulation of the Transcription Factor CEBPbeta. *Front Immunol,* 9**,** 2515.

VIDYA, M. K., KUMAR, V. G., SEJIAN, V., BAGATH, M., KRISHNAN, G. & BHATTA, R. 2018. Toll-like receptors: Significance, ligands, signaling pathways, and functions in mammals. *Int Rev Immunol,* 37**,** 20-36.

WALSH, D., MCCARTHY, J., O'DRISCOLL, C. & MELGAR, S. 2013. Pattern recognition receptors--molecular orchestrators of inflammation in inflammatory bowel disease. *Cytokine Growth Factor Rev,* 24**,** 91-104.

WALSH, J. T., HENDRIX, S., BOATO, F., SMIRNOV, I., ZHENG, J., LUKENS, J. R., GADANI, S., HECHLER, D., GOLZ, G., ROSENBERGER, K., KAMMERTONS, T., VOGT, J., VOGELAAR, C., SIFFRIN, V., RADJAVI, A., FERNANDEZ-CASTANEDA, A., GAULTIER, A., GOLD, R., KANNEGANTI, T. D., NITSCH, R., ZIPP, F. & KIPNIS, J. 2015. MHCII-independent CD4+ T cells protect injured CNS neurons via IL-4. *J Clin Invest,* 125**,** 699-714.

WALSH, N. C., KENNEY, L. L., JANGALWE, S., ARYEE, K. E., GREINER, D. L., BREHM, M. A. & SHULTZ, L. D. 2017. Humanized Mouse Models of Clinical Disease. *Annu Rev Pathol,* 12**,** 187-215.

WALTERS, A., KEETON, R., LABUSCHAGNE, A., HSU, N. J. & JACOBS, M. 2021. TNFRp75-dependent immune regulation of alveolar macrophages and neutrophils during early Mycobacterium tuberculosis and Mycobacterium bovis BCG infection. *Immunology,* 162**,** 220-234.

WANG, L. Y., TU, Y. F., LIN, Y. C. & HUANG, C. C. 2016. CXCL5 signaling is a shared pathway of neuroinflammation and blood-brain barrier injury contributing to white matter injury in the immature brain. *J Neuroinflammation,* 13**,** 6.

WANG, Z. Q., XING, W. M., FAN, H. H., WANG, K. S., ZHANG, H. K., WANG, Q. W., QI, J., YANG, H. M., YANG, J., REN, Y. N., CUI, S. J., ZHANG, X., LIU, F., LIN, D. H., WANG, W. H., HOFFMANN, M. K. & HAN, Z. G. 2009. The novel lipopolysaccharide-binding protein CRISPLD2 is a critical serum protein to regulate endotoxin function. *J Immunol,* 183**,** 6646-56.

WEIERGRABER, M., HENRY, M., HESCHELER, J., SMYTH, N. & SCHNEIDER, T. 2005. Electrocorticographic and deep intracerebral EEG recording in mice using a telemetry system. *Brain Res Brain Res Protoc,* 14**,** 154-64.

WHO 2020. Global tuberculosis report 2020. *In:* WORLD HEALTH ORGANIZATION. (ed.). Geneva.

WHO 2022. Global tuberculosis report 2022. *In:* WORLD HEALTH ORGANIZATION. (ed.). Geneva.

WIECZOREK, M., ABUALROUS, E. T., STICHT, J., ALVARO-BENITO, M., STOLZENBERG, S., NOE, F. & FREUND, C. 2017. Major Histocompatibility Complex (MHC) Class I and MHC Class II Proteins: Conformational Plasticity in Antigen Presentation. *Front Immunol,* 8**,** 292.

WIELAND, C. W., VAN DER WINDT, G. J., WIERSINGA, W. J., FLORQUIN, S. & VAN DER POLL, T. 2008. CD14 contributes to pulmonary inflammation and mortality during murine tuberculosis. *Immunology,* 125**,** 272-9.

WLODARCZYK, A., LOBNER, M., CEDILE, O. & OWENS, T. 2014. Comparison of microglia and infiltrating CD11c(+) cells as antigen presenting cells for T cell proliferation and cytokine response. *J Neuroinflammation,* 11**,** 57.

WOLDEAMANUEL, Y. W. & GIRMA, B. 2014. A 43-year systematic review and meta-analysis: case-fatality and risk of death among adults with tuberculous meningitis in Africa. *J Neurol,* 261**,** 851-65.

WOLF, A. J., DESVIGNES, L., LINAS, B., BANAIEE, N., TAMURA, T., TAKATSU, K. & ERNST, J. D. 2008. Initiation of the adaptive immune response to Mycobacterium tuberculosis depends on antigen production in the local lymph node, not the lungs. *J Exp Med,* 205**,** 105-15.

XIA, A., LI, X., QUAN, J., CHEN, X., XU, Z. & JIAO, X. 2021. Mycobacterium tuberculosis Rv0927c Inhibits NF-kappaB Pathway by Downregulating the Phosphorylation Level of IkappaBalpha and Enhances Mycobacterial Survival. *Front Immunol,* 12**,** 721370.

XIA, X., LI, H., SATHEESAN, S., ZHOU, J. & ROSSI, J. J. 2019. Humanized NOD/SCID/IL2rgammanull (hu-NSG) Mouse Model for HIV Replication and Latency Studies. *J Vis Exp*.

XIAHOU, Z., WANG, X., SHEN, J., ZHU, X., XU, F., HU, R., GUO, D., LI, H., TIAN, Y., LIU, Y. & LIANG, H. 2017. NMI and IFP35 serve as proinflammatory DAMPs during cellular infection and injury. *Nature Communications,* 8**,** 950.

XING, Z., WANG, J., CROITORU, K. & WAKEHAM, J. 1998. Protection by CD4 or CD8 T cells against pulmonary Mycobacterium bovis bacillus Calmette-Guerin infection. *Infect Immun,* 66**,** 5537-42.

XUAN, C., WANG, Q., HAN, X., DUAN, Y., LI, L., SHI, L., WANG, Y., SHAN, L., YAO, Z. & SHANG, Y. 2013. RBB, a novel transcription repressor, represses the transcription of HDM2 oncogene. *Oncogene,* 32**,** 3711-21.

YADAV, R. & SRIVASTAVA, P. 2018. Clustering, Pathway Enrichment, and Protein-Protein Interaction Analysis of Gene Expression in Neurodevelopmental Disorders. *Adv Pharmacol Sci,* 2018**,** 3632159.

YAN, Y., CHEN, R., WANG, X., HU, K., HUANG, L., LU, M. & HU, Q. 2019. CCL19 and CCR7 Expression, Signaling Pathways, and Adjuvant Functions in Viral Infection and Prevention. *Front Cell Dev Biol,* 7**,** 212.

YANG, Q., CAI, Y., ZHAO, W., WU, F., ZHANG, M., LUO, K., ZHANG, Y., LIU, H., ZHOU, B., KORNFELD, H. & CHEN, X. 2014. IP-10 and MIG are compartmentalized at the site of disease during pleural and meningeal tuberculosis and are decreased after antituberculosis treatment. *Clin Vaccine Immunol,* 21**,** 1635-44.

YIN, J., VALIN, K. L., DIXON, M. L. & LEAVENWORTH, J. W. 2017. The Role of Microglia and Macrophages in CNS Homeostasis, Autoimmunity, and Cancer. *J Immunol Res,* 2017**,** 5150678.

YUN, H. J., KIM, E. H. & KIM, B. G. 2018. Neuron-Macrophage Co-cultures to Activate Macrophages Secreting Molecular Factors with Neurite Outgrowth Activity. *J Vis Exp*.

ZANONI, I. & GRANUCCI, F. 2013. Role of CD14 in host protection against infections and in metabolism regulation. *Front Cell Infect Microbiol,* 3**,** 32.

ZHANG, B., LI, H., ZHANG, J., HANG, Y. & XU, Y. 2022. Activating transcription factor 3 protects alveolar epithelial type II cells from Mycobacterium tuberculosis infection-induced inflammation. *Tuberculosis (Edinb),* 135**,** 102227.

ZHANG, H., LI, Y., CHENG, Q., CHEN, X., YU, Q. & LI, Z. 2020a. Abnormal Expression of Dysferlin in Blood Monocytes Supports Primary Dysferlinopathy in Patients Confirmed by Genetic Analyses. *Front Neurol,* 11**,** 540098.

ZHANG, L., TAN, J., JIANG, X., QIAN, W., YANG, T., SUN, X., CHEN, Z. & ZHU, Q. 2017. Neuron-derived CCL2 contributes to microglia activation and neurological decline in hepatic encephalopathy. *Biol Res,* 50**,** 26.

ZHANG, M., YANG, W., WANG, P., DENG, Y., DONG, Y. T., LIU, F. F., HUANG, R., ZHANG, P., DUAN, Y. Q., LIU, X. D., LIN, D., CHU, Q. & ZHONG, B. 2020b. CCL7 recruits cDC1 to promote antitumor immunity and facilitate checkpoint immunotherapy to non-small cell lung cancer. *Nat Commun,* 11**,** 6119.

ZHAO, J., YANG, Q., LIU, Z., XU, P., TIAN, L., YAN, J., LI, K., LIN, B., BIAN, L., XI, Z. & LIU, X. 2023. The impact of subchronic ozone exposure on serum metabolome and the mechanisms of abnormal bile acid and arachidonic acid metabolisms in the liver. *Ecotoxicol Environ Saf,* 252**,** 114573.

ZHAO, K., YI, Y., MA, Z. & ZHANG, W. 2021. INHBA is a Prognostic Biomarker and Correlated With Immune Cell Infiltration in Cervical Cancer. *Front Genet,* 12**,** 705512.

ZHOU, H., XU, M., HU, P., LI, Y., REN, C., LI, M., PAN, Y., WANG, S. & LIU, X. 2023. Identifying hub genes and common biological pathways between COVID-19 and benign prostatic hyperplasia by machine learning algorithms. *Frontiers in Immunology,* 14.

ZHU, X. & ZHU, J. 2020. CD4 T Helper Cell Subsets and Related Human Immunological Disorders. *Int J Mol Sci,* 21.

Appendix

Table A-1: SPIA pathway analysis results.
The significantly perturbed pathways identified by the SPIA method is shown together the specific pathway ID and status. There is a KEGG link given which will visually display the differentially expressed genes in the respective pathways.

Pathway Name	Status	Perturbation Score (t_A)	False discovery rate (p_{GFdr})	KEGGLINK
Herpes simplex infection	Activated	41,45	1E-16	http://www.genome.jp/dbget-bin/show_pathway?mmu05168+22029+22030+14281+12266+142980+24088+17874+54123+18035+18036+21926+16193+20304+230073+71586+15957+18854+22059+19106+23961+246728+246730+15979+15977+20846+20847+16391+21354+21355+14964+14972+14990+15007+15013+15018+15024+15040+12702+14969+14102+21937
Cytokine-cytokine receptor interaction	Activated	39,73	1E-15	http://www.genome.jp/dbget-bin/show_pathway?mmu04060+12984+16180+16178+16177+12167+12156+16323+57916+21939+14102+21948+15979+12978+18596+329244+15977+12977+13857+53603+18414+56708+16878+16156+16193+20305+20304+20306+20293+24047+13051+20312+56744+20315+15945+17329+20311+21937+27279+18383+21933+22035+21926+20310+14825+12778
Influenza A	Activated	8,03	1E-11	http://www.genome.jp/dbget-bin/show_pathway?mmu05164+230073+71586+217069+142980+18035+18036+54123+320207+170743+17874+66824+77125+15977+20846+20847+16391+17858+23961+246728+246730+56417+18854+14969+12702+20304+15894+16193+21926+19106+22035+21933+58185+15945+14102+15979+21937
NF-kappa B signaling pathway	Activated	18,79	2E-11	http://www.genome.jp/dbget-bin/show_pathway?mmu04064+18035+17874+22030+16177+21937+21926+18034+19698+21939+21929+22029+20315+230073+12475+12046+12047+234779+12229+17060+17873+217069+19225+22329+20310+24047+15894
Chemokine signaling pathway	Activated	61,85	1E-09	http://www.genome.jp/dbget-bin/show_pathway?mmu04062+13051+14825+15945+17329+20293+20296+20304+20305+20306+20310+20311+20312+20315+24047+56744+320207+14710+66066+22324+11513+17969+20846+20847+20848+19354+18035+18036+277360

HTLV-I infection	Activated	6,62	5E-09	http://www.genome.jp/dbget-bin/show_pathway?mmu05166+22329+15894+18018+18019+14964+14972+14990+15007+15013+15018+15024+15040+17532+20130+11513+11910+17127+18973+12575+30939+18035+16193+18034+19698+21939+21937+16177+16178+18596+320207+57265+12579+23872+14281+13653+13654+14283+14969+22059+17865+17701+17702+22695+21926
Measles	Activated	12,29	7E-09	http://www.genome.jp/dbget-bin/show_pathway?mmu05162+170743+17874+54123+24088+230073+18035+18036+71586+15977+20846+20847+16391+23961+246728+246730+15979+12487+320207+20848+16193+17858+19106+14102+22035+21933+21929+22059+56417
Toxoplasmosis	Activated	20,42	2E-07	http://www.genome.jp/dbget-bin/show_pathway?mmu05145+17874+18035+18036+21926+329581+18126+20846+14969+11689+12703+20848+320207+18783+16772+16775+16776+16782+226519+24088+15979+21939+21937+16835+16145
Chagas disease (American trypanosomiasis)	Activated	18,67	1E-06	http://www.genome.jp/dbget-bin/show_pathway?mmu05142+24088+12266+12259+12260+12262+17874+14281+21926+15977+18035+15979+18126+21937+17127+18787+320207+14102+16193+20304+21899
Hepatitis C	Activated	6,47	3E-06	http://www.genome.jp/dbget-bin/show_pathway?mmu05160+230073+54123+142980+18035+15977+20846+20847+16391+58187+12702+20848+23961+246728+246730+19106+16362+15957+320207+22059+12575+21926+21937+22030+16835
Toll-like receptor signaling pathway	Activated	13,47	3E-06	http://www.genome.jp/dbget-bin/show_pathway?mmu04620+15977+17874+26410+54123+15945+21939+16193+20304+20846+18035+21926+24088+142980+21899+12475+17329+320207+170743+14281
Leishmaniasis	Activated	19,88	4E-06	http://www.genome.jp/dbget-bin/show_pathway?mmu05140+14131+12266+17969+20846+14969+24088+17874+18035+18036+18126+21926+15170+14281+15979+19225
Cytosolic DNA-sensing pathway	Activated	5,07	1E-05	http://www.genome.jp/dbget-bin/show_pathway?mmu04623+66824+58203+15977+54123+15945+56532+56417+16193+230073+77125+18035+18036+20304+22040

Tuberculosis	Activated	20,34	2E-05	http://www.genome.jp/dbget-bin/show_pathway?mmu05152+17533+13033+108058+12323+20698+14131+20846+24088+12608+12475+17874+21899+21926+21937+14969+13040+16193+16411+12796+192656+56619+14127+15979+12266+18126+15977
Apoptosis	Activated	15,87	2E-05	http://www.genome.jp/dbget-bin/show_pathway?mmu04210+22059+329581+12364+18035+320207+17874+22030+12984+16177+16180+21937+21933+14102+18049+21926+22035
Antigen processing and presentation	Activated	4,84	3E-05	http://www.genome.jp/dbget-bin/show_pathway?mmu04612+13040+19141+21356+14964+14972+14990+15007+15013+15018+15024+15040+14969+21354+21355+21926
Epstein-Barr virus infection	Activated	0,63	7E-05	http://www.genome.jp/dbget-bin/show_pathway?mmu05169+14964+14972+14990+15007+15013+15018+15024+15040+15507+22059+22029+22030+18035+18036+18037+18034+19698+12495+21939+12505+15894+21929+320207+234779+230073+19106+12575+20848
Staphylococcus aureus infection	Activated	2,80	7E-05	http://www.genome.jp/dbget-bin/show_pathway?mmu05150+12266+14962+50908+50909+12259+12260+12262+12273+14131+14969+12267+15894+20345
MAPK signaling pathway	Activated	8,49	1E-04	http://www.genome.jp/dbget-bin/show_pathway?mmu04010+19252+70686+18783+18034+19698+17532+20130+240168+18596+14184+14164+12064+18049+15370+22059+15507+26408+53608+13197+17873+22030+12475+14102+16177+16178+21937+21926+19354+18019+68794+26410+14281
Legionellosis	Activated	8,06	2E-04	http://www.genome.jp/dbget-bin/show_pathway?mmu05134+66824+17952+18035+12266+18034+24088+12475+17874+21926+16193+14825+20310
ECM-receptor interaction	Activated	2,56	3E-04	http://www.genome.jp/dbget-bin/show_pathway?mmu04512+16772+16775+16776+16782+226519+12833+12834+21923+329278+20971+15530+16419+319480+16402+109700+12505

RIG-I-like receptor signaling pathway	Activated	3,39	3E-04	http://www.genome.jp/dbget-bin/show_pathway?mmu04622+230073+71586+217069+67664+54123+15977+18035+18036+80861+100038882+22030+21926+15945
Malaria	Activated	5,74	3E-04	http://www.genome.jp/dbget-bin/show_pathway?mmu05144+15894+20971+71683+22329+24088+17874+16193+21926+21939+20339
Viral myocarditis	Activated	0,36	8E-04	http://www.genome.jp/dbget-bin/show_pathway?mmu05416+21939+14969+14964+14972+14990+15007+15013+15018+15024+15040+12487+15894+71960+12389+19354
Rheumatoid arthritis	Activated	3,39	8E-04	http://www.genome.jp/dbget-bin/show_pathway?mmu05323+21926+16193+16156+12977+17392+14969+15894+12487+20315+20311+24088+14281+20304
Amoebiasis	Activated	6,34	8E-04	http://www.genome.jp/dbget-bin/show_pathway?mmu05146+16772+16775+16776+16782+226519+16193+16177+16178+21926+18126+24088+15507+12475+320207+18788+20708
Jak-STAT signaling pathway	Activated	2,41	4E-03	http://www.genome.jp/dbget-bin/show_pathway?mmu04630+320207+18712+12702+12703+16391+20846+20847+20848+15170+12984+13857+15979+18414+16156+16193+16878+56708+53603+15977+329244
Adipocytokine signaling pathway	Activated	0,93	4E-03	http://www.genome.jp/dbget-bin/show_pathway?mmu04920+18035+18036+18037+12702+12894+433256+20528+20848+22030+21937+19017+21926
African trypanosomiasis	Activated	1,81	7E-03	http://www.genome.jp/dbget-bin/show_pathway?mmu05143+17874+21926+20339+22329+16775+16193+15894+14102

Prion diseases	Activated	6,15	1E-02	http://www.genome.jp/dbget-bin/show_pathway?mmu05020+226519+12259+12260+12262+13653+20304+16193+12364
Focal adhesion	Activated	3,85	2E-02	http://www.genome.jp/dbget-bin/show_pathway?mmu04510+16419+109700+16402+319480+68794+228785+320207+22793+12833+12834+16772+16775+16776+16782+21923+226519+329278+12389+18596+16000+19354+22324
Salmonella infection	Activated	0,81	2E-02	http://www.genome.jp/dbget-bin/show_pathway?mmu05132+14281+12475+17874+68794+74764+66824+15979+18126+16193+14825+20310
Intestinal immune network for IgA production	Activated	-4,58	1E-11	http://www.genome.jp/dbget-bin/show_pathway?mmu04672+16193+21939+57916+12487+14969+17123+20315+50723
Osteoclast differentiation	Inhibited	-27,21	2E-07	http://www.genome.jp/dbget-bin/show_pathway?mmu04380+12978+22030+12977+18383+18035+18018+15977+20846+20847+16391+320207+16177+15979+14281+14282+14283+16477+14131+22177+12229+17060+234779+17342+21926+21937+12702+12703+18034+19698+17969+18733+83433
Natural killer cell mediated cytotoxicity	Inhibited	-10,45	7E-07	http://www.genome.jp/dbget-bin/show_pathway?mmu04650+18018+18019+22035+15979+234779+21926+23900+14127+22177+15170+15977+14102+21933+12506+15894+320207+19354+22324+14131+14964+14972+15040+19370+77777
B cell receptor signaling pathway	Inhibited	-2,52	3E-06	http://www.genome.jp/dbget-bin/show_pathway?mmu04662+18035+18036+18037+22324+320207+68713+16331+16332+14281+240168+18018+18019+19354+234779+17060+12229+15170+18733
Pertussis	Inhibited	0	3E-05	http://www.genome.jp/dbget-bin/show_pathway?mmu05133+17874+18126+16193+20311+16402+50909+50908+12259+12260+12262+12258+12266+14281+21926+12475+15900+16362+66824

Allograft rejection	Inhibited	0	4E-05	http://www.genome.jp/dbget-bin/show_pathway?mmu05330+14964+14969+14972+14990+15007+15013+15018+15024+15040+21939+14102+12487+21926
Graft-versus-host disease	Inhibited	0	5E-04	http://www.genome.jp/dbget-bin/show_pathway?mmu05332+14969+14102+14964+14972+14990+15007+15013+15018+15024+15040+12487+21926+16193
Transcriptional misregulation in cancer	Inhibited	0	6E-04	http://www.genome.jp/dbget-bin/show_pathway?mmu05202+14247+56312+12575+16000+12608+16193+80859+17392+16178+12394+18854+12046+12047+12475+19696+22029+21939+14011+15364+17132+22059+12978+17095+15242
Type I diabetes mellitus	Inhibited	-6,03	8E-04	http://www.genome.jp/dbget-bin/show_pathway?mmu04940+12487+14969+14964+14972+14990+15007+15013+15018+15024+15040+14102+21926
NOD-like receptor signaling pathway	Inhibited	0	1E-03	http://www.genome.jp/dbget-bin/show_pathway?mmu04621+192656+18035+18036+14825+20310+20304+21926+66824+16193+21929+17952
Autoimmune thyroid disease	Inhibited	-0,65	3E-03	http://www.genome.jp/dbget-bin/show_pathway?mmu05320+14969+21939+14102+14964+14972+14990+15007+15013+15018+15024+15040+12487
Small cell lung cancer	Inhibited	-0,09	3E-03	http://www.genome.jp/dbget-bin/show_pathway?mmu05222+22059+320207+16772+16775+16776+16782+226519+329581+18126+19225+18035+22029+22030+12579
Complement and coagulation cascades	Inhibited	-8,45	5E-03	http://www.genome.jp/dbget-bin/show_pathway?mmu04610+18787+12061+12266+14962+12273+12267+12258+50908+50909+12259+12260+12262

Viral carcinogenesis	Inhibited	0	6E-03	http://www.genome.jp/dbget-bin/show_pathway?mmu05203+22059+16391+22029+22030+26427+20848+320207+18034+19696+13654+12579+12575+18035+54123+12266+14964+14972+14990+15007+15013+15018+15024+15040+19106
Fc gamma R-mediated phagocytosis	Inhibited	-4,83	2E-02	http://www.genome.jp/dbget-bin/show_pathway?mmu04666+320207+16331+16332+234779+18783+22324+19354+18805+230837+17909+17969+20698
p53 signaling pathway	Inhibited	-2,91	2E-02	http://www.genome.jp/dbget-bin/show_pathway?mmu04115+13197+17873+16000+18787+12575+14102+22059+66940+140742
Glioma	Inhibited	-9,20	3E-02	http://www.genome.jp/dbget-bin/show_pathway?mmu05214+16000+18596+108058+12323+320207+22059+234779+12575

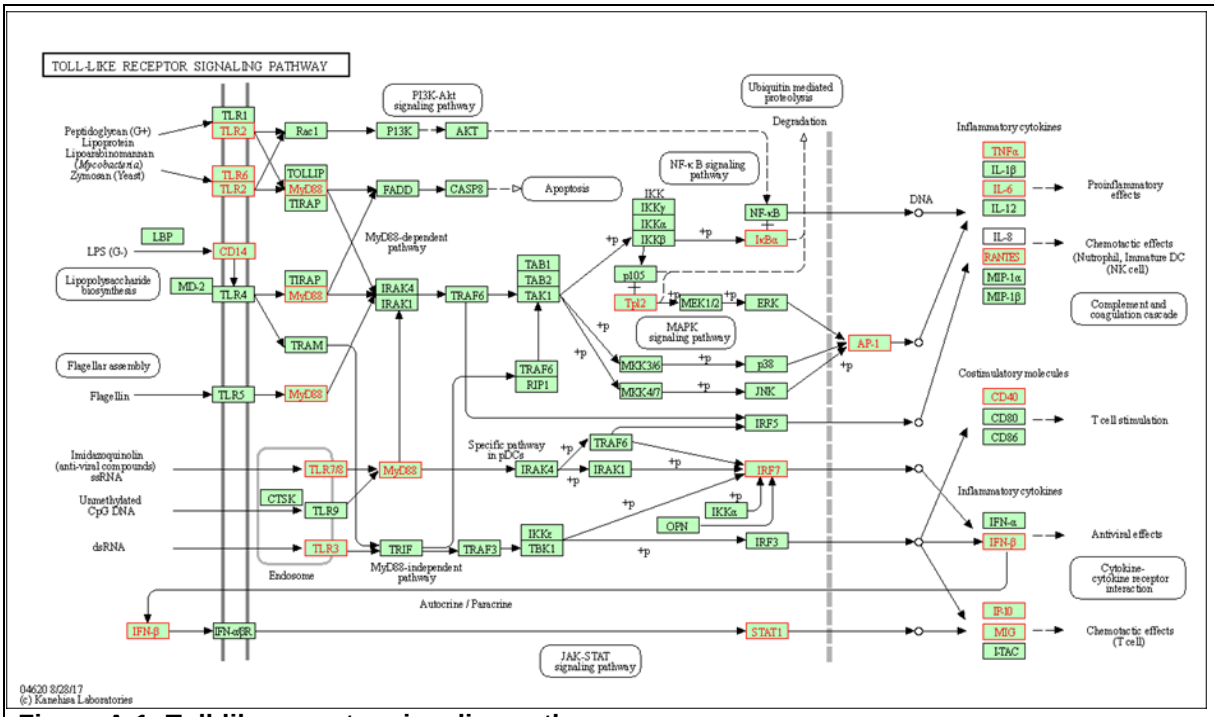

Figure A-1: Toll-like receptor signaling pathway.
The Toll-like receptor signaling pathway shows differentially expressed genes in red and green boxes, and unaltered genes in black and green boxes.

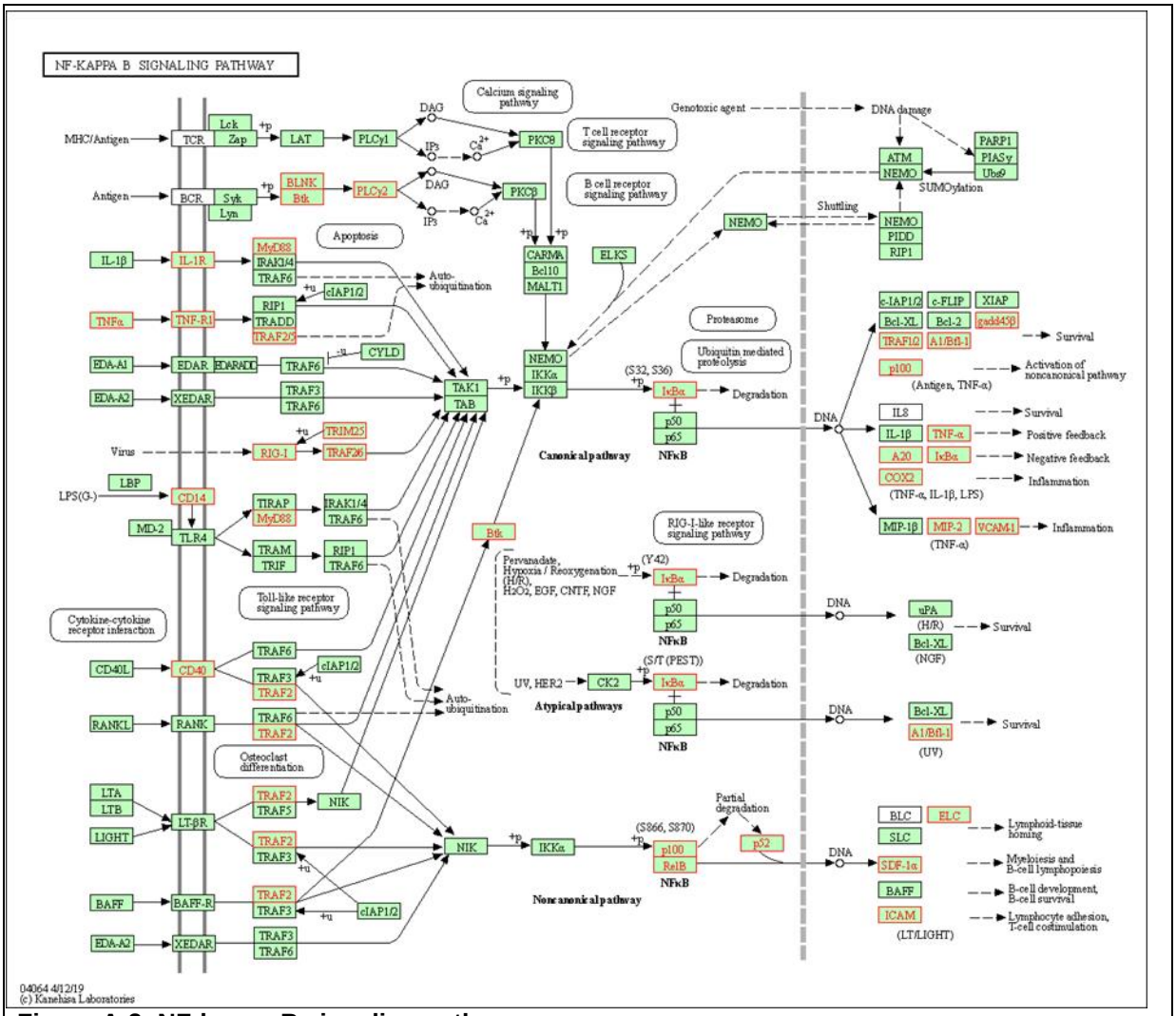

Figure A-2: NF-kappa B signaling pathway.
This pathway shows the up and down stream proteins which are linked to NF-kappa B signaling. Differentially expressed genes are shown by the red and green boxes, and unaltered genes in black and green boxes.

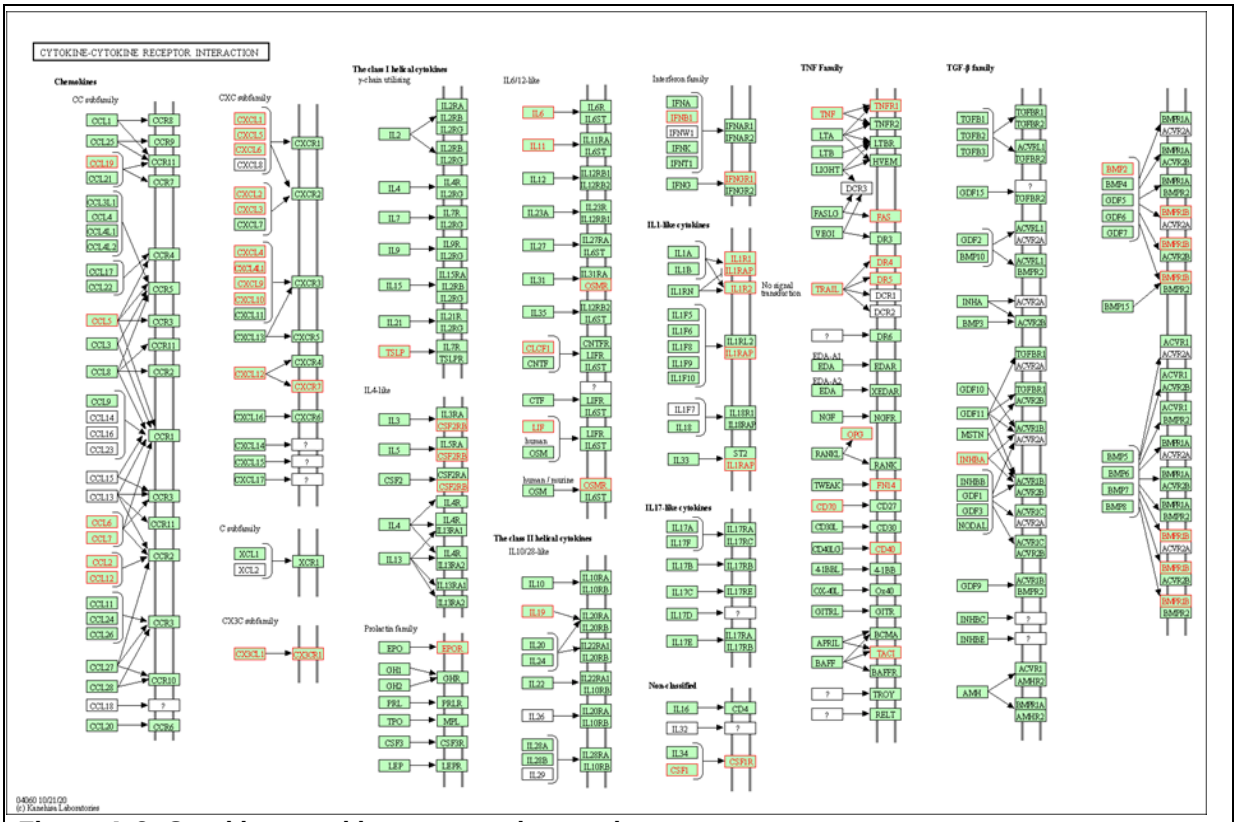

Figure A-3: Cytokine-cytokine receptor interaction.
This figure shows the interaction of cytokines and chemokines with the respective ligands. Genes that have been differentially expressed are highlighted by red and green boxes, and unaltered genes in black and green boxes.

Table A-2: Gene module enrichment.
Gene modules are displayed according to significance (0.05>p-value) together with their respective effect sizes. The modules are ranked based on most significant at the top to least significant.

Module ID	Title	Effect size	p-Value
LI.M4.0	Cell cycle and transcription	7,46E-01	6,15E-18
LI.M27.0	Chemokine cluster (I)	8,51E-01	4,39E-13
LI.M75	Antiviral IFN signature	9,67E-01	5,03E-13
LI.M11.0	Enriched in monocytes (II)	7,24E-01	5,03E-13
LI.M37.0	Immune activation - generic cluster	6,63E-01	1,36E-11
LI.M86.0	Chemokines and inflammatory molecules in myeloid cells	9,13E-01	3,67E-10
LI.M111.0	Viral sensing & immunity; IRF2 targets network (I)	9,72E-01	7,47E-10
LI.M68	RIG-1 like receptor signaling	9,87E-01	1,32E-09
LI.M20	AP-1 transcription factor network	9,07E-01	4,47E-09
LI.M89.0	Putative targets of PAX3	9,11E-01	7,79E-09
LI.M111.1	Viral sensing & immunity; IRF2 targets network (II)	9,54E-01	1,07E-08
LI.M127	Type I interferon response	9,49E-01	1,14E-08
LI.M13	Innate activation by cytosolic DNA sensing	9,03E-01	3,25E-08
LI.M27.1	Chemokine cluster (II)	7,59E-01	4,98E-08
LI.M165	Enriched in activated dendritic cells (II)	7,59E-01	1,86E-07

LI.S10	Resting dendritic cell surface signature	7,79E-01	2,73E-07
LI.M43.0	Myeloid, dendritic cell activation via NFkB (I)	8,92E-01	3,22E-07
LI.S4	Monocyte surface signature	7,12E-01	1,08E-06
LI.M5.0	Regulation of antigen presentation and immune response	7,38E-01	1,37E-06
LI.M4.1	Cell cycle (I)	7,46E-01	4,96E-06
LI.M160	Leukocyte differentiation	8,16E-01	5,17E-06
LI.M112.0	Complement activation (I)	9,57E-01	6,34E-06
LI.M118.0	Enriched in monocytes (IV)	7,07E-01	6,34E-06
LI.M16	TLR and inflammatory signaling	8,28E-01	6,35E-06
LI.M43.1	Myeloid, dendritic cell activation via NFkB (II)	8,04E-01	1,41E-05
LI.M67	Activated dendritic cells	8,40E-01	1,93E-05
LI.M64	Enriched in activated dendritic cells/monocytes	8,50E-01	2,26E-05
LI.M29	Pro-inflammatory cytokines and chemokines	8,31E-01	2,72E-05
LI.M89.1	Putative targets of PAX3	8,71E-01	3,21E-05
LI.M35.0	Signaling in T cells (I)	8,05E-01	3,86E-05
LI.S5	DC surface signature	7,15E-01	6,46E-05
LI.M40	Complement and other receptors in DCs	9,61E-01	7,72E-05

LI.M94	Growth factor induced, enriched in nuclear receptor subfamily 4	8,78E-01	8,33E-05
LI.M54	BCR signaling	9,26E-01	8,35E-05
LI.M24	Cell activation (IL15, IL23, TNF)	7,73E-01	8,35E-05
LI.M23	RA, WNT, CSF receptors network (monocyte)	9,22E-01	8,89E-05
LI.M31	Cell cycle and growth arrest	9,57E-01	8,89E-05
LI.M150	Innate antiviral response	8,77E-01	8,89E-05
LI.M0	Targets of FOSL1/2	7,56E-01	2,17E-04
LI.M73	Enriched in monocytes (III)	8,72E-01	2,48E-04
LI.M91	Adhesion and migration, chemotaxis	8,67E-01	5,16E-04
LI.M38	Chemokines and receptors	7,70E-01	5,21E-04
LI.M3	Regulation of signal transduction	6,67E-01	6,68E-04
LI.M33	Inflammatory response	9,80E-01	6,88E-04
LI.M95.1	Enriched in antigen presentation (III)	8,91E-01	8,35E-04
LI.M92	Lipid metabolism, endoplasmic reticulum	7,46E-01	1,62E-03
LI.M87	Transmembrane transport (I)	7,58E-01	2,00E-03
LI.M189	Extracellular region cluster (GO)	7,58E-01	2,11E-03
LI.M2.1	Extracellular matrix (II)	5,93E-01	2,11E-03

LI.M215	Small GTPase mediated signal transduction	8,04E-01	2,46E-03
LI.M135.1	Enriched in plasma membrane proteins (II)	8,50E-01	2,64E-03
LI.M81	Enriched in myeloid cells and monocytes	6,65E-01	2,86E-03
LI.M122	Enriched for cell migration	7,25E-01	3,16E-03
LI.M45	Leukocyte activation and migration	8,57E-01	3,77E-03
LI.M71	Enriched in antigen presentation (I)	8,07E-01	3,79E-03
LI.M53	Inflammasome receptors and signaling	7,03E-01	6,97E-03
LI.M78	Myeloid cell cytokines, metallopeptidases and laminins	8,74E-01	7,39E-03
LI.M42	Platelet activation (III)	8,07E-01	7,58E-03
LI.M86.1	Pro-inflammatory dendritic cell, myeloid cell response	7,02E-01	7,58E-03
LI.M155	G protein coupled receptors cluster	8,77E-01	8,81E-03
LI.M6	Mitotic cell division	8,18E-01	1,01E-02
LI.M112.1	Complement activation (II)	7,85E-01	1,01E-02
LI.S11	Activated (LPS) dendritic cell surface signature	7,11E-01	1,10E-02
LI.M50	CD1 and other DC receptors	8,53E-01	1,18E-02
LI.M210	Extracellular matrix, collagen	6,56E-01	1,28E-02
LI.M56	Suppression of MAPK signaling	6,96E-01	1,28E-02

LI.M115	Cytokines - receptors cluster	8,30E-01	1,46E-02
LI.M124	Enriched in membrane proteins	7,70E-01	1,53E-02
LI.M95.0	Enriched in antigen presentation (II)	7,65E-01	1,54E-02
LI.M47.2	Enriched in B cells (III)	7,43E-01	1,82E-02
LI.M11.1	Blood coagulation	7,46E-01	1,82E-02
LI.M85	Platelet activation and degranulation	5,64E-01	1,96E-02
LI.M140	Extracellular matrix, complement	8,77E-01	2,06E-02
LI.M118.1	Enriched in monocytes (surface)	6,41E-01	2,12E-02
LI.M4.3	Myeloid cell enriched receptors and transporters	7,02E-01	2,16E-02
LI.M109	Receptors, cell migration	6,92E-01	2,86E-02
LI.M22.0	Mismatch repair (I)	8,30E-01	2,86E-02
LI.M163	Enriched in neutrophils (II)	8,65E-01	3,26E-02
LI.M139	Lysosomal/endosomal proteins	7,37E-01	3,58E-02
LI.M36	T cell surface, activation	7,02E-01	3,62E-02
LI.M47.4	Enriched in B cells (V)	8,80E-01	3,75E-02
LI.M9	B cell development	7,58E-01	3,88E-02
LI.M119	Enriched in activated dendritic cells (I)	6,20E-01	3,88E-02

LI.M10.0	E2F1 targets (Q3)	7,13E-01	3,93E-02
LI.S1	NK cell surface signature	6,47E-01	3,93E-02
LI.M39	Integrin mediated leukocyte migration	7,78E-01	4,22E-02
LI.M223	Enriched in T cells (II)	9,43E-01	4,54E-02
LI.M25	TLR8-BAFF network	6,93E-01	4,54E-02
LI.M49	Transcription regulation in cell development	6,68E-01	4,54E-02

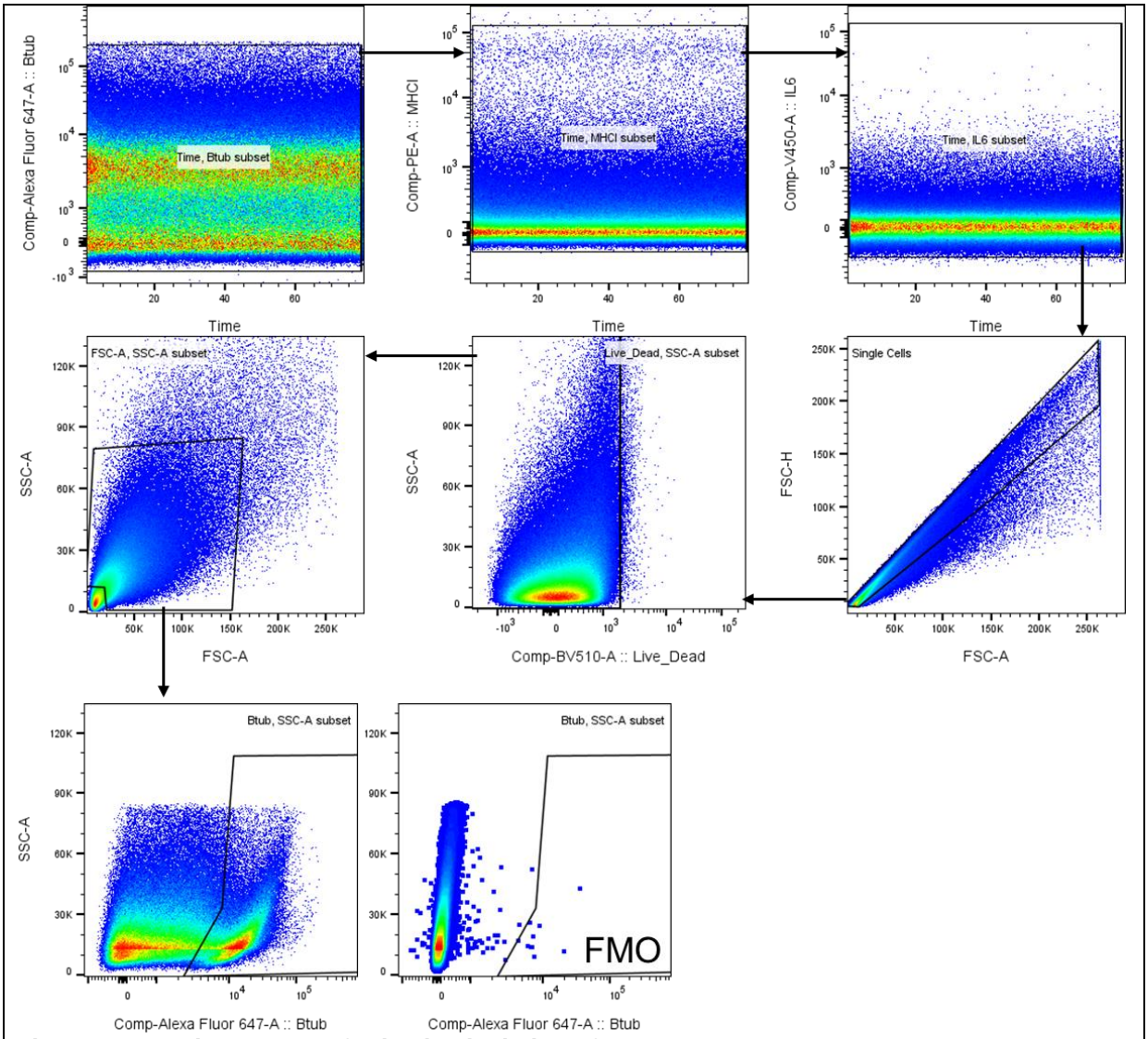

Figure A-4: Gating strategy for in vivo isolation of neurons.
Neurons from single cell brain samples were isolated by assessing appropriate flow with the time gates of the various lasers and removing doublets with the singlets gate. Live cells were gated on before discarding debris and selecting for B-III-Tubulin^{+} cells.

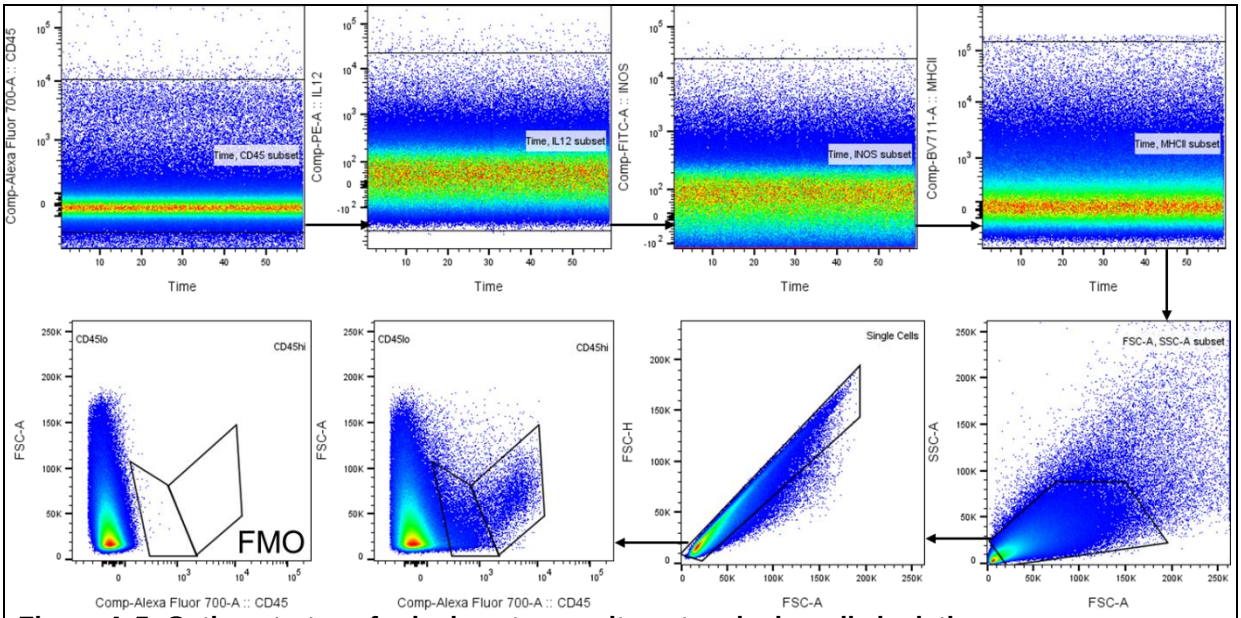

Figure A-5: Gating strategy for leukocyte recruitment and microglia isolation.
Gating strategy for the isolation of resident microglia and recruited leukocytes. Time gate demonstrating regular flow followed by FSC-A vs SSC-A gate to remove debris. The singlet gate to select for single cells and finally the $CD45^{lo}$ and $CD45^{hi}$ gates to differentiate between resident and recruited cells.

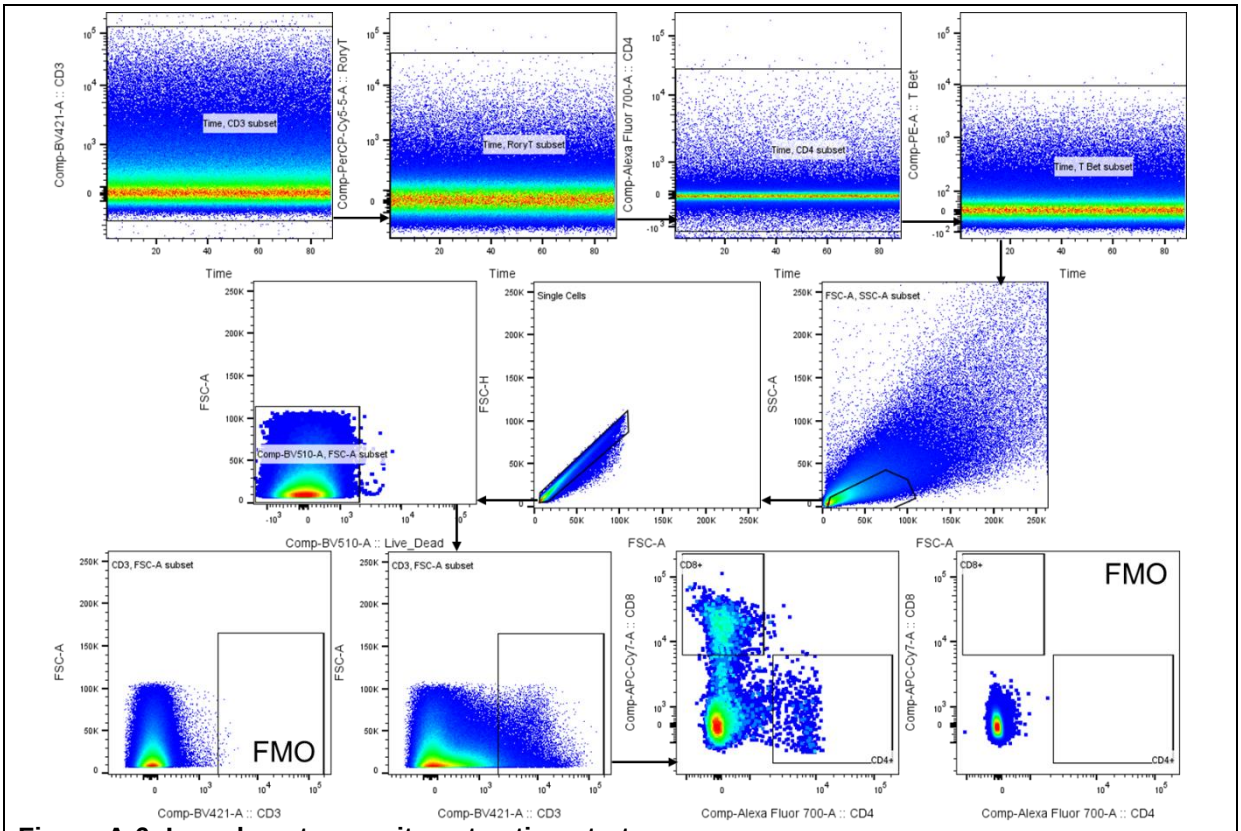

Figure A-6: Lymphocyte recruitment gating strategy.
Single cell suspended brain samples were processed for flow cytometry analysis. Leukocytes were gated for based on the forward scatter and side scatter parameters. Next, only live cells were selected for followed by the specific isolation of $CD3^{+}CD4^{+}$ and $CD3^{+}CD8^{+}$ positive cells.

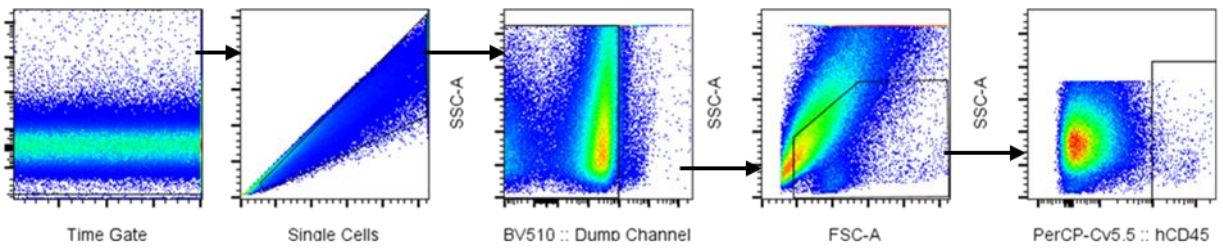

Figure A-7: Human lymphocyte recruitment gating strategy.
Single cell suspensions generated from humanized mice brains were processed for flow cytometry analysis. Leukocytes were gated for based on the forward scatter and side scatter parameters and human leukocytes were isolated by selecting for $hCD45^+$ cells.